REACTIVE OXYGEN SPECIES GENERATED IN THE PEROXYGEN SYSTEMS

By

MIAO YU

A dissertation submitted in partial fulfillment of
the requirements for the degree of

DOCTOR OF PHILOSOPHY

WASHINGTON STATE UNIVERSITY
Department of Civil and Environmental Engineering

JULY 2013

To the Faculty of Washington State University:

The members of the Committee appointed to examine the dissertation of MIAO YU find it satisfactory and recommend that it be accepted.

Richard J. Watts, Ph.D., Chair

Amy L. Teel, Ph.D.

David R. Yonge, Ph.D.

I. Francis Cheng, Ph.D.

ACKNOWLEDGEMENT

I would like to thank Dr. Richard Watts for his support and help during all the past five years. I'm grateful that he provided me the opportunity to work in the chemical oxidation lab and pursue my graduate study. I truly appreciate his guidance for me and expertise in this field. Dr. Watts has set up a role model for me to my future research and work. I would like to thank Dr. Amy Teel, Dr. David Yonge and Dr. I. Francis Cheng for being my committee members and their guidance and help on my dissertation. I'm very grateful for Dr. Teel's help on revising my dissertation and improving my writing skill. I would like to thank Dr. Akram Hossain for being substitute committee member and reviewing my dissertation.

I also would like to thank all of my lab mates: Dr. Mushtaque Ahmad, Marissa, Shannon, Farah and Sattam. My thanks go to Dr. Ahmad for all of his helpful suggestions during my PhD and discussions with me on my research. I also would like to thank Shannon for editing my dissertation. I'm grateful for working in this wonderful lab with these nice lab mates.

My special thanks go to my husband Dr. Shuai Shao for his love, encouragement and support. My appreciation goes to my parents Qian Zhang and Qinghui Yu, for everything they did for me.

REACTIVE OXYGEN SPECIES GENERATED IN THE PEROXYGEN SYSTEMS

Abstract

by Miao Yu, Ph.D.
Washington State University
July 2013

Chair: Richard J. Watts

Three different topics related to peroxymonosulfate activation by subsurface minerals, soluble irons and iron chelate, and the reactive species generated in modified Fenton's systems with different concentrations of hydrogen peroxide were studied. Chapter one presented an introduction of theory for this research. In chapter two, peroxymonosulfate activation by four subsurface minerals and three soil fractions was investigated. Rates of peroxymonosulfate decomposition and generation rates of reactive species were studied in the presence of minerals. Hematite activated peroxymonosulfate system most effectively degraded the hydroxyl radical probe nitrobenzene. Use of the probe compound anisole in conjunction with scavengers demonstrated that both sulfate radical and hydroxyl radical are generated in mineral-activated peroxymonosulfate systems. The natural soil did not effectively promote the generation of oxidants; however, the SOM was found to promote the generation of reductants.

In chapter three, peroxymonosulfate activation by iron (II) sulfate, iron (III) sulfate and iron (III)–EDTA was compared using nitrobenzene as an oxidant probe and hexachloroethane as a reductant probe, and the model groundwater contaminants perchloroethylene(PCE) and

trichloroethylene(TCE). $FeSO_4$, $Fe_2(SO_4)_3$, and Fe (III)–EDTA were each able to effectively activate peroxymonosulfate to generate oxidants, but not to generate reductants. PCE and TCE loss in $FeSO_4$– and $Fe_2(SO_4)_3$–activated peroxymonosulfate was due to hydroxyl radical activity, while both hydroxyl radical and sulfate radical were responsible for PCE and TCE degradation in Fe (III)–EDTA–activated peroxymonosulfate.

The fourth chapter investigated the degradation of the reactive species responsible for PCE and TCE by catalyzed hydrogen peroxide propagation (CHP) using concentrations of H_2O_2 in increments between 0.01M and 1 M. The addition of scavenger confirmed that the degradation of PCE and TCE was mainly due to hydroxyl radical. The TCE degradation with scavenger became higher when H_2O_2 concentrations increased, suggesting that more superoxide was generated with greater H_2O_2 concentration. Results similar to PCE and TCE degradation were obtained with nitrobenzene destruction, indicating that there was less hydroxyl radical in CHP systems with high H_2O_2 concentrations. Tetranitromethane degradation further confirmed that higher reactivity of superoxide was generated due to increased H_2O_2 concentrations in CHP systems.

TABLE OF CONTENTS

LIST OF TABLES

LIST OF FIGURES

CHAPTER 4: REACTIVE SPECIES GENERATION IN MODIFIED FENTON'S SYSTEMS WITH DIFFERENT CONCENTRATIONS OF HYDROGEN PEROXIDE

DEDICATION

This dissertation is dedicated to my

grandparents

Tongqi Zhang and Yuying Yang

parents

Qian Zhang and Qinghui Yu

husband

Shuai Shao

CHAPTER 1

Introduction

Soil and groundwater contamination has been the result of improper disposal of biorefractory and toxic organic pollutants. The remediation of soil and groundwater is challenging, even after over twenty years of research on remediation technologies. Ex situ technologies, such as excavation of the contaminated source area and pump–and-treat remediation of groundwater, was used during 1980s and 1990s, but has only limited use today. Since ex situ technologies are not cost efficient, in situ processes are more commonly used today.

In situ bioremediation has been used extensively for the degradation of contaminants in soil and groundwater. Although bioremediation technology has been investigated for years, and many advances on this area have been established, it is often ineffective because bioremediation cannot degrade sorbed contaminants or dense non aqueous phase liquids (DNAPLs). In addition, bioremediation is a slow process and sometimes it is even slower than natural attenuation. Thermal methods are effective processes in remediation, but are often too expensive to use; furthermore, they leave a large carbon footprint. Numerous other in situ remediation technologies such as air sparging, permeable reactive barriers, soil vapor extraction and bioventing have also been applied to saturated or unsaturated zones. However, each of these has limitations including low reactivity with contaminants or mass transfer problems with DNAPLs and sorbed contaminants, resulting in difficulty of meeting clean up goals (Watts and Teel, 2006).

In situ chemical oxidation (ISCO) has become a popular technology over the past twenty years. ISCO processes deliver strong oxidants to the subsurface for the treatment of biorefractory organic pollutants. ISCO has four commonly used processes: catalyzed hydrogen peroxide propagations (CHP) (modified Fenton's reagent), ozone, permanganate and persulfate (Watts and Teel, 2006). CHP, permanganate, and persulfate are the primary oxidant sources. Reactive oxygen species, including hydroxyl radical (OH•) and superoxide radical (O_2•$^-$) are generated during ISCO processes. The sulfate radical (SO_4•$^-$) is only produced in the activated persulfate systems. Successful cleanup using ISCO process is based on the proper selection from the four processes mentioned above, because each of them has advantages and limitations.

Catalyzed H_2O_2 propagations (CHP) can degrade a wide range of organic contaminants, such as perchloroethylene (PCE), trichloroethylene (TCE), dichloroethylene (DCE), BTEX, chlorobenzene, phenols, MTBE, explosives, etc. It can effectively degrade sorbed contaminants and DNAPLs more rapidly than rate of desorption and dissolution (Watts and Teel, 2005; Smith et al., 2006; Corbin et al., 2007). Reactive species; such as hydroxyl radical, superoxide, hydroperoxide anion (HO_2^-) and perhydroxyl radical ($HO_2^{\bullet}$), are generated in the CHP reactions and are responsible for the degradation of organic contaminants. However, the high rate of hydrogen peroxide decomposition is a limitation of CHP. Hydrogen peroxide is unstable in the subsurface, making it difficult to distribute and place in contact with contaminants (Watts and Teel, 2006).

Permanganate is often the oxidant choice for remediation of PCE and TCE in groundwater. Permanganate is a selective oxidant, and reacts only with alkenes and benzene derivatives with

ring activating groups. The most common use of permanganate for ISCO is to degrade organic compounds such as PCE, TCE, DCE, vinyl chloride (VC), and phenols. The advantage of permanganate is its stability; it can last for months in the field. However, its reactivity is limiting and it is not able to degrade chlorinated alkanes or chlorinated aromatics.

Ozone based ISCO process is not commonly used as CHP or permanganate though it can potentially treat contaminated soils and groundwater. The mechanism of ozone oxidation is mainly through hydroxyl radical-mediated oxidation (Watts and Teel, 2006). Although it can degrade contaminants such as PCE, TCE, DCE, VC, BTEX, PAHs, phenols, high explosives, etc.; it has low stability that limits its use.

The oxidant source persulfate has become increasingly popular in the past few years. Persulfate is a strong oxidant that has been used for the destruction of a wide range of soil and groundwater contaminants. The high stability of persulfate in the subsurface provides the potential for its transport from the point of injection to contaminants in low permeability regions, which may broaden its use for ISCO. Persulfate is usually activated for ISCO applications. Activation of persulfate has been achieved most commonly through the use of chelated metals or base. The chelation of iron with EDTA maintains iron solubility at all pH regimes, providing effective activation of persulfate (Kwan and Chu, 2007). Hydroxyl radical, sulfate radical, superoxide, hydroperoxide anion are generated through the base activation of persulfate (Furman et al., 2010). Moreover, Ahmad et al. 2010 showed that persulfate can be activated by some types of iron and manganese minerals to generate hydroxyl radical. The generation of the reactive oxygen species provides the widespread reactivity of persulfate. However, persulfate is often too stable and

difficult to activate in the field. Since each of the four ISCO processes has limitations that may lead to an ineffective cleanup in contaminated soil and groundwater, a new oxidant source is needed for effective ISCO remediation.

Peroxymonosulfate chemistry

The triple salt $2KHSO_5 \cdot KHSO_4 \cdot K_2SO_4$ is the source of the strong oxidant peroxymonosulfate ($KHSO_5$) which may have advantages over other ISCO sources. Peroxymonosulfate is a peroxygen with one hydrogen and one sulfate moiety : $[\ H\text{-}O\text{-}O\text{-}SO_3]^-$, which suggests that it may be highly reactive like hydrogen peroxide, but may be longer lived in the subsurface and stable compared to hydrogen peroxide. Like other peroxygens, peroxymonosulfate needs activation when used as oxidant source for remediation. Peroxymonosulfate can be activated by transition metals such as cobalt or iron (II) to generate sulfate radicals (Anipsitakis and Dionysiou, 2004). Anipsitakis et al. (2006) demonstrated that generation of sulfate radical from cobalt-mediated peroxymonosulfate can degrade phenolic compounds. Most previous studies indicate that transition metal-activated peroxymonosulfate is able to generate sulfate radical for remediation. However, similar to activated persulfate, peroxymonosulfate may be activated by other methods such as base or subsurface minerals to generate reactive species for remediation. Moreover, activated peroxymonosulfate may not only generate sulfate radical, but also other radicals such as hydroxyl radical and superoxide. Peroxymonosulfate activation by other methods and the generation of reactive oxygen species has not been investigated to date.

Catalyzed hydrogen peroxide propagation (CHP) reactions

Catalyzed hydrogen peroxide propagation (CHP) reactions are based on soluble iron, iron chelates, or minerals catalyzing the decomposition of hydrogen peroxide to generate reactive species such as hydroxyl radical. It is a modification of Fenton's reagents which dilute hydrogen peroxide is added to an excess iron (II) solution to generate hydroxyl radical (Walling 1975):

$$Fe^{2+} + H_2O_2 \rightarrow Fe^{3+} + OH^{\bullet} + OH^{-} \quad (1)$$

When higher concentrations of hydrogen peroxide (0.6-3.6 M) are used in CHP reactions, hydroxyl radical is not the only reactive species generated. The hydroxyl radicals generated through initial Fenton's reaction promote the following propagation reactions to generate superoxide, perhydroxyl radical, and hydroperoxide anion (Watts and Teel, 2006):

$$OH^{\bullet} + H_2O_2 \rightarrow HO_2^{\bullet} + H_2O \quad (2)$$

$$HO_2^{\bullet} \rightarrow O_2^{\bullet -} + H^{+} \ (pKa = 4.8) \quad (3)$$

$$HO_2^{\bullet} + Fe^{2+} \rightarrow Fe^{3+} + HO_2^{-} \quad (4)$$

Perhydroxyl radical is a relatively weak oxidant, and hydroperoxide anion is a strong nucleophile. Hydroxyl radical is a strong oxidant that has high reaction rate with alkenes, aromatics or heterocyclic ring compounds as shown in Table 1. Due to its widespread reactivity, hydroxyl radical is considered the most important reactive species for contaminant degradation in ISCO.

Superoxide radical anion is a weak reductant and nucleophile in aqueous system. However, Smith et al. (2004) demonstrated that even dilute concentrations of solvents enhanced the

superoxide reactivity in water. Superoxide and hydroperoxide can degrade highly oxidized contaminants, such as TCE, PCE, hexachloroethane (HCA) and tetranitromethane. Smith et al. (2006) demonstrated that superoxide is responsible for the degradation of DNAPL contaminants PCE and TCE. Superoxide is becoming more important and has wide applications for contaminant degradation in ISCO.

Objectives

Peroxymonosulfate can be activated by transition metals such as cobalt or iron (II) to generate sulfate radicals (Anipsitakisand and Dionysiou, 2004). However, peroxymonosulfate activation by minerals has not been investigated to date. Like other peroxygens, activated peroxymonosulfate may generate sulfate radical, hydroxyl radical, and superoxide radical, but the generation of these reactive oxygen species in the peroxymonosulfate system has not been investigated. Hydrogen peroxide reacts rapidly with minerals in the subsurface (Teel et al., 2007) but persulfate is not (Ahmad et al., 2010). The purpose of this research was to 1) investigate the activation of peroxymonosulfate by typical subsurface minerals, 2) document the reactive oxygen species generated during its activation, 3) evaluate the activation of peroxymonosulfate by minerals in a natural soil.

Although Co (II), Ru (III), and Fe (II) catalyze peroxymonosulfate to generate mainly sulfate radical, more detailed study of peroxymonosulfate activation by transition metals and the resulting reactive oxygen species is necessary. Since a suite of reactive species is generated in CHP and iron (II) activated persulfate systems, such a range of reactants may also be generated in iron–activated peroxymonosulfate systems. The purpose of this study was to investigate the

generation of reactive species in iron (II) sulfate–, iron (III) sulfate– and iron (III) chelate–activated peroxymonosulfate systems using reaction-specific compounds, and to confirm the reactivity of activated peroxymonosulfate with two model groundwater contaminants.

As the chemical structures of PCE and TCE both exhibit the characteristics of degradation by oxidants and reductants, the mechanism of their degradation is more complex. Smith et al. (2009) showed that both hydroxyl radical and superoxide were involved in TCE and PCE DNAPL degradation, and the degradation may be due primarily to the activity of superoxide in CHP system. Since hydroxyl radical is short-lived and its reactivity is limited by diffusion-controlled rates in aqueous solutions, it may not be reactive with sorbed contaminants (Sedlak and Andren, 1994). However, the PCE and TCE degradation mechanism may be different when dissolved in water rather than in DNAPLs. Moreover, as the results from Smith et al. (2009) were based on a CHP system only with 2 M hydrogen peroxide, the PCE and TCE degradation under varying hydrogen peroxide concentrations in CHP requires elucidation. The purpose of this study was to investigate which reactive species were responsible for PCE and TCE degradation in aqueous phase and the reactive species generation in CHP systems with different concentrations of hydrogen peroxide.

References

Ahmad, M., Teel, A.L., Watts, R.J. 2010. Persulfate activation by subsurface minerals. J. Contam. Hydrol. 115(1-4): 34-45.

Anipsitakis, G.P., Dionysiou D.D., 2004. Radical generation by the interaction of transition metals with common oxidants. Environ. Sci. Technol. 38, 3705-3742.

Anipsitakis, G.P., Dionysiou D.D., 2006. Cobalt –mediated activation of peroxymonosulfate and sulfate radical attack on phenolic compounds. Implication of chloride ions. Environ. Sci. Technol. 40, 1000-1007.

Corbin, J.R., Teel, A.L., Allen-King, R.M., Watts, R.J., 2007. Reductive oxygen species responsible for the enhanced desorption of dodecane in modified Fenton's system. Water Environ. Res. 79(1), 37-42.

Furman, O., Teel, A.L., Watts, R.J. 2010. Mechanism of base activation of persulfate. Environ. Sci. Technol. 44(16), 6423-6428.

Kwan C.Y., Chu W., 2007. The role of organic ligands in ferrous-induced photochemical degradation of 2, 4-dichlorophenoxyacetic acid. Chemosphere. 67 (8), 1601–1611.

Sedlak, D. L. and Andren, A. W., 1994. The effect of sorption on the oxidation of polychlorinated biphenyls _PCBs_ by hydroxyl radical. Water Res.; 28(5):1207–1215.

Smith, B.A., Teel, A.L., Watts, R.J. 2004. Identification of the reactive oxygen species responsible for carbon tetrachloride degradation in modified Fenton's systems. Environ. Sci. Technol. 38, 5465-5469.

Smith, B.A., Teel, A.L., Watts, R.J. 2006. Mechanism for the destruction of carbon tetrachloride and chloroform DNAPLs by modified Fenton's reagent. J. Contam. Hydrol. 85(3-4), 229-246.

Smith, B.A., Teel, A.L., Watts, R.J., 2009. Destruction of trichloroethylene and perchloroethylene DNAPLs by catalyzed H_2O_2 propagations. J. Environ. Eng.; 135(7):536–543. Teel, A.J., Finn, D.D., Schmidt, J.T., Cutler, L.M., Watts, R.J., 2007. J. of Environ. Eng. 133(8), 853-858.

Walling, C. 1975. "Fenton's reagent revisited." Acc. Chem. Res., 8(1), 125-131.

Watts, R.J., Teel, A.L. 2005. Chemistry of modified Fenton's reagent (catalyzed H_2O_2 Propagation CHP) for in situ soil and groundwater remediation. J. Environ. Eng. 131(4), 612-622.

Watts, R.J., Teel, A.L. 2006. Treatment of contaminated soils and groundwater using ISCO. Pract. Period. Hazard. Tox. Radio Waste Manag. 10(1), 2-9.

Table 1 Reaction rates between hydroxyl radical and aliphatic and aromatic compounds (Watts and Teel, 2006)

Substrate	**$K_{OH^\cdot}$ ($M^{-1}s^{-1}$)**
methanol	9.7×10^8
ethanol	1.9×10^9
2-propanol	2.0×10^9
tert-butanol	5.2×10^8
1-hexanol	5.2×10^9
benzene	7.8×10^9
benzoic acid	4.0×10^9
anisole	6.0×10^9
nitrobenzene	3.9×10^9

CHAPTER 2

Activation of Peroxymonosulfate by Subsurface Minerals

Introduction

The remediation of soil and groundwater contaminated with toxic and biorefractory organic contaminants remains a challenge, even after over twenty years of research on remediation technologies. Although bioremediation has widespread application for degrading contaminants, it is often ineffective for the remediation of contaminated soils and groundwater. Thermal remediation methods are effective, but are often too expensive and leave a large carbon footprint. In situ chemical oxidation (ISCO) is a group of increasing technologies that have been developed over the past twenty years. Catalyzed hydrogen peroxide propagations (CHP), permanganate, and persulfate are the primary ISCO processes. Each of these ISCO processes has limitations. As the CHP oxidant source, hydrogen peroxide is unstable in the subsurface, making it difficult to distribute and place in contact with contaminants (Watts and Teel, 2006). Although permanganate is stable, it is reactive only with chlorinated alkenes, which limits its application (Watts and Teel, 2006). Activated persulfate is stable relative to hydrogen peroxide and reactive with a wide range of contaminants compared to permanganate; however, it is expensive and difficult to activate in the field. Thus, a new oxidant source is needed for effective ISCO remediation.

Peroxymonosulfate is an oxidant that may have advantages over other ISCO sources. Peroxymonosulfate is a peroxygen with one hydrogen and one sulfate moiety, which suggests that it may be highly reactive like hydrogen peroxide, but may be longer lived in the subsurface

compared to hydrogen peroxide. Peroxymonosulfate can be activated by transition metals such as cobalt or iron (II) to generate sulfate radicals (Anipsitakisand and Dionysiou, 2004). However, peroxymonosulfate activation by minerals has not been investigated to date. Like other peroxygens, activated peroxymonosulfate may generate sulfate radical, hydroxyl radical, and superoxide radical, but the generation of these reactive oxygen species in the peroxymonosulfate system has not been investigated. Hydrogen peroxide reacts rapidly with minerals in the subsurface (Teel et al., 2007) but persulfate is not (Ahmad et al., 2010). The purpose of this research was to 1) investigate the activation of peroxymonosulfate by typical subsurface minerals, 2) document the reactive oxygen species generated during its activation, 3) evaluate the activation of peroxymonosulfate by minerals in a natural soil.

Methodology

Chemicals

Potassium monopersulfate, anisole, and hexachloroethane (HCA) were obtained from Sigma Aldrich (St. Louis, MO). Sodium hydroxide, nitrobenzene, sodium bicarbonate, acetic acid, hydrochloric acid, potassium permanganate, *tert*-butanol, 2-propanol, and potato starch were purchased from J.T. Baker (Phillipsburg, NJ). N hexane, potassium iodide, and sodium thiosulfate were obtained from Fisher Scientific (Fair Lawn, NJ). Hydroxylamine hydrochloride was purchased from VWR (West Chester, PA). Barnstead NANOpure II Ultrapure system was used to purify double-deionized water to >18 MΩ·cm.

Minerals

Three iron minerals (hematite, goethite, ferrihydrite) and one manganese mineral (birnessite) were used to study the mineral activation of peroxymonosulfate. Hematite, goethite, and ferrihydrite were purchase from J.T. Baker, Strem Chemicals (Newburyport, MA) and Mach I (King of Prussia, PA), respectively. Birnessite was prepared by the dropwise of 250 ml of hydrochloric acid to 1L of 1M potassium permanganate solution while maintaining the solution temperature between 55 ℃ and 60 ℃ (Mckenzie, 1971). Particle size distribution was determined by the pipette method (Gee and Bauder, 1986) and surface area was determined by Brunauer, Emmett, and Teller (BET) analysis under liquid nitrogen on a Coulter SA 3100 (Carter et al., 1986). Particle size distribution and surface area for the four minerals are listed in Table 1.

Soils

A natural surface soil and its two soil fractions (the mineral fraction and the iron fraction) were investigated for the mineral activation of peroxymonosulfate in this study. The surface soil was sampled from the Palouse region of Washington State, USA. The soil was ground to pass through a 300 μm sieve. The soil mineral fraction was the product of removal its soil organic matter (SOM) by successive addition of 30% of hydrogen peroxide with heating up the slurry to 55 ℃ to 60 ℃ (Robinson, 1927). The soil iron fraction was the product of removing the manganese oxides from the mineral fraction, leaving only the iron mineral fraction using acidic hydroxylamine hydrochloride. Both of these two soil fractions were washed with deionized water to remove extractant residuals and to bring the soil pH to neutral. Each of the fractions was

then dried at 55 ℃ and ground to pass a 300 μm sieve before use. The characteristics of the soil and soil fractions are listed in Table 2.

Probe compounds

Nitrobenzene, hexachloroethane (HCA) and anisole were used as reaction-specific probe compounds to investigate the mineral activation of peroxymonosulfate. Nitrobenzene was used to detect hydroxyl radical but not sulfate radical ($k_{OH\cdot} = 3.9 \times 10^9$ $M^{-1}s^{-1}$; $k_{SO4\cdot-} = 8.4 \times 10^5$ $M^{-1}s^{-1}$) (Buxton et al., 1988). HCA was used as reductant superoxide probe because it is reactive with superoxide in the presence of cosolvents (Smith et al., 2004), but is not oxidized by hydroxyl radical or sulfate radical ($k_{OH\cdot} < 10^6$ $M^{-1}s^{-1}$; $k_{SO4\cdot-} < 10^6$ $M^{-1}s^{-1}$). Anisole was used to detect both hydroxyl radical and sulfate radical ($k_{OH\cdot} = 5.4 \times 10^9$ $M^{-1}s^{-1}$; $k_{SO4\cdot-} = 4.9 \times 10^9$ $M^{-1}s^{-1}$) (O'Neill et al., 1975; Buxton et al., 1988). The initial concentration of nitrobenzene and anisole was 1 mM and the initial concentration of HCA was 1 μM.

Hydroxyl radical and sulfate radical scavengers

2-Propanol was used to scavenge both hydroxyl radical and sulfate radical ($k_{OH\cdot} = 1.9 \times 10^9$ $M^{-1}s^{-1}$; $k_{SO4\cdot-} = 8.2 \times 10^7$ $M^{-1}s^{-1}$) (Buxton et al., 1988; Clifton and Huie, 1989), and *tert*-Butanol was used to scavenge hydroxyl radical only ($k_{OH\cdot} = 5.2 \times 10^{10}$ $M^{-1}s^{-1}$; $k_{SO4\cdot-} = 8.4 \times 10^5$ $M^{-1}s^{-1}$). The molar ratio between the probe scavenger and probe compounds was 1000:1.

Experimental procedures

All reactions were conducted in 20 ml borosilicate reactors with minerals or soils and a mixture of peroxymonosulfate and sodium hydroxide to produce a near neutral pH environment. The reactions were conducted at 20 ± 2 ℃ in triplicate. For reactions containing four of the minerals, the system consisted of 0.1 M peroxymonosulfate and sodium hydroxide with 1:1 molar ratio, 2 g hematite or goethite, 0.25 g ferrihydrite, or 1 g birnessite along with one of the probe compounds. The total volume in each reaction was 5 ml for nitrobenzene system or anisole and 20 ml for HCA system. For reactions containing the three soils, reactors consisted of 0.1 M peroxymonosulfate and sodium hydroxide with 1:1 molar ratio, 5 g of soil and the probe compounds. The total volume of this system was 10 ml for nitrobenzene or anisole and 20 ml for HCA. Reaction vials were extracted with hexane at selected time points, and the extractants were analyzed by gas chromatograph. Control experiments were conducted using deionized water in place of peroxymonosulfate. Positive control experiments were conducted with peroxymonosulfate without minerals or soils. Peroxymonosulfate concentrations and pH of the systems in the presence of four minerals were monitored in triplicate as reactions proceeded.

Analysis

Peroxymonosulfate concentrations were measured by iodometric titration using 0.01N sodium thiosulfate (Kolthoff and Stenger, 1947). System pH was measured using a Fisher Accumet 900 pH meter. A Hewlett-Packard 5890 gas chromatography (GC) with flame ionization detector (FID) fitted with a 15 m × 0.53 mm SPB-5 capillary column was used to analyze nitrobenzene and anisole extracts. For nitrobenzene analysis, the initial oven temperature and final temperature were 60 ℃ and 180 ℃ respectively; the program rate was 30 ℃/min, the injector temperature

was 200 ℃, and the detector temperature was 250 ℃. For anisole analysis, the initial oven temperature and final temperature were 50 ℃ and 180 ℃ with a program rate of 30 ℃/min. The injector temperature was 150 ℃, and the detector temperature was 180 ℃. HCA extracts were analyzed using a Hewlett-Packard 5890 GC equipped with 30 m × 0.53 mm Equity-5 capillary column and electron capture detector (ECD). The initial oven temperature and final temperature were 100 ℃ and 160 ℃ with a program rate of 50 ℃ /min; the injector and detector temperatures were 220 ℃ and 270 ℃, respectively.

Results and Discussion

Peroxymonosulfate decomposition in the presence of minerals

Peroxymonosulfate activation was studied in the presence of one manganese oxide mineral and three iron oxide minerals. Peroxymonosulfate decomposition in the presence of the four minerals over 7 d is shown in Figure 1. Although ferrihydrite promoted the most rapid peroxymonosulfate decomposition (84%), all of the decomposition occurred within the first 4 hr. For the other three minerals, birnessite promoted 78% of peroxymonosulfate decomposition, followed by hematite (69%) and goethite (67%). Peroxymonosulfate decomposition in the presence of the minerals varied significantly from the positive control (α=0.05). The decomposition rates of peroxymonosulfate are likely proportional to surface area of the minerals (Khan and Watts, 1996; Valentine and Wang, 1998; Kwan and Voelker, 2003). Data from Figure 1 were calculated to fit the first order kinetics and the surface areas of the four minerals used to normalize the observed peroxymonosulfate decomposition rate constants. As shown in Table 3, the normalized rate constant for peroxymonosulfate decomposition catalyzed by birnessite is the greatest compared

to the other three minerals. Similar results were found in previous studies; birnessite promoted rapid decomposition of hydrogen peroxide, and goethite catalyzed hydrogen peroxide decomposition was found to be much slower (Watts and Teel, 2005). In addition, Ahmad et al. (2010) found that, in the study of mineral-activated persulfate, the greatest persulfate decomposition rate occurred in birnessite systems. Normalized rate constant of peroxymonosulfate decomposition for goethite is lower than for hematite. The same results were found for the goethite and hematite-activated persulfate systems studied by Ahmad et al. (2010). Although ferrihydrite has the highest surface area, its normalized rate constant is lower than the other minerals, which may be due to surface scavenging of reactive species (Ahmad et al., 2010). This may be the same mechanism in the ferrihydrite-activated peroxymonosulfate system. In summary, the decomposition of peroxymonosulfate in the presence of minerals was proportional to surface areas (for birnessite, hematite and goethite), but was also likely a function of the catalytic nature of the mineral surface (for ferrihydrite). Because the surface scavenging rate in ferrihydrite-activated hydrogen peroxide system was larger than the hydrogen peroxide decomposition rate, lower oxidant decomposition occurred (Huang et al., 2001, Miller and Valentine, 1999).

pH changes in the mineral- activated peroxymonosulfate systems

Changes in pH in mineral-activated peroxymonosulfate systems over 7 d are shown in Figure 2. In all of the peroxymonosulfate systems, the pH dropped rapidly from neutral pH to pH 3-4 over the first 12 hr, and remained stable over the next 6 d. The pH drop is likely due to the formation of sulfuric acid from the decomposition of peroxymonosulfate. However, the pH drop does not

correlate entirely with the decomposition of peroxymonosulfate (Figure 1). The differences in pH may be due to the variation in the acidity or buffering capacities of the four minerals.

Generation of reactive oxygen species in mineral-activated peroxymonosulfate systems

Nitrobenzene was used as probe compound to investigate hydroxyl radical generation in mineral-activated peroxymonosulfate systems. The degradation of nitrobenzene in the four mineral-activated peroxymonosulfate systems over 7 d is shown in Figure 3. The greatest nitrobenzene degradation was 87% in the presence of hematite, followed by 42% goethite-catalyzed system. For birnessite- and ferrihydrite-activated peroxymonosulfate systems, nitrobenzene degradation was 15% and 20% respectively, which was lower than nitrobenzene degradation in the positive control system (21%). The results of Figure 3 demonstrate that hematite promoted the greatest generation of hydroxyl radical with nominal hydroxyl radical generation in the hematite system. However, birnessite and ferrihydrite appeared to scavenge hydroxyl radical. Miller and Valentine (1995) reported that iron oxides can quench the generation of hydroxyl radical. The low oxidant generation rate in the ferrihydrite and birnessite systems may be due to the scavenging of hydroxyl radical (Ahmad et al., 2010). Data from Figure 3 were calculated to fit the first order kinetics and the surface areas of four minerals were used to normalize the observed nitrobenzene degradation rate constants, which are shown in Table 4. The normalized rate constants correlated with the results in Figure 3; hematite still promoted the highest rate of oxidant generations compared to the other three minerals.

Generation of reductant species in mineral-activated peroxymonosulfate systems

Hexachloroethane (HCA) was used as probe compound to investigate the reductant superoxide generation in mineral-activated peroxymonosulfate systems. The degradation of HCA in the four mineral-activated peroxymonosulfate systems, as well as in control and positive control systems, are shown in Figure 4. The greatest HCA degradation was 27% in the presence of goethite, followed by 11% degradation with ferrihydrite. The HCA degradation rate in hematite and birnessite activated peroxymonosulfate systems were significant lower at 9% and 0%, respectively. HCA degradation rates in ferrihydrite, hematite and birnessite systems were not significantly different from the positive control (α=0.05), and in the birnessite system, the degradation of HCA was lower than in the positive control. The results of Figure 4 demonstrate that neither iron minerals nor manganese mineral promoted the generation of reductants or superoxide in peroxymonosulfate systems.

Sulfate and hydroxyl radical activities of hematite- activated peroxymonosulfate system

Because the greatest oxidant generation was observed in the presence of hematite (Figure 3), the relative activities of sulfate radical and hydroxyl radical were further investigated in the hematite-activated peroxymonosulfate system. Anisole was used as a probe compound to investigate the activity of the two reactive oxygen species because it reacts rapidly with both sulfate radical and hydroxyl radical. The hydroxyl radical scavenger *tert*-butanol and the hydroxyl radical + sulfate radical scavenger 2-propanol were added to separate reactors to identify the radicals generated. As shown in Figure 5, 83% of anisole loss was observed in the absence of scavengers, followed by 51% in the presence of *tert*-butanol. However, there was 7% loss of anisole when 2-propanol was used, which is close to anisole loss in the control system

(4%). These results demonstrate that the hematite-catalyzed peroxymonosulfate system generated both of the hydroxyl and sulfate radicals; and both radicals were dominant oxidants in the hematite-activated peroxymonosulfate system.

Sulfate and hydroxyl radical activities of ferrihydrite- and birnessite-activated peroxymonosulfate systems

Although ferrihydrite and birnessite did not effectively activate peroxymonosulfate to degrade nitrobenzene, these catalysts may promote the generation of sulfate radical. Therefore, ferrihydrite- and birnessite-activated peroxymonosulfate systems were investigated using the sulfate + hydroxyl radical probe anisole with and without scavengers. Anisole degradation in these two systems is shown in Figure 6 (a) and (b). In the ferrihydrite system, 54% of anisole loss was observed in the absence of scavengers within 10 min. In the presence of excess *tert*-butanol, 32% anisole degradation occurred and 2% anisole degradation was found when 2-propanol was added to the system. The anisole loss remained constant for the remaining 80 min of the reactions, which may be due to the rapid peroxymonosulfate decomposition in the presence of ferrihydrite (Figure 1), which resulted in lack of the oxidant. Nonetheless, the anisole loss within the first 10 min was the result of the oxidation by both hydroxyl and sulfate radicals. In the birnessite system, there was 67% of anisole loss without scavengers, and 47% loss and 21% loss in the presence of *tert*-butanol and 2-propanol, respectively. These results indicated that both of the hydroxyl and sulfate radicals were generated in the birnessite system; however, the contribution of sulfate radical to the anisole loss (46%) was greater than that of hydroxyl radical (20%).

Sulfate and hydroxyl radical activities of goethite-activated peroxymonosulfate system

The effect of scavenging to isolate the relative effects of sulfate radical vs. hydroxyl radical, quantified using the probe compound anisole in goethite-activated peroxymonosulfate systems, is shown in Figure 7. Anisole loss (99%) without scavenging showed significant oxidant production over 36 hr. However, scavenging of sulfate and hydroxyl radicals also resulted in changes in the rate of anisole oxidation (Figure 7). These results suggest that both sulfate and hydroxyl radical are not the dominant oxidants in goethite-activated peroxymonosulfate system. Kitajima et al. (1978) documented that minerals can assume a positive charge in the presence of hydrogen peroxide. A similar mechanism may be occurring in the peroxymonosulfate system; i.e., a positive charge may also develop on the goethite surface as shown below:

$$\text{Goethite} + \text{peroxymonosulfate} \text{ ----- } \text{Goethite}^{+} + \text{peroxymonosulfate}^{-} \quad (1)$$

The oxidized goethite surface may be responsible for anisole oxidation by a pathway other than sulfate and hydroxyl radical.

Generation of reactive oxygen species in peroxymonosulfate systems containing soil and soil fractions

A natural soil, which was sampled from the Palouse region of Washington State, was used to further investigate mineral activation of peroxymonosulfate. Oxidant generation rates in peroxymonosulfate systems containing total soil, and two soil mineral fractions were investigated. Degradation of hydroxyl radical probe nitrobenzene degradation in the presence of three soil fractions is shown in Figure 8. Nitrobenzene degradation in the total soil-activated

peroxymonosulfate system was not significantly different from the positive control (α=0.05); however, in the peroxymonosulfate systems containing only the mineral fraction and iron fraction, the degradation was 95% within 72 hr and 99% within 3 hr, which were significantly different from the positive control (α=0.05). Similar results were found in a persulfate system at both low and high pH regimes with the same soil and soil fractions (Ahmad et al., 2010). The low reactivity in the total soil may be due to the scavenging of hydroxyl radical by soil organic matter (SOM) (Bissey et al., 2006; Liang et al., 2008a), or scavenging by inorganic constituents of the soil (Miller and Valentine, 1995). Although the total soil did not promote net activation of peroxymonosulfate to generate hydroxyl radical, the other two soil fractions promoted the effective hydroxyl radical generation. The soil mineral fraction was prepared by removal of the SOM from the total soil leaving only the iron and manganese minerals in the soil. Peroxymonosulfate was activated by these minerals (Figure 3) to generate hydroxyl radical, and hydroxyl radical was not scavenged by SOM and responsible for the degradation of nitrobenzene. The soil iron fraction was prepared by removal of manganese oxide from soil mineral fraction, leaving only the iron minerals in the soil. Iron minerals such as hematite and goethite catalyze peroxymonosulfate to generate hydroxyl radical; however, birnessite did not promote the generation of oxidants, and even inhibited oxidant production (Figure 3). This may be the reason why soil iron fraction can activate peroxymonosulfate to generate hydroxyl radical. These results correspond to the normalized nitrobenzene degradation rate constant trends shown in Table 5.

Generation of reductant species in peroxymonosulfate systems containing soil and soil fractions

Reductant generation rates in the peroxymonosulfate systems containing total soil and two soil fractions were studied by quantifying the degradation of reductant superoxide probe HCA. The HCA degradation in the presence of the Palouse total soil and two fractions is shown in Figure 9. After 7 d, the degradation of HCA in the two soil mineral fractions were less than 20% and not significantly different from the positive control (α=0.05), indicating that neither iron mineral nor manganese mineral can activate peroxymonosulfate to generate reductants. However, the degradation of HCA in the total soil-peroxymonosulfate system was 86% after 7 days. Reductants can be generated through the reactions of persulfate with phenolic compounds in the presence of SOM (Ahmad et al; 2013). Similar reactions may occur in the peroxymonosulfate system with total soil, which also contained the SOM. The results correspond to the normalized HCA degradation rate constant trends shown in Table 6.

Sulfate and hydroxyl radical activities of soil-activated peroxymonosulfate systems

Because oxidants were generated in the soil activated peroxymonosulfate systems, the relative activities of sulfate radical and hydroxyl radical generation was investigated further. Anisole was used as a probe compound to investigate the activity of the two reactive oxygen species. The hydroxyl and sulfate radical scavenger 2-propanol and the hydroxyl radical scavenger *tert*-butanol were added to the systems in access to identify the radicals that were generated. In the whole soil-activated peroxymonosulfate system (Figure 10), 54% of anisole loss was observed in the absence of scavengers in 36 hr, followed by 24% in the presence of *tert*-butanol and 10% loss of anisole when 2-propanol was used, which is close to anisole loss in the control system (4%). The low anisole degradation rate in total soil-activated peroxymonosulfate system may be due to

the scavenging of hydroxyl radical by SOM. In the mineral fraction activated peroxymonosulfate system (Figure 11), 82% of anisole loss was observed in the absence of the scavengers in 6 hr, followed by 68% in the presence of *tert*-butanol and 20% loss of anisole when 2-propanol was used. In the iron fraction activated peroxymonosulfate system in (Figure 12), > 99% of anisole loss was observed in the absence of scavengers in 2 hr, followed by 50% loss in the presence of *tert*-butanol and 7% loss of anisole when 2-propanol was used. These results demonstrate that the greatest amount of anisole degradation was achieved in the soil iron fraction-catalyzed peroxymonosulfate system. The two soil fractions-catalyzed peroxymonosulfate systems generated both of hydroxyl radical and sulfate radical. The hydroxyl radical and the sulfate radical were documented in both of the soil mineral and iron fraction-activated peroxymonosulfate systems.

Conclusion

The potential for peroxymonosulfate as an ISCO oxidant source was investigated using three iron oxides (hematite, goethite, ferrihydrite) and one manganese oxide (birnessite) as potential activators. In the mineral-activated peroxymonosulfate systems, the decomposition of peroxymonosulfate was significantly different from the positive control system containing peroxymonosulfate only. Ferrihydrite, which has the highest surface area among the four minerals studied, promoted the greatest peroxymonosulfate decomposition. A positive control system containing peroxymonosulfate and sodium hydroxide without minerals did not generate hydroxyl radical. Hematite-activated peroxymonosulfate provided the greatest generation of oxidants, followed by goethite. However, ferrihydrite and birnessite appeared to inhibit the

generation of hydroxyl radical. The activity of sulfate radical and hydroxyl radical generated in mineral-activated peroxymonosulfate reactions was further investigated using the probe compound anisole in conjunction with sulfate radical and hydroxyl radical scavengers. The oxidation activity in all mineral-activated peroxymonosulfate systems was the result of both sulfate radical and hydroxyl radical activities.

A natural soil and two of its fractions (one with SOM removed; the second with SOM and manganese oxide removed) were also used to study peroxymonosulfate activation. The natural soil minerals in the whole soil were not effective in catalyzing peroxymonosulfate to generate oxidants. However, SOM in the whole soil was highly active in promoting the generation of reductants. The two soil fractions were found to effectively generate oxidants in peroxymonosulfate systems. The oxidation activity in peroxymonosulfate systems catalyzed by the two soil fractions was the result of both sulfate radical and hydroxyl radical activities.

The results of this research demonstrate that peroxymonosulfate can be activated by subsurface minerals to generate reactive oxygen species-hydroxyl radical and sulfate radical; furthermore, SOM can promote the generation of reductants in peroxymonosulfate ISCO applications.

References

Ahmad, M., Teel, A.L., Watts, R.J., 2010. Persulfate activation by subsurface minerals. J. Contam. Hydrol. 115, 34-45.

Ahmad, M., Teel, A.L., Watts, R.J., 2013. Mechanism of Persulfate Activation by Phenoxides. Environ.
Sci.Technol. (Accepted).

Anipsitakisand, G.P., Dionysiou D.D., 2004. Radical generation by the interaction of transition metals with common oxidants. Environ. Sci. Technol. 38, 3705-3742.

Bissey, L.L., Smith, J.L., Watts, R.J., 2006. Soil organic matter-hydrogen peroxide dynamics in the treatment of contaminated soils and groundwater using catalyzed H_2O_2 propagations (modified Fenton's reagent). Water Res. 40 (13), 2477-2484.

Buxton, G.V., Greenstock, CL., Helman, W.P., Ross, A.B., 1988. Critical review of rate constants for reactions of hydrated electrons, hydrogen atoms and hydroxyl radicals in aqueous solution. J. Phys. Chem. Ref. Data 17, 513-531.

Carter, D.L., Mortland, M.M., Kemper, W.D., 1986. Specific surface. In: Klute, A. (Ed.), Methods of Soil Analysis. Part 1: Physical and Mineralogical Methods. American Society of Agronomy and Soil Science Society of America, Madison, WI, pp. 413–423.

Clifton, C.L., and Huie, R.E., 1989. Rate constants for hydrogen abstraction reactions of the sulfate radical, Alcohols. Int. J. Chem. Kinet. 21(8), 677-687.

Gee, G.W., Bauder, J.W., 1986. Methods of soil analysis. In: Klute, A. (Ed.), Part 1: Physical and Mineralogical Methods. American Society of Agronomy and Soil Science Society of America, Madison, WI, pp. 383–399.

Kitajima, N., Fukuzumi, S., Ono, Y., 1978. Formation of superoxide ion during the decomposition of hydrogen peroxide on supported metal oxides. J. Phys. Chem., 82, 1505.

Kolthoff, I.M., Stenger, V.A., 1947. Volumetric analysis, second ed. Vol. I: Theoretical fundamentals. Vol II: Titration Methods: Acid-Base, Precipitation and Complex Reactions. Interscience Publishers Inc., New York.

Liang, C.J., Huang, C.F., Yan-Jyun Chen, Y.J., 2008a. Potential for activated persulfate degradation of BTEX contamination.Water Res. 42, 4091–4100.

McKenzie, R.M., 1971. The synthesis of birnessite, cryptomelane, and some other oxides and hydroxides of manganese. Mineralog. Mag. 38, 493-502.

Miller, C.M., Valentine, R.L., 1995. Hydrogen peroxide decomposition and quinolone degradation in the presence of aquifer material. Water Res. 29, 2353–2359.

O'Neill, P., Steenken, S., and Schulte-Frohinde, D., 1975. Formation of radical cations of methoxylated benzenes by reaction with OH radicals, Ti^{2+}, Ag^{2+}, sulfate radical in aqueous solution. An optical and conductometric pulse radioanalysis and in situ radiolysis electron spin resonance study. J. Phys. Chem. 79(25), 2773-2779.

Sethna, S.M., 1951. The Elbs persulfate oxidation. Chem. Rev. 49 (1), 91–101.

Teel, A.J., Finn, D.D., Schmidt, J.T., Cutler, L.M., Watts, R.J., 2007. J. of Environ. Eng. 133(8), 853-858.

Watts, R.J., Teel, A.L., 2005. Chemistry of modified Fenton's reagent (catalyzed H_2O_2 propagation-CHP) for in situ soil and groundwater remediation. J. Environ. Eng. 131(4), 612-622.

Watts, R.J., Teel, A.L., 2006. Treatment of contaminated soils and groundwater using ISCO. Pract. Period. Hazard. Toxic Radioact. Waste Manage. 10(1), 2-9.

Table 1 Particle size distribution (PSD) and surface area of minerals

PSD (mm)	Goethite (%)	Hematite (%)	Ferrihydrite (%)	Birnessite (%)
2.00-0.25	0.12	2.40	0	2.40
0.05-0.002	8.24	89.10	0	5.60
<0.002	91.64	8.50	100	92.00
Surface Area (m^2/g)	37	28	233	44

Table 2 Characteristics of the total soil and soil fractions

	Total Soil	Soil mineral fraction	Soil iron fraction
Organic carbon (%)	1.617	0.083	0.050
Amorphous oxides			
Fe (mg/kg)	4780	4190	3660
Mn (mg/kg)	610	420	170
Crystalline oxides			
Fe (mg/kg)	3900	2700	2700
Mn (mg/kg)	260	210	90

Cation exchange capacity (cmol(+)/kg)	19	12	9
Surface area (m^2/g)	23.5	24	19
Particle size distribution			
Sand (%)	7.77	9.23	7.83
Clay (%)	69.15	70.67	76.7
Silt (%)	23.08	20.10	15.46
Texture	Silt loam	Silt loam	Silt loam

Table 3 Peroxymonosulfate decomposition rate constants in mineral-activated peroxymonosulfate systems

	Iron minerals			Manganese mineral
	Hematite	Goethite	Ferrihydrite	Birnessite
Mass used (g)	2	2	0.25	1
Surface area(m^2/g)	28	37	233	44
k_{obs}	0.147 ± 0.024	0.150 ± 0.019	0.082 ± 0.071	0.268 ± 0.058
k_{norm}	$2.625 \pm 0.429 \times 10^{-3}$	$2.027 \pm 0.257 \times 10^{-3}$	$1.408 \pm 1.219 \times 10^{-3}$	$6.091 \pm 1.318 \times 10^{-3}$

95% confidence intervals shown.

kobs = observed 1st order rate constant (d^{-1}) calculated from the data of Fig. 1; knorm=kobs / ((surface area)(mass)), (d^{-1}/m^2).

Table 4 Nitrobenzene degradation rate constants in mineral-activated peroxymonosulfate systems

	Iron minerals			Manganese mineral
	Hematite	Goethite	Ferrihydrite	Birnessite
Mass used (g)	2	2	0.25	1
Surface area(m^2/g)	28	37	233	44
k_{obs}	0.266 ± 0.023	0.074 ± 0.012	0.035 ± 0.024	0.018 ± 0.010
k_{norm}	$4.750 \pm 0.410 \times 10^{-3}$	$1.000 \pm 0.162 \times 10^{-3}$	$0.601 \pm 0.412 \times 10^{-3}$	$0.409 \pm 0.227 \times 10^{-3}$

95% confidence intervals shown.

kobs = observed 1st order rate constant (d^{-1}) calculated from the data of Fig. 1; knorm=kobs / ((surface area)(mass)), (d^{-1}/m^2).

Table 5 Nitrobenzene degradation rate constants in natural soil-activated peroxymonosulfate systems

	Soil KB1	Mineral fraction	Iron fraction
Mass used (g)	5	5	5
Surface area(m^2/g)	23.5	24	19
k_{obs}	0.00493 ± 0.001	0.03784 ± 0.009	1.17442 ± 0.124
k_{norm}	$0.042 \pm 0.009 \times 10^{-3}$	$0.315 \pm 0.075 \times 10^{-3}$	$12.362 \pm 1.305 \times 10^{-3}$

95% confidence intervals shown.

kobs = observed 1st order rate constant (d^{-1}) calculated from the data of Fig. 1; knorm=kobs / ((surface area)(mass)), (d^{-1}/m^2).

Table 6 HCA degradation rate constants in natural soil-activated peroxymonosulfate systems

	Soil KB1	Mineral fraction	Iron fraction
Mass used (g)	5	5	5
Surface area(m^2/g)	23.5	24	19
k_{obs}	0.2738 ± 0.0315	0.0251 ± 0.0240	0.0165 ± 0.0103
k_{norm}	$11.651 \pm 1.340 \times 10^{-3}$	$1.046 \pm 1.000 \times 10^{-3}$	$0.868 \pm 0.542 \times 10^{-3}$

95% confidence intervals shown.

kobs = observed 1st order rate constant (d^{-1}) calculated from the data of Fig. 1; knorm=kobs / ((surface area)(mass)), (d^{-1}/m^2).

List of Figures

Figure 1

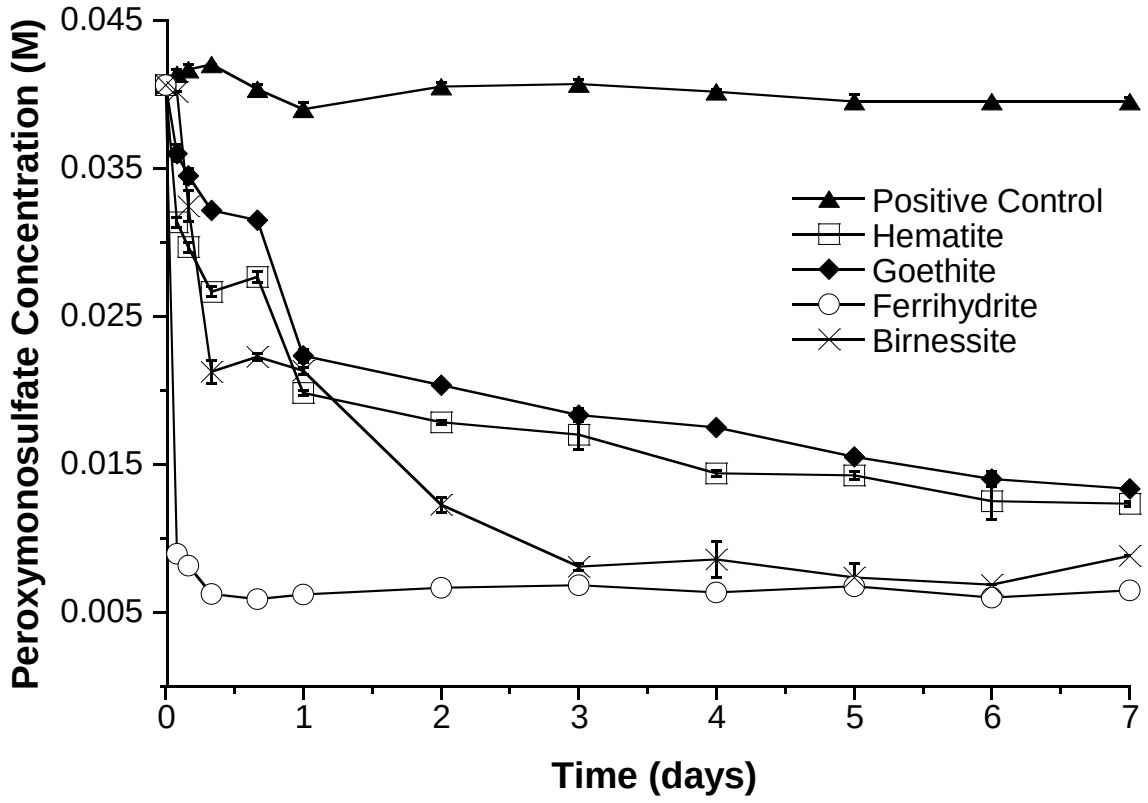
Peroxymonosulfate Concentration (M)
0.045
0.035
0.025
0.015
0.005
0
1
2
3
4
5
6
7
Time (days)
Positive Control
Hematite
Goethite
Ferrihydrite
Birnessite

Figure 2

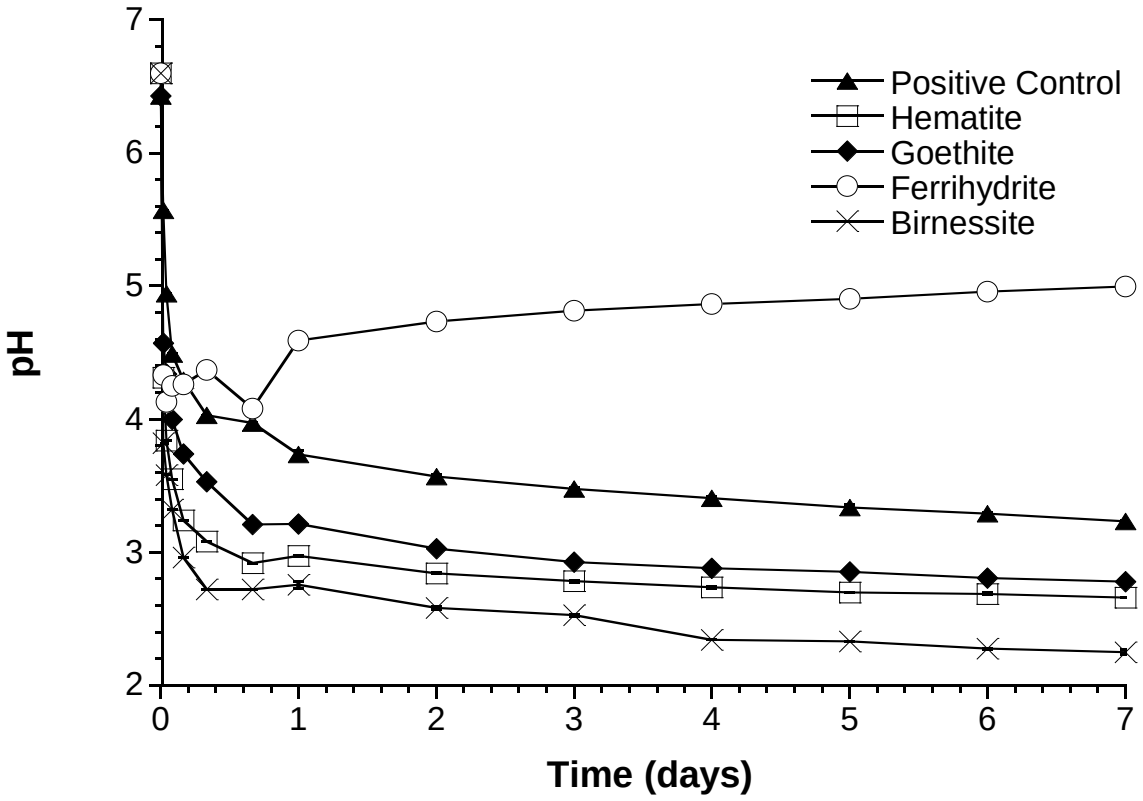
Positive Control
Hematite
Goethite
Ferrihydrite
Birnessite
pH
Time (days)
7
6
5
4
3
2
0
1
2
3
4
5
6
7

Figure 3

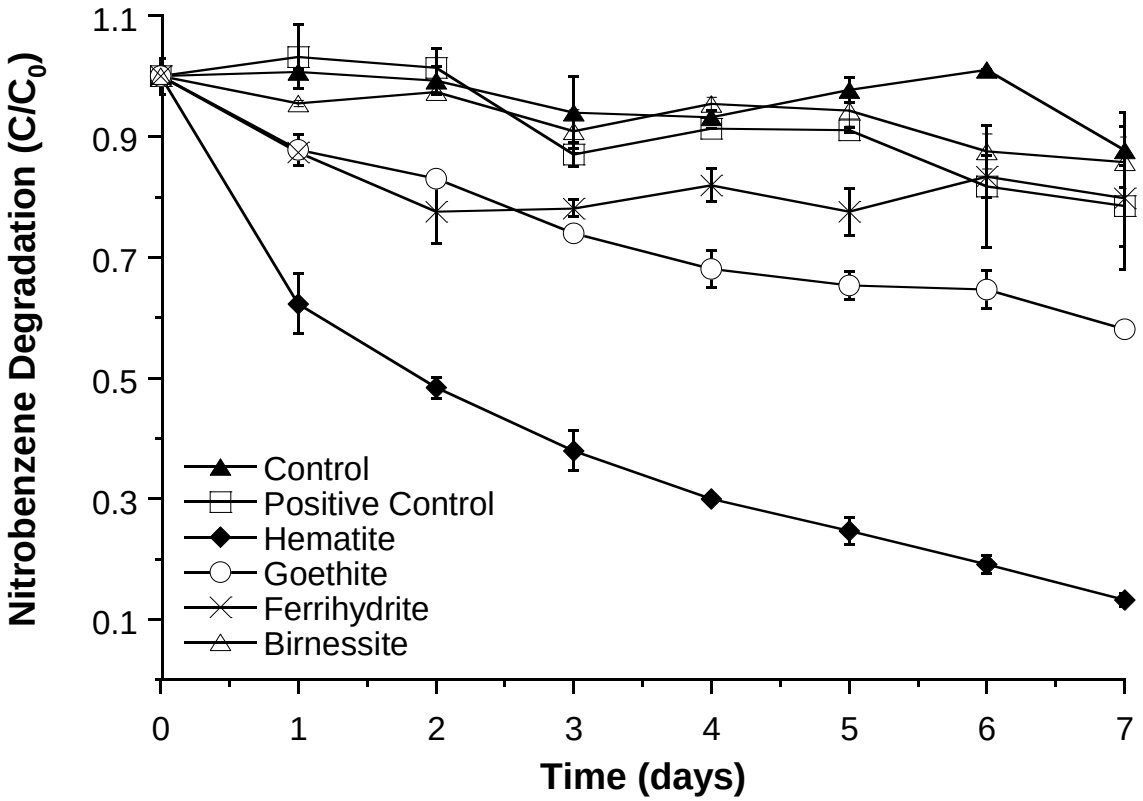
Nitrobenzene Degradation (C/C0)
1.1
0.9
0.7
0.5
0.3
0.1
0
1
2
3
4
5
6
7
Time (days)
Control
Positive Control
Hematite
Goethite
Ferrihydrite
Birnessite

Figure 4

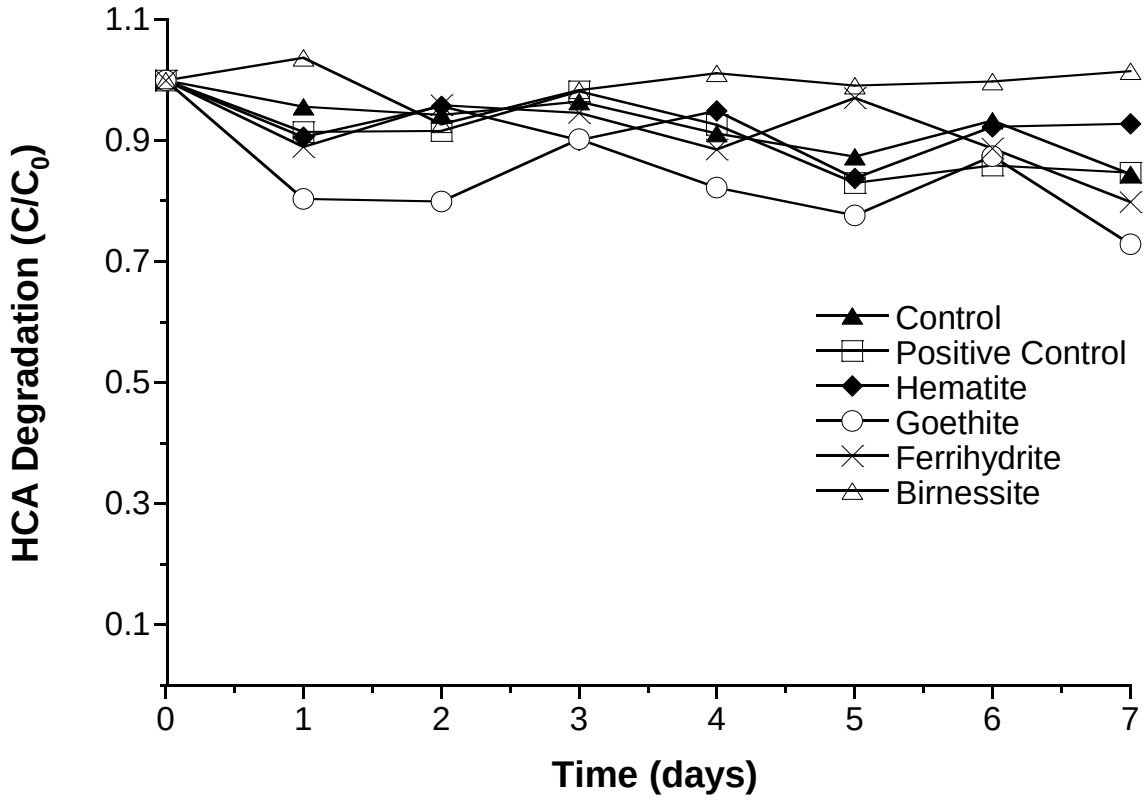
1.1
0.9
0.7
0.5
0.3
0.1
HCA Degradation (C/C0)
0
1
2
3
4
5
6
7
Time (days)
Control
Positive Control
Hematite
Goethite
Ferrihydrite
Birnessite

Figure 5

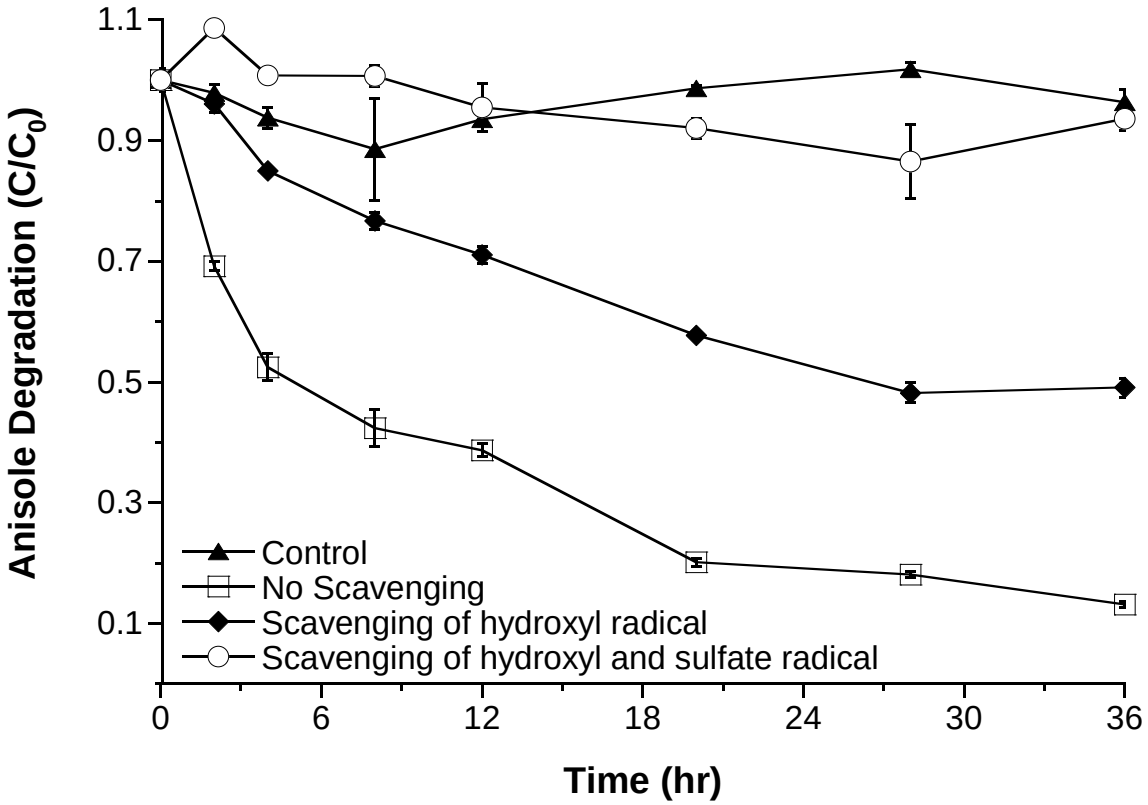
Anisole Degradation (C/C0)
1.1
0.9
0.7
0.5
0.3
0.1
0
6
12
18
24
30
36
Time (hr)
Control
No Scavenging
Scavenging of hydroxyl radical
Scavenging of hydroxyl and sulfate radical

Figure 6 (a)

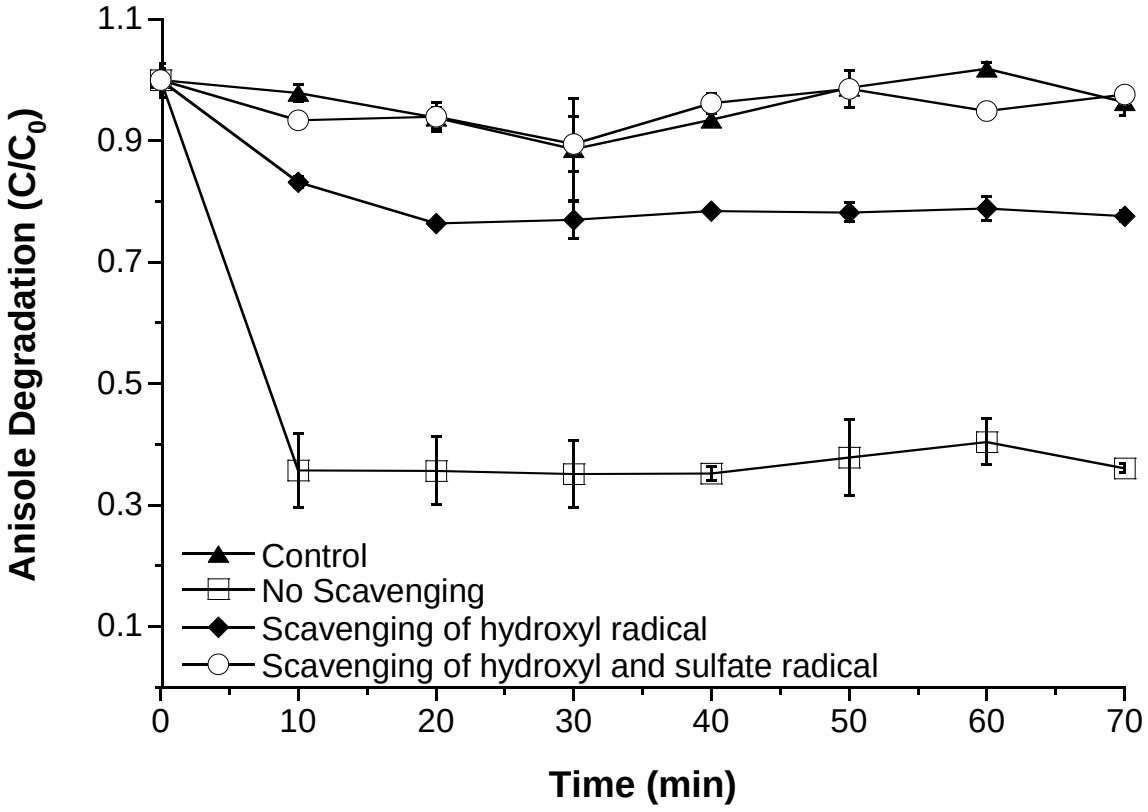
Anisole Degradation (C/C0)
1.1
0.9
0.7
0.5
0.3
0.1
0
10
20
30
40
50
60
70
Time (min)
Control
No Scavenging
Scavenging of hydroxyl radical
Scavenging of hydroxyl and sulfate radical

Figure 6 (b)

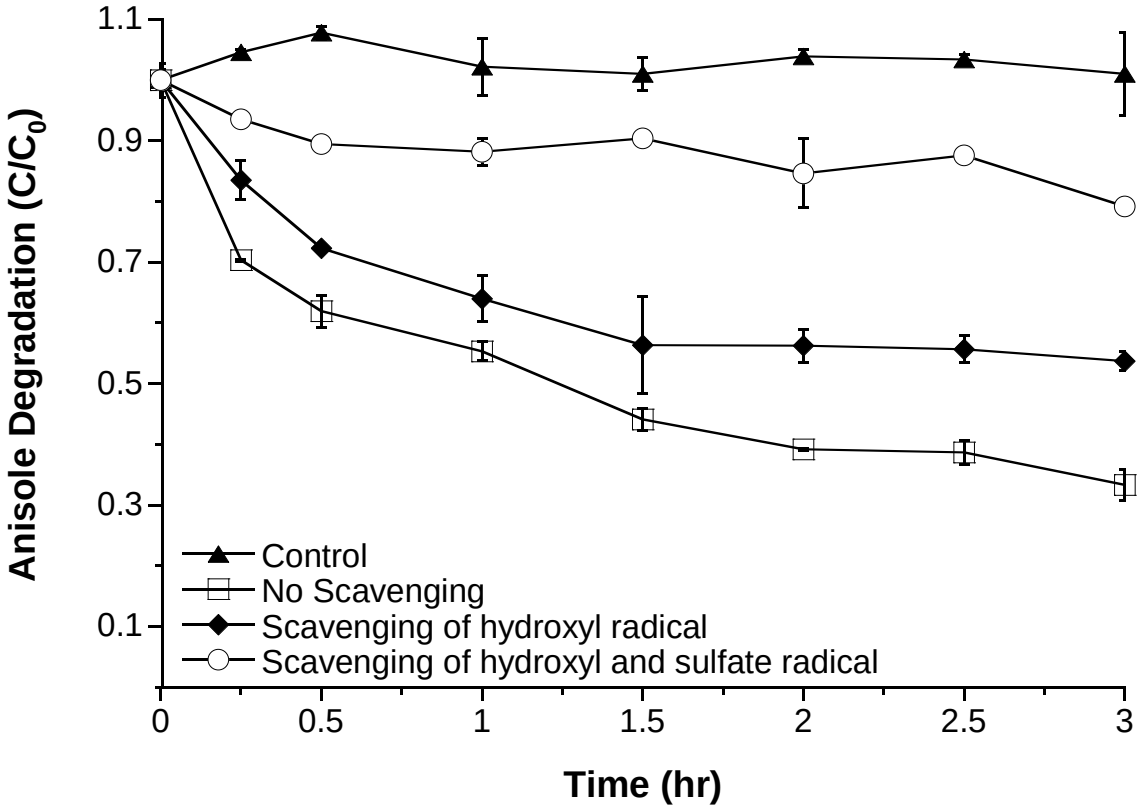
Anisole Degradation (C/C0)
1.1
0.9
0.7
0.5
0.3
0.1
0
0.5
1
1.5
2
2.5
3
Time (hr)
Control
No Scavenging
Scavenging of hydroxyl radical
Scavenging of hydroxyl and sulfate radical

Figure 7

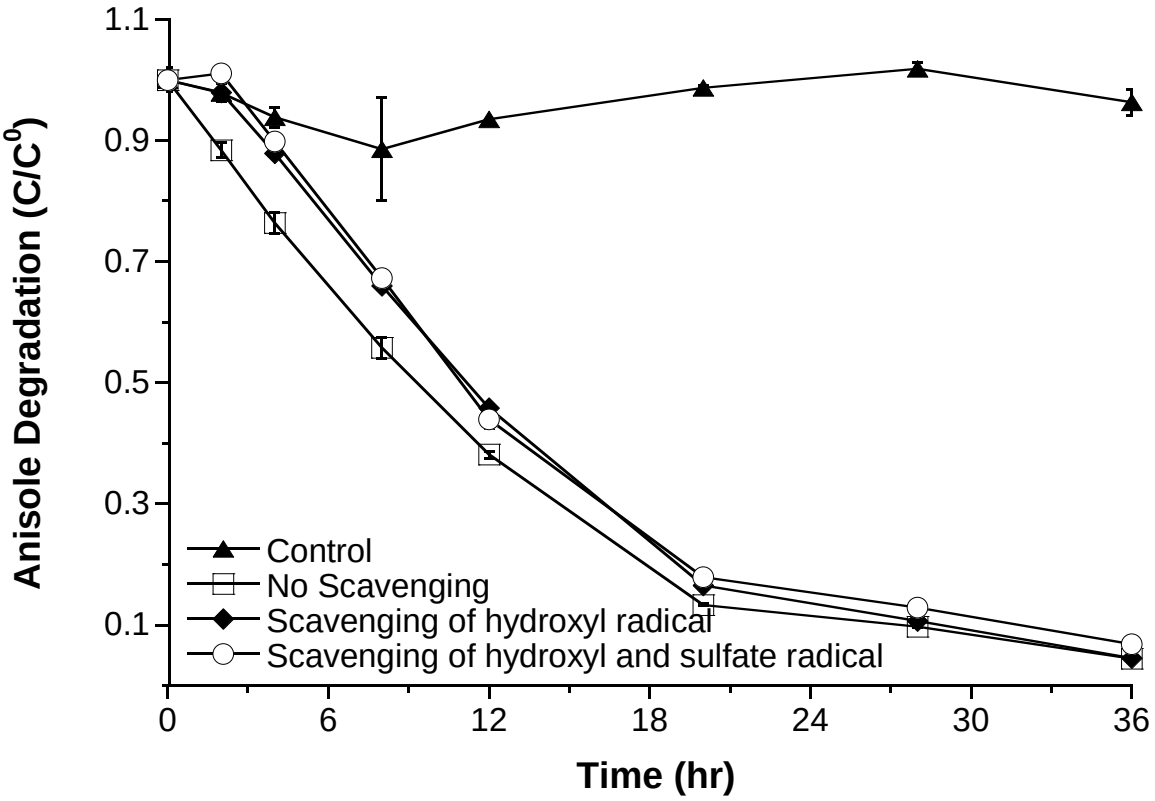
Anisole Degradation (C/C^0)
1.1
0.9
0.7
0.5
0.3
0.1
0
6
12
18
24
30
36
Time (hr)
Control
No Scavenging
Scavenging of hydroxyl radical
Scavenging of hydroxyl and sulfate radical

Figure 8

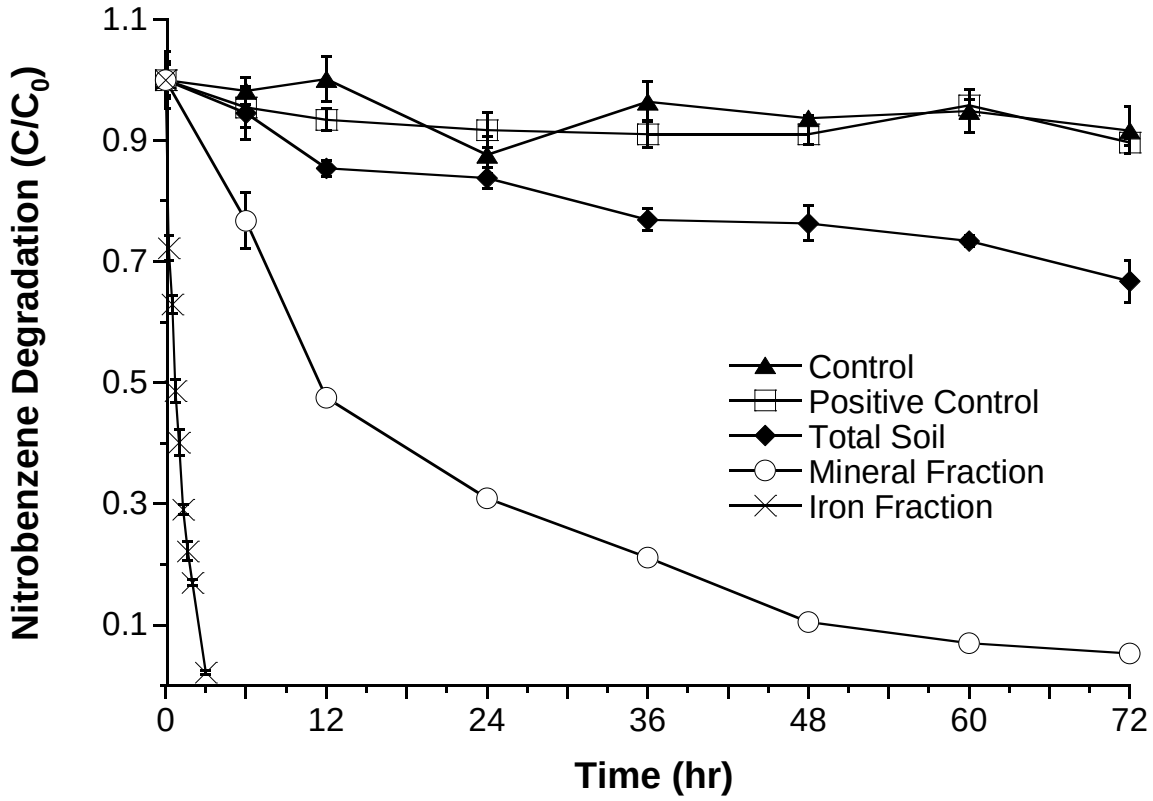
Nitrobenzene Degradation (C/C0)
1.1
0.9
0.7
0.5
0.3
0.1
0
12
24
36
48
60
72
Time (hr)
Control
Positive Control
Total Soil
Mineral Fraction
Iron Fraction

Figure 9

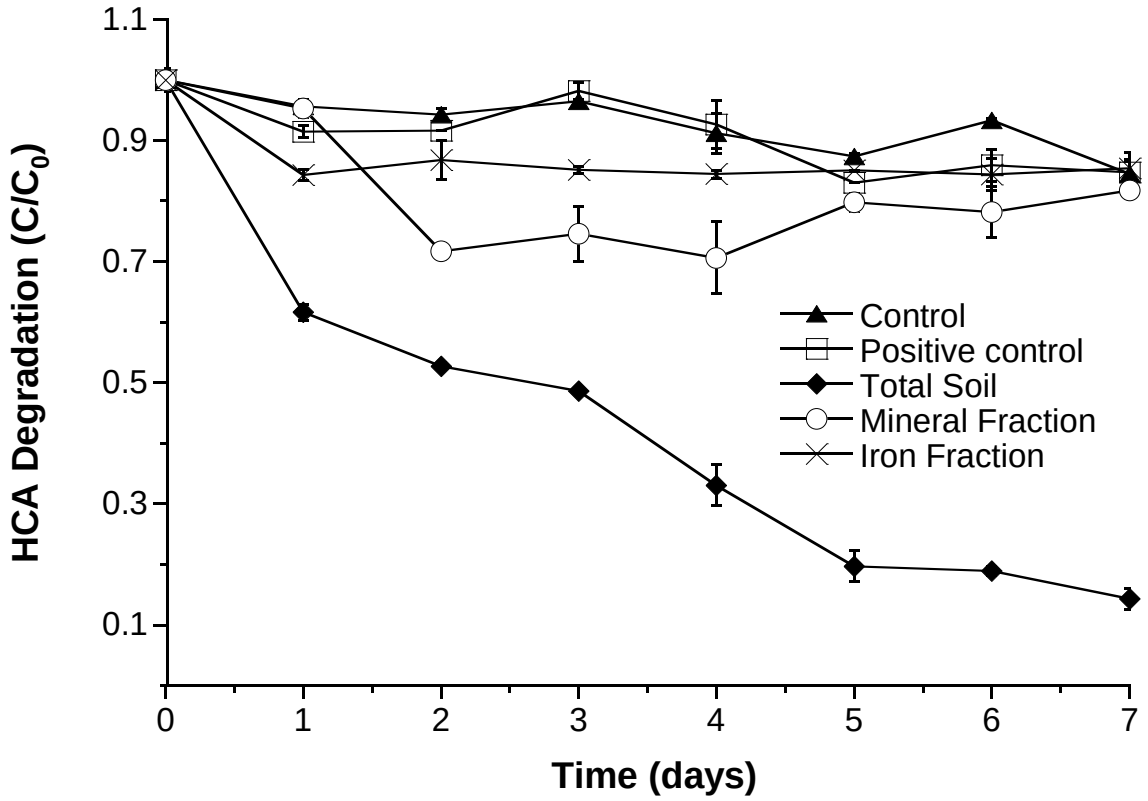
HCA Degradation (C/C0)
Time (days)
1.1
0.9
0.7
0.5
0.3
0.1
0
1
2
3
4
5
6
7
Control
Positive control
Total Soil
Mineral Fraction
Iron Fraction

Figure 10

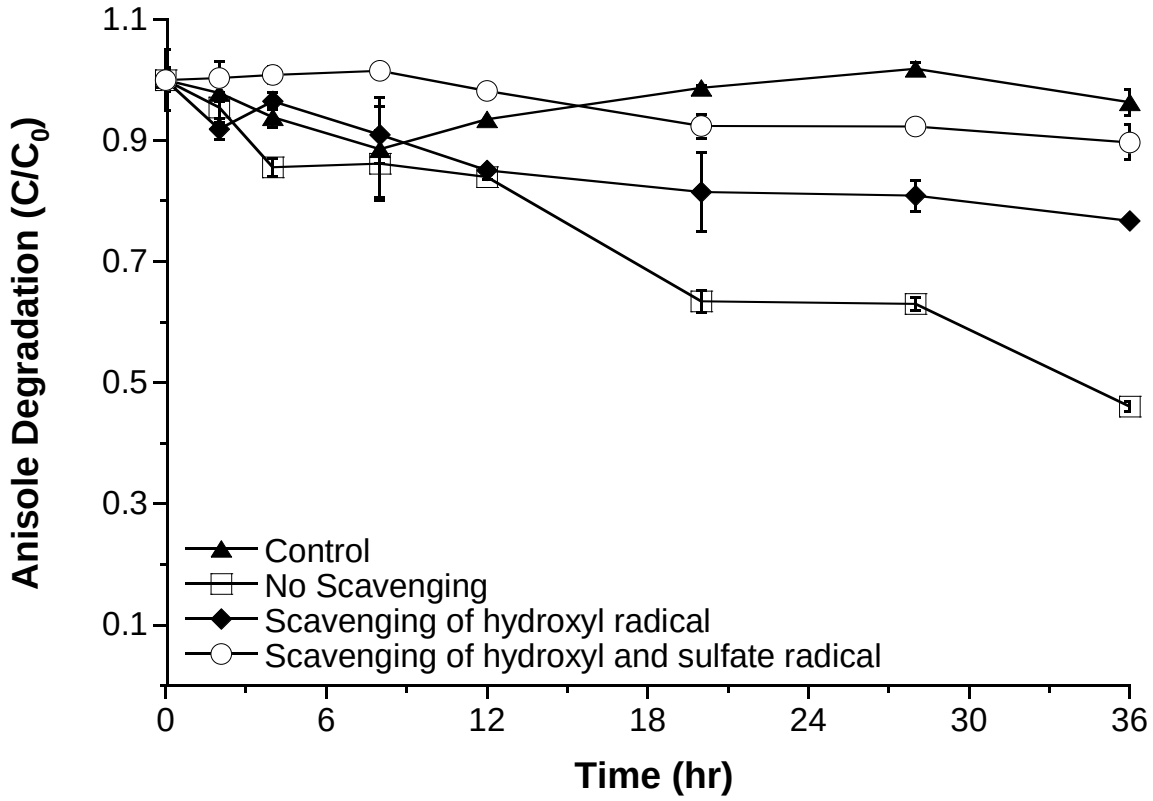
Anisole Degradation (C/C0)
1.1
0.9
0.7
0.5
0.3
0.1
0
6
12
18
24
30
36
Time (hr)
Control
No Scavenging
Scavenging of hydroxyl radical
Scavenging of hydroxyl and sulfate radical

Figure 11

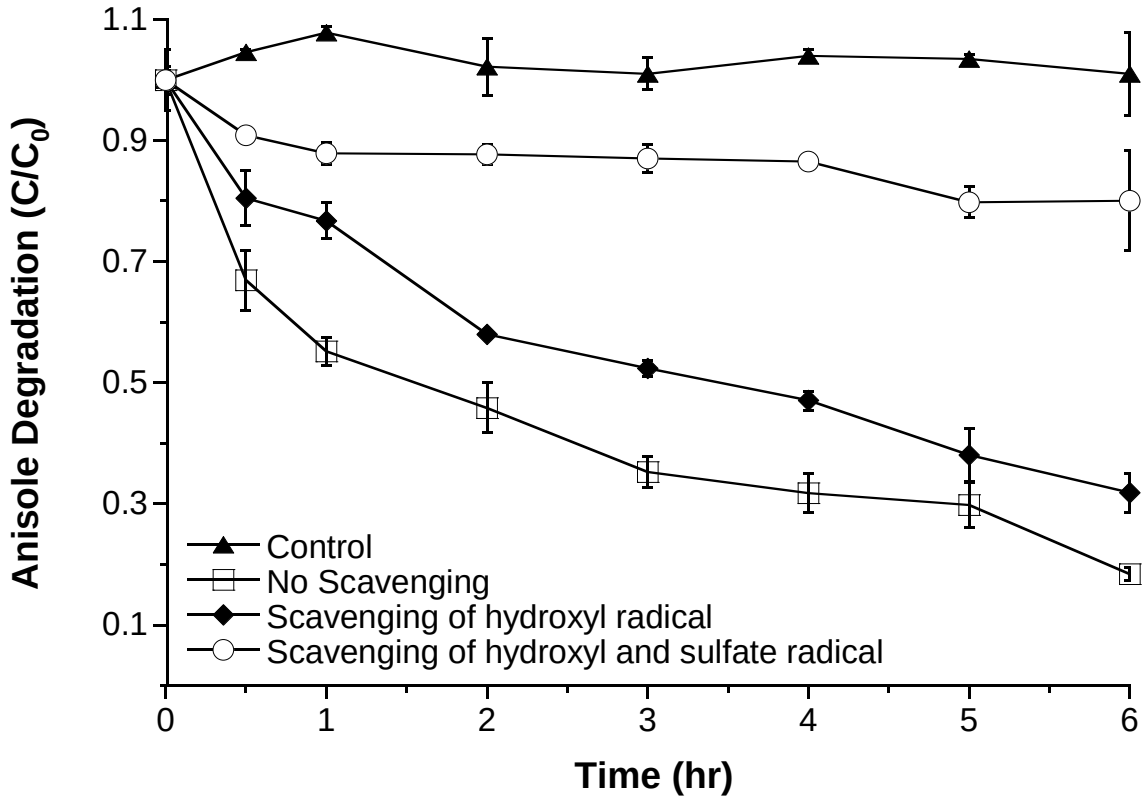
Anisole Degradation (C/C0)
1.1
0.9
0.7
0.5
0.3
0.1
0
1
2
3
4
5
6
Time (hr)
Control
No Scavenging
Scavenging of hydroxyl radical
Scavenging of hydroxyl and sulfate radical

Figure 12

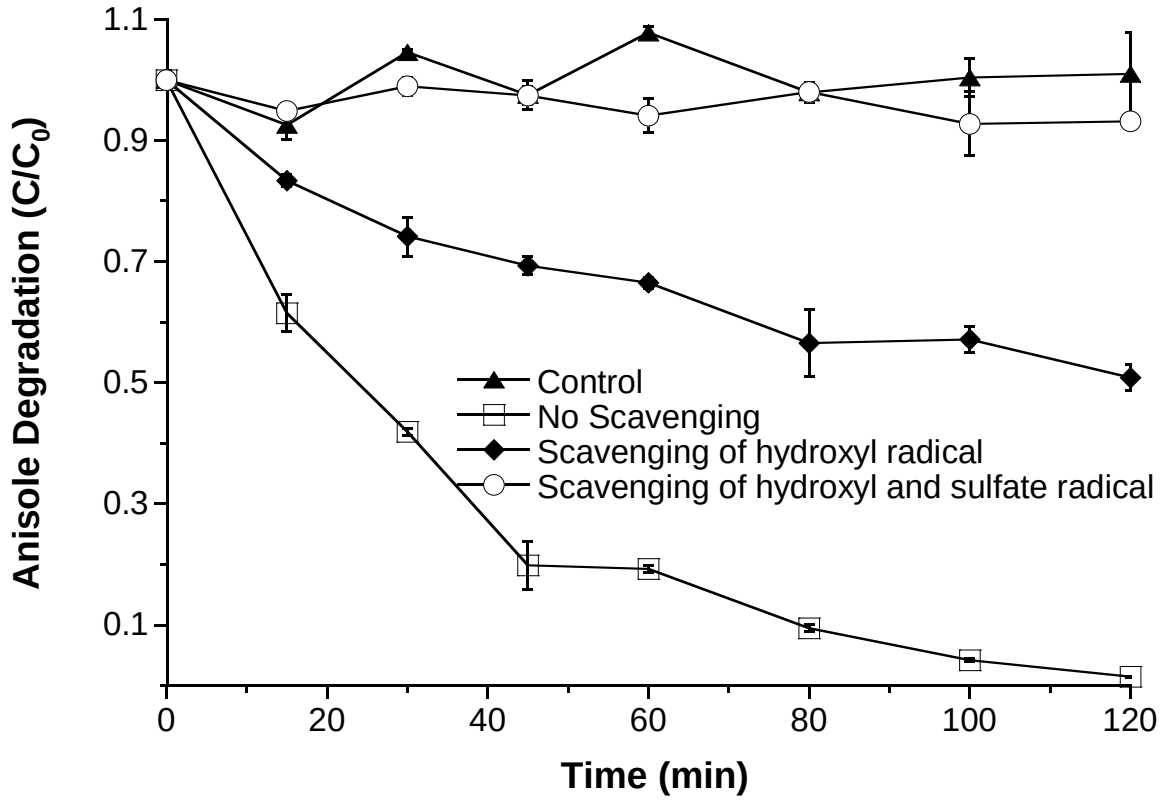
Anisole Degradation (C/C0)
1.1
0.9
0.7
0.5
0.3
0.1
0
20
40
60
80
100
120
Time (min)
Control
No Scavenging
Scavenging of hydroxyl radical
Scavenging of hydroxyl and sulfate radical

CHAPTER 3

Peroxymonosulfate Activation by Soluble Irons and Iron Chelate

Introduction

In situ chemical oxidation (ISCO) has been used extensively to treat soil and groundwater contamination over the past 15 years. ISCO processes deliver strong oxidants to the subsurface for the treatment of biorefractory organic pollutants. Three processes are commonly used for ISCO: catalyzed hydrogen peroxide propagations (CHP) (modified Fenton's reagent), permanganate, and activated persulfate (Watts and Teel, 2006). Permanganate is stable and reactive with chlorinated alkenes; however, it is consumed by natural organic matter in the subsurface (Siegrist et al., 2001) and its reactivity is limited. Therefore, CHP and activated persulfate are more widely used as ISCO processes.

Transition metals are often used as activators for CHP and persulfate to promote the generation of reactive oxygen species, which are responsible for the degradation of organic contaminants. Iron is the most common transition metal used in CHP system and persulfate activation. The Fenton initiation reaction of hydrogen peroxide with iron (II) leads to the generation of hydroxyl radical ($OH^{\bullet}$):

$$Fe^{2+} + H_2O_2 \rightarrow Fe^{3+} + OH^{\bullet} + OH^{-} \quad (1)$$

Hydroxyl radical generated through the Fenton initiation reaction can promote propagation reactions to generate superoxide radical anion ($O_2^{\bullet-}$), perhydroxyl radical ($HO_2^{\bullet}$), and

hydroperoxide anion (HO_2^-). Similar to the Fenton initiation reaction, iron (II) can activate persulfate, generating sulfate radical and hydroxyl radical (Kolthoff et al., 1951):

$$^-O_3S\text{-}O\text{-}O\text{-}SO_3^- + Fe^{2+} \rightarrow Fe^{3+} + SO_4^{\bullet -} + SO_4^{2-} \quad (2)$$

$$SO_4^{\bullet -} + H_2O \rightarrow SO_4^{2-} + OH^{\bullet} + H^+ \quad (3)$$

Although CHP and activated persulfate have widespread reactivity with organic contaminants, they have limitations for ISCO. The application of CHP in the subsurface is limited by rapid hydrogen peroxide decomposition, while persulfate is too stable to activate easily in the field. Thus, the oxidant peroxymonosulfate, which is a peroxygen with one hydrogen and one sulfate moiety, is investigated in the present study as a new oxidant source for ISCO.

Similarly to hydrogen peroxide and persulfate, peroxymonosulfate can be activated by transition metals to generate reactive oxygen species. Anipsitakis et al. (2004) found that sulfate radicals are primarily generated when transition metals such as Co (II), Ru (III), and Fe (II) react with peroxymonosulfate for the degradation of 2,4-dichlorophenol, atrazine, and naphthalene (Anipsitakis and Dionysiou, 2003). Co (II) and Ru (III) were found to be the best metal initiators for the peroxymonosulfate activation:

$$Co^{2+} + HSO_5^- \rightarrow Co^{3+} + SO_4^{\bullet -} + OH^- \quad (4)$$

A combination of sulfate and hydroxyl radicals was formed when V (III) was used as a catalyst for the activation of peroxymonosulfate (Anipsitakis and Dionysiou, 2004):

$$V^{3+}+HSO_5^- \rightarrow V^{4+}+SO_4^{\bullet -}+OH^- \quad (5)$$

$$V^{3+}+HSO_5^- \rightarrow V^{4+}+SO_4^{2-}+OH^{\bullet} \quad (6)$$

Rastogi et al. (2009) reported the degradation of a series of chlorophenols using Fe (II) – activated peroxymonosulfate. Although Co (II), Ru (III), and Fe (II) catalyze peroxymonosulfate to generate mainly sulfate radical, more detailed study of peroxymonosulfate activation by transition metals and the resulting reactive oxygen species is necessary. Since a suite of reactive species is generated in CHP and iron (II) activated persulfate systems, such a range of reactants may also be generated in iron–activated peroxymonosulfate systems. The purpose of this study was to investigate the generation of reactive species in iron (II) sulfate–, iron (III) sulfate– and iron (III) chelate–activated peroxymonosulfate systems using reaction-specific compounds, and to confirm the reactivity of activated peroxymonosulfate with two model groundwater contaminants.

Methodology

Chemicals

Potassium monopersulfate, iron (III) sulfate, anisole, hexachloroethane (HCA), perchloroethylene (PCE) and trichloroethylene (TCE) were purchased from Sigma Aldrich (St. Louis, MO). Sodium hydroxide, nitrobenzene, sodium bicarbonate, acetic acid, hydrochloric acid,

potassium permanganate, *tert*-butanol, isopropanol, potato starch, iron (II) sulfate, the iron chelate ethylenediaminetetraacetic acid iron (III) sodium salt hydrate (iron [III]–EDTA), and ethylenediaminetetraacetic acid disodium salt (Na_2-EDTA) were obtained from J.T. Baker (Phillipsburg, NJ). N hexane, potassium iodide and sodium thiosulfate were purchased from Fisher Scientific (Fair Lawn, NJ). Double-deionized water (>18 MΩ·cm) was produced and purified using a Barnstead NANOpure II Ultrapure water purification system.

Activators

Activation of peroxymonosulfate was investigated using iron (II) sulfate, iron (III) sulfate, iron (III)–EDTA and Na_2–EDTA. Stock solutions (5mM) of activators were prepared by dissolving iron (II) sulfate, iron (III) sulfate, iron (III)–EDTA, and Na_2–EDTA in deionized water.

Probe compounds

Nitrobenzene and HCA were used as reactant-specific probe compounds to investigate the iron (II), iron (III) and iron chelate activation of peroxymonosulfate. Nitrobenzene was used as oxidant probe to detect hydroxyl radical because it has high reactivity with hydroxyl radical ($k_{OH\cdot} = 3.9 \times 10^9\ M^{-1}s^{-1}$) but not sulfate radical ($k_{SO4\cdot-} = 8.4 \times 10^5\ M^{-1}s^{-1}$) (Buxton et al., 1988). HCA was used as a probe compound for reductants but not oxidants (Smith et al., 2004). It has low reactivity with hydroxyl radical and sulfate radical ($k_{OH\cdot} < 10^6\ M^{-1}s^{-1}$, $k_{SO4\cdot-} < 10^6\ M^{-1}s^{-1}$). TCE and PCE were used as model groundwater contaminants to confirm the reactivity of the reactive species generated during the activation of peroxymonosulfate**.**

Hydroxyl radical and sulfate radical scavengers

Tert-butanol was used as a hydroxyl radical scavenger ($k_{OH\cdot} = 5.2 \times 10^{10}$ $M^{-1}s^{-1}$; $k_{SO4\cdot-} = 8.4 \times 10^{5}$ $M^{-1}s^{-1}$) and isopropanol was used to scavenge both hydroxyl radical and sulfate radical ($k_{OH\cdot} = 1.9 \times 10^{9}$ $M^{-1}s^{-1}$; $k_{SO4\cdot-} = 8.2 \times 10^{7}$ $M^{-1}s^{-1}$) (Buxton et al., 1988; Clifton and Huie, 1989). The molar ratio of scavenger to probe compounds was 1000:1.

Reaction procedures

Reactions containing probe compounds or contaminants were conducted in triplicate at 20 ± 2 ℃ in 20 ml borosilicate reactors with iron (II) sulfate, iron (III) sulfate, iron (III)–EDTA, or Na_2–EDTA and a mixture of peroxymonosulfate and sodium hydroxide solutions to produce a near-neutral pH environment. The reaction system contained 0.5 M peroxymonosulfate and 0.5 M sodium hydroxide for a 1:1 molar ratio, 5 mM of iron (II) sulfate, iron (III) sulfate, iron (III)–EDTA or Na_2–EDTA. Probe compound concentrations were 1 mM for nitrobenzene, 1 μM for HCA, and 100 μM for PCE and TCE. The total volume of the reactor contents was 10 ml for nitrobenzene, PCE and TCE, and 20 ml for HCA. During the reaction, hexane (5 ml or 2 ml) was used to extract the entire reactor contents at selected time points, and hexane extracts were analyzed by gas chromatography. Control experiments were conducted in parallel using deionized water in place of peroxymonosulfate. Positive control experiments were also conducted in parallel using deionized water in place of the iron activators. Peroxymonosulfate concentrations and system pH were monitored in triplicate at selected time points.

Analysis

Extracts containing nitrobenzene were analyzed using a gas chromatography (Hewlett-Packard 5890 series) with a flame ionization detector (FID) fitted with a 15 m × 0.53 mm SPB-5 capillary column. For nitrobenzene analysis, the injector temperature was 200 ℃, the detector temperature was 250 ℃, and the initial and final oven temperatures were 60 ℃ and 180 ℃, respectively, with a program rate of 30 ℃ /min. PCE, TCE, and HCA extracts were analyzed by the gas chromatography equipped with a 30 m × 0.53 mm Equity-5 capillary column and electron capture detector. For PCE, TCE, or HCA analysis, the injector and detector temperatures were 220 ℃ and 270 ℃, and the initial and final oven temperatures were 100 ℃ and 160 ℃, respectively, with a program rate of 30 ℃ /min for PCE and TCE and 50 ℃ /min for HCA. Concentrations of peroxymonosulfate were quantified by iodometric titration with 0.01 N sodium thiosulfate (Kolthoff and Stenger, 1947). Solution pH was measured using a Fisher Accumet 900 pH meter.

Results and Discussion

Peroxymonosulfate decomposition

The decomposition of peroxymonosulfate in systems containing 5 mM iron (II) sulfate, iron (III) sulfate, iron (III)–EDTA, and Na_2–EDTA is shown in Figure 1, and the pseudo first-order rate constants for peroxymonosulfate loss are listed in Table 1. The rate constant for peroxymonosulfate decomposition in the positive control with no activator was low, with a pseudo first-order rate constant of $4.7 \pm 4.1 \times 10^{-4}$ h^{-1}. Peroxymonosulfate loss in the presence of iron (II) sulfate, iron (III) sulfate, iron (III)–EDTA and Na_2–EDTA were significantly different from the positive control, with rate constants of $4.9 \pm 0.1 \times 10^{-3}$ h^{-1}, $4.7 \pm 0.1 \times 10^{-3}$ h^{-1}, $1.5 \pm 0.6 \times 10^{-2}$ h^{-1}, $2.8 \pm 1.8 \times 10^{-3}$ h^{-1}, respectively ($p < 0.05$). The results shown in Figure 1 and Table 1

demonstrate that peroxymonosulfate was decomposed by iron (II) sulfate, iron (III) sulfate, iron (III)–EDTA, and Na_2-EDTA. Iron (III)–EDTA promoted the greatest peroxymonosulfate decomposition compared to the other catalysts. Peroxymonosulfate decomposition rates in the presence of iron (II) sulfate and iron (III) sulfate were similar. Na_2–EDTA without iron promoted a smaller degree of peroxymonosulfate decomposition than iron (III)–EDTA.

Generation of reactive oxidant species in iron (II) sulfate, iron (III) sulfate and iron (III)-EDTA–activated peroxymonosulfate systems

The generation of hydroxyl radical in the iron (II) sulfate–, iron (III) sulfate–, iron (III)–EDTA–, and Na_2–EDTA–activated peroxymonosulfate systems, with and without the presence of the hydroxyl radical scavenger *tert*-butanol, was quantified by nitrobenzene degradation, as shown in Figure 2. Pseudo first-order rate constants for nitrobenzene loss with or without scavenger are listed in Table 2. Nitrobenzene loss was non-detectable in the deionized water control over 120 hours, with a rate constant of $2.3 \pm 5.1 \times 10^{-4}$ h^{-1}. Nitrobenzene was degraded by 8.9% in the Na_2–EDTA system, with a rate constant of $0.7 \pm 7.9 \times 10^{-4}$ h^{-1}, which was not significantly different from the control ($p > 0.05$) indicating that no measurable hydroxyl radical was generated with peroxymonosulfate activated by Na_2-EDTA. In the iron (II) sulfate–, iron (III) sulfate–, and iron (III)–EDTA–activated peroxymonosulfate systems, nitrobenzene degradation was 94.8%, 87.4%, and 94.7% over 120 hours, with rate constants of 0.024 ± 0.003, 0.016 ± 0.001, and 0.022 ± 0.003 h^{-1}, respectively. Nitrobenzene oxidation rates were not significantly different between iron (II) sulfate– and iron (III)–EDTA–activated peroxymonosulfate systems; however, the degradation rate of iron (III) sulfate was significantly lower ($p < 0.05$). Overall, the results demonstrate that the iron (II) sulfate, iron (III) sulfate, and iron (III)–EDTA were much

more effective in activating peroxymonosulfate to generate hydroxyl radical than Na_2–EDTA. When *tert*-butanol was added to the iron (II) sulfate–, iron (III) sulfate–, and iron (III)–EDTA–activated peroxymonosulfate systems to scavenge hydroxyl radical, 2.0%, 0.8%, and 1.6% nitrobenzene loss was observed with rate constants of $4.8 \pm 9.5 \times 10^{-4}$, $0.5 \pm 3.5 \times 10^{-4}$, and $3.7 \pm 5.3 \times 10^{-4}$ h^{-1}, respectively, which were not significantly different from the deionized water control ($p > 0.05$), further confirming that the loss of nitrobenzene was due to hydroxyl radical activity. Similar results with iron (III)–EDTA activation of persulfate to generate hydroxyl radical have been reported by Ahmad et al. (2012). The results of Figure 2 indicate that iron (II) sulfate, iron (III) sulfate, and iron (III)–EDTA can activate peroxymonosulfate to generate hydroxyl radical.

Generation of reactive reductant species in iron (II) sulfate, iron (III) sulfate and iron (III) – EDTA–activated peroxymonosulfate systems

The generation of reductants in iron (II) sulfate–, iron (III) sulfate–, iron (III)–EDTA–, and Na_2–EDTA–activated peroxymonosulfate systems was quantified by HCA degradation as shown in Figure 3. Pseudo first-order rate constants for HCA loss are listed in Table 3. Loss of HCA in the iron (II) sulfate–, iron (III) sulfate–, iron (III)–EDTA, and Na_2–EDTA–catalyzed peroxymonosulfate systems over seven days was 12.9%, 15.0%, 10.5%, and 12.9%, respectively. The corresponding rate constants were 0.024, 0.024, 0.004, and 0.003 day^{-1}, which were not significantly different from the deionized water control rate constant of 0.019 day^{-1} ($p > 0.05$). Unlike the results of Figure 2, neither iron (II), iron (III), nor iron (III)–EDTA activated peroxymonosulfate to generate reductants.

Degradation of Model Groundwater Contaminants PCE and TCE

PCE and TCE are the most commonly detected groundwater contaminants and have been widely used as model contaminants for CHP and activated persulfate systems (Liang et al. 2008; Liang et al. 2009). In the present study, PCE and TCE were used as model groundwater contaminants to confirm iron (II) sulfate–, iron (III) sulfate–, and iron (III)–EDTA–activated peroxymonosulfate reactivity. The hydroxyl radical scavenger *tert*-butanol and the hydroxyl radical and sulfate radical scavenger isopropanol were added to the activated peroxymonosulfate systems to compare hydroxyl radical and sulfate radical activities. Figure 4 shows the degradation of PCE over one hour in the iron (II) sulfate–, iron (III) sulfate– and iron (III)–EDTA–activated peroxymonosulfate systems; Table 4 lists the corresponding pseudo first-order PCE degradation rate constants. The PCE degradation rate in the control system was $2.9 \pm 1.8 \times 10^{-4}$ h^{-1}. PCE degradation in the iron (II) sulfate–activated system in the presence of isopropanol and *tert*-butanol was 2.6% and 10.2%, respectively, with rate constants of $5.0 \pm 0.9 \times 10^{-4}$ h^{-1} and $1.8 \pm 0.3 \times 10^{-3}$ h^{-1} (Figure 4a). In contrast, 70.1% degradation of PCE was observed without scavengers, with a rate constant of 1.8×10^{-2} h^{-1}. This result indicates that 60% of the PCE degradation was due to hydroxyl radical activity, and that sulfate radical was responsible for only 7.6% of the PCE loss.

Similar results were obtained with the iron (III) sulfate–activated system, with PCE degradation of 1.2% and 10.9% with isopropanol and *tert*-butanol, respectively, and 78.2% without scavengers (Figure 4b). These results indicate that 67% of the PCE degradation occurred through hydroxyl radical activity while 9.7% was due to sulfate radical activity.

The results of Figure 4a and 4b demonstrate that the degradation of PCE in the iron (II) sulfate– and iron (III) sulfate–activating peroxymonosulfate systems was mainly due to the activity of hydroxyl radical. In contrast, in the iron (III)–EDTA–activated peroxymonosulfate system (Figure 4c), 12.9% and 55.2% of PCE loss was observed in the presence of isopropanol and *tert*-butanol, respectively, compared to 95.4% PCE loss without scavengers, indicating that 40% of the PCE degradation was due to hydroxyl radical and 42% of the PCE degradation was due to sulfate radical,. This result shows that, unlike the results in the iron (II)– and iron (III)–activated peroxymonosulfate systems, both hydroxyl radical and sulfate radical were responsible for PCE degradation in the iron (III)–EDTA–activated peroxymonosulfate system. The rate constant for PCE degradation in the iron (III)–EDTA system was 2.7 to 1.9-fold higher than that of iron (II) sulfate and iron (III) sulfate, respectively, indicating that iron (III)–EDTA may be a more effective activator for peroxymonosulfate than iron (II) sulfate and iron (III) sulfate.

TCE was another model groundwater contaminant used to confirm the reactivity of iron (II)–, iron (III)–, and iron chelate–activated peroxymonosulfate. As shown in Figure 5(a) and in Table 4, TCE was degraded by 86.7% over one hour in iron (II) sulfate–activated peroxymonosulfate, with a rate constant of $3.3 \pm 0.3 \times 10^{-2}$ h^{-1}. Scavenging with isopropanol resulted in non-detectable TCE degradation, and scavenging with *tert*-butanol resulted in 16.5% degradation with $3.0 \pm 0.4 \times 10^{-3}$ h^{-1} rate constant, compared to control system rate of $4.6 \pm 1.9 \times 10^{-4}$. This result suggested that 70% of TCE degradation was attributable to hydroxyl radical, with only 17% of TCE degradation attributable to sulfate radical. Peroxymonosulfate activated by iron (III) sulfate resulted in 86.5% TCE degradation at a rate constant of $2.4 \pm 1.0 \times 10^{-2}$ h^{-1}. Scavenging with isopropanol resulted in non-detectable TCE degradation, and scavenging with *tert*-butanol

resulted in 15.7% degradation with a $1.8 \pm 1.1 \times 10^{-3}$ h^{-1} rate constant. This result indicates that hydroxyl radical was responsible for 71% TCE degradation, with only 16% of TCE degradation attributable to sulfate radical. In the iron (III)–EDTA–activated peroxymonosulfate system without scavengers, 97.6% of TCE was degraded with a rate constant of $5.6 \pm 1.0 \times 10^{-2}$ h^{-1}. In the presence of isopropanol, 26.1% of the TCE degraded with a rate constant of $5.3 \pm 0.3 \times 10^{-3}$ h^{-1}, while 64.9% degradation with a rate constant of $1.9 \pm 0.2 \times 10^{-2}$ h^{-1} was observed in the presence of *tert*-butanol, suggesting that 33% of TCE degradation occurred due to hydroxyl radical versus 39% due to sulfate radical. Similar to the results of Figure 4, both hydroxyl radical and sulfate radical were responsible for TCE degradation in the iron (III)–EDTA–activated peroxymonosulfate system, while hydroxyl radical was the major reactant for TCE degradation in the soluble iron systems. The rate constant for TCE degradation in the iron (III)–EDTA–activated peroxymonosulfate system was 1.7 to 2.3-fold higher than iron (II) sulfate and iron (III) sulfate, which further confirmed that iron (III)–EDTA may be a more effective activator for peroxymonosulfate than iron (II) sulfate and iron (III) sulfate. These results are consistent with those of Ahmad et al. (2012), who found that that iron (III)–EDTA was a more effective activator for persulfate than iron (II)–EDTA.

Conclusion

The activation of peroxymonosulfate was investigated by using the activators iron (II) sulfate, iron (III) sulfate, iron (III)–EDTA, and Na_2–EDTA. The generation of oxidants and reductants in activated peroxymonosulfate systems was investigated using reactant-specific compounds and model groundwater contaminants. The relative activity of the oxidants hydroxyl radical and

sulfate radical was isolated using radical scavengers. The results demonstrated that iron (II) sulfate, iron (III) sulfate, and iron (III)–EDTA each effectively activated peroxymonosulfate to promote hydroxyl radical generation, but not reductant generation. The activated peroxymonosulfate systems were effective in the degradation of the model groundwater contaminants PCE and TCE. Iron (III)–EDTA was a more effective activator than iron (II) sulfate and iron (III) sulfate. In iron (II) sulfate– and iron (III) sulfate–activated peroxymonosulfate systems, the dominant oxidant for model groundwater contaminants loss was hydroxyl radical rather than sulfate radical. However, in the iron (III)–EDTA–activated peroxymonosulfate system, both hydroxyl radical and sulfate radical were dominant oxidants. The results of this research show that iron (II) sulfate–, iron (III) sulfate–, and iron (III)–EDTA–activated peroxymonosulfate systems can effectively generate oxidants responsible for the degradation of model groundwater contaminants, such as PCE or TCE, and have potential for the degradation of other biorefractory contaminants.

References

Ahmad, M., Teel, A.L., 2012. Oxidative and reductive pathways in iron-ethylenediaminetetraacetic cid-activated persulfate systems. J. Environ. Eng.-ASCE; 138: 411–418.

Anipsitakis, G.P., Dionysiou, D.D., 2003. Degradation of organic contaminants in water with sulfate radicals generated by the conjunction of peroxymonosulfate with cobalt. Environ. Sci. Technol. 37(20), 4790–4797.

Anipsitakis, G.P., Dionysiou D.D., 2004. Radical generation by the interaction of transition metals with common oxidants. Environ. Sci. Technol. 38, 3705-3742.

Buxton, G. E. P., V., Greenstock, C. L., Helman, W. P., Ross, A. B. 1987. Critical review of rate constants for reactions of hydrated electrons, hydrogen atoms and hydroxyl radicals (OH•/ •O-) in aqueous solution. J. Phys. Chem. Ref. Data, 17 (2), 513-886.

Clifton, C.L., Huie, R.E. 1989. Rate constants for hydrogen abstraction reactions of the sulfate radicals. Int. J. Chem. Knet. 21, 677-687.

Kolthoff, I.M., Miller, I.K. 1951. The chemistry of persulfate. I. The kinetics and mechanism of the decomposition of the persulfate ion in aqueous medium. J. Am. Chem. Soc. 73, 3055-3059.

Liang, C.J. and Lee, I.L. 2008. In situ iron activated persulfate oxidative fluid sparging treatment of TCE contamination-A proof of concept study. J. Contam. Hydrol., 100(3-4), 91-100.

Liang, C.J. and Lee, I.L. 2008. Persulfate oxidation of trichloroethyelene with and without iron activation in porous media. Chemosphere, 70(3), 426-435.

Rastogi, A., Dionysiou, D.D., 2009. Effect of inorganic, synthetic and naturally occurring chelating agents on Fe(II) mediated advanced oxidation of chlorophenols. Water Research, 43, 684-694.

Siegrist, R.L., Urynowicz, M.A., (2001). Principles and practices of in situ chemical oxidation using permanganate, Batelle Press, Columbus, OH.

Smith, B.A., Teel, A.L., Watts, R.J. 2004. Identification of the reactive oxygen species responsible for carbon tetrachloride degradation in modified Fenton's systems. Environ. Sci.

Tec. 38, 5465-5469.

Watts, R.J., Teel, A.L., 2006. Treatment of contaminated soils and groundwater using ISCO. Pract. Period. Hazard. Toxic Radioact. Waste Manage. 10(1), 2-9.

Table 1 Pseudo First-Order Peroxymonosulfate Decomposition Rate Constants in the Presence of 5 mM Iron (II) Sulfate, Iron (III) Sulfate, Iron (III)–EDTA, and Na_2-EDTA

	Peroxymonosulfate decomposition rate constant (h^{-1})
Control	$4.7 \pm 4.1 \times 10^{-4}$
$FeSO_4$	$4.9 \pm 0.1 \times 10^{-3}$
$Fe_2(SO_4)_3$	$4.7 \pm 0.1 \times 10^{-3}$
Fe (III)–EDTA	$1.5 \pm 0.6 \times 10^{-2}$
Na_2-EDTA	$2.8 \pm 1.8 \times 10^{-3}$

Table 2 Pseudo First-order Nitrobenzene Degradation Rate Constants in Peroxymonosulfate Systems Activated by 5 mM Iron (II) Sulfate, Iron (III) Sulfate, Iron (III)–EDTA and Na_2-EDTA

		Nitrobenzene degradation rate constant (h^{-1})
Control		$2.3 \pm 5.1 \times 10^{-4}$
$FeSO_4$	No scavenger	$2.4 \pm 0.3 \times 10^{-2}$
	tert-Butanol	$4.8 \pm 9.5 \times 10^{-4}$
$Fe_2(SO_4)_3$	No scavenger	$1.6 \pm 0.1 \times 10^{-2}$
	tert-Butanol	$0.5 \pm 3.5 \times 10^{-4}$
Fe (III)–EDTA	No scavenger	$2.2 \pm 0.3 \times 10^{-2}$
	tert-Butanol	$3.7 \pm 5.3 \times 10^{-4}$
Na_2-EDTA	No scavenger	$0.7 \pm 7.9 \times 10^{-4}$
	tert-Butanol	$6.2 \pm 6.5 \times 10^{-4}$

Table 3 Pseudo First-order Probe Compound HCA Degradation Rate Constants in Peroxymonosulfate Systems Activated by 5 mM Iron (II) Sulfate, Iron (III) Sulfate, Iron (III)–EDTA and Na_2-EDTA

	HCA degradation rate constant (day^{-1})
Control	$1.9 \pm 0.8 \times 10^{-2}$
$FeSO_4$	$2.4 \pm 1.2 \times 10^{-2}$
$Fe_2(SO_4)_3$	$2.4 \pm 1.3 \times 10^{-2}$
Fe (III)–EDTA	$0.4 \pm 1.6 \times 10^{-2}$
Na_2-EDTA	$0.3 \pm 0.8 \times 10^{-2}$

Table 4 Pseudo First-order PCE and TCE Degradation Rate Constants in Peroxymonosulfate Systems Activated by 5 mM Iron (II) Sulfate, Iron (III) Sulfate, and Iron (III)–EDTA

		PCE degradation rate constant (h^{-1})	TCE degradation rate constant (h^{-1})
Control		$2.9 \pm 1.8 \times 10^{-4}$	$4.6 \pm 1.9 \times 10^{-4}$
$FeSO_4$	Isopropanol	$5.0 \pm 0.9 \times 10^{-4}$	$2.9 \pm 4.5 \times 10^{-4}$
	tert-Butanol	$1.8 \pm 0.3 \times 10^{-3}$	$3.0 \pm 0.4 \times 10^{-3}$
	No scavenger	$1.8 \pm 0.3 \times 10^{-2}$	$3.3 \pm 0.3 \times 10^{-2}$
$Fe_2(SO_4)_3$	Isopropanol	$2.7 \pm 0.9 \times 10^{-4}$	$0.8 \pm 1.8 \times 10^{-4}$
	tert-Butanol	$1.9 \pm 0.3 \times 10^{-3}$	$1.8 \pm 1.1 \times 10^{-3}$
	No scavenger	$2.6 \pm 0.4 \times 10^{-2}$	$2.4 \pm 1.0 \times 10^{-2}$
Fe (III)–EDTA	Isopropanol	$2.2 \pm 0.1 \times 10^{-3}$	$5.3 \pm 0.3 \times 10^{-3}$
	tert-Butanol	$1.3 \pm 0.1 \times 10^{-2}$	$1.9 \pm 0.2 \times 10^{-2}$
	No scavenger	$4.9 \pm 0.4 \times 10^{-2}$	$5.6 \pm 1.0 \times 10^{-2}$

List of Figures

Figure 1

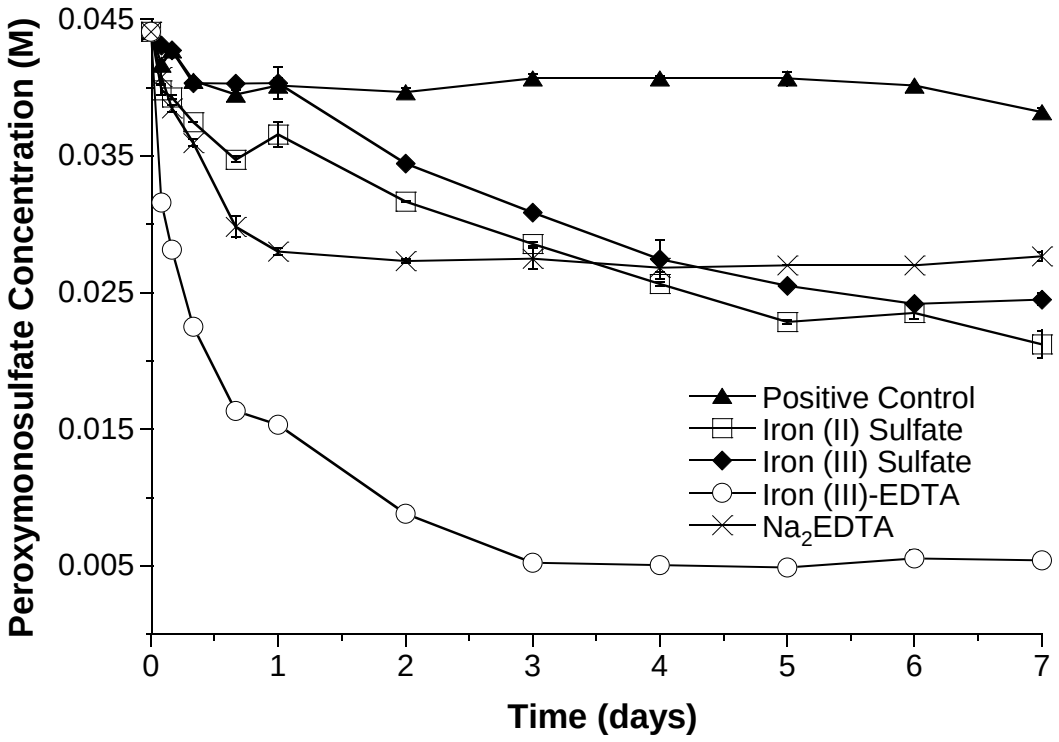
Peroxymonosulfate Concentration (M)
0.045
0.035
0.025
0.015
0.005
0
1
2
3
4
5
6
7
Time (days)
Positive Control
Iron (II) Sulfate
Iron (III) Sulfate
Iron (III)-EDTA
Na2EDTA

Figure 2 (a)

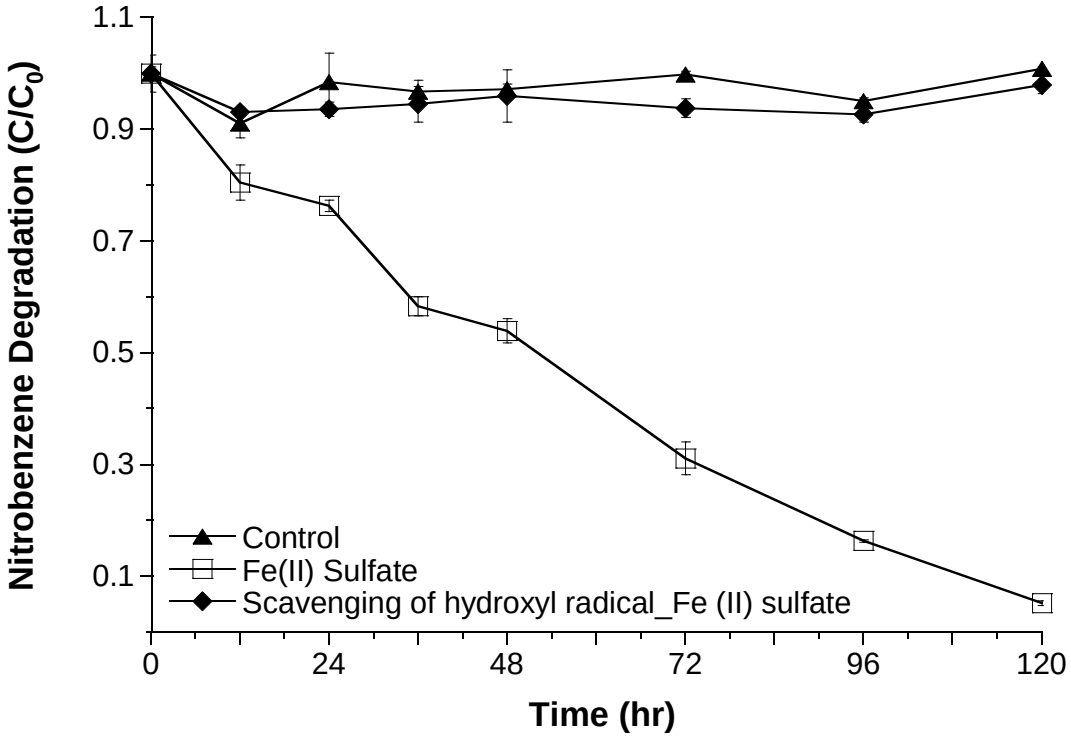
Nitrobenzene Degradation (C/C0)
1.1
0.9
0.7
0.5
0.3
0.1
0
24
48
72
96
120
Time (hr)
Control
Fe(II) Sulfate
Scavenging of hydroxyl radical_Fe (II) sulfate

(b)

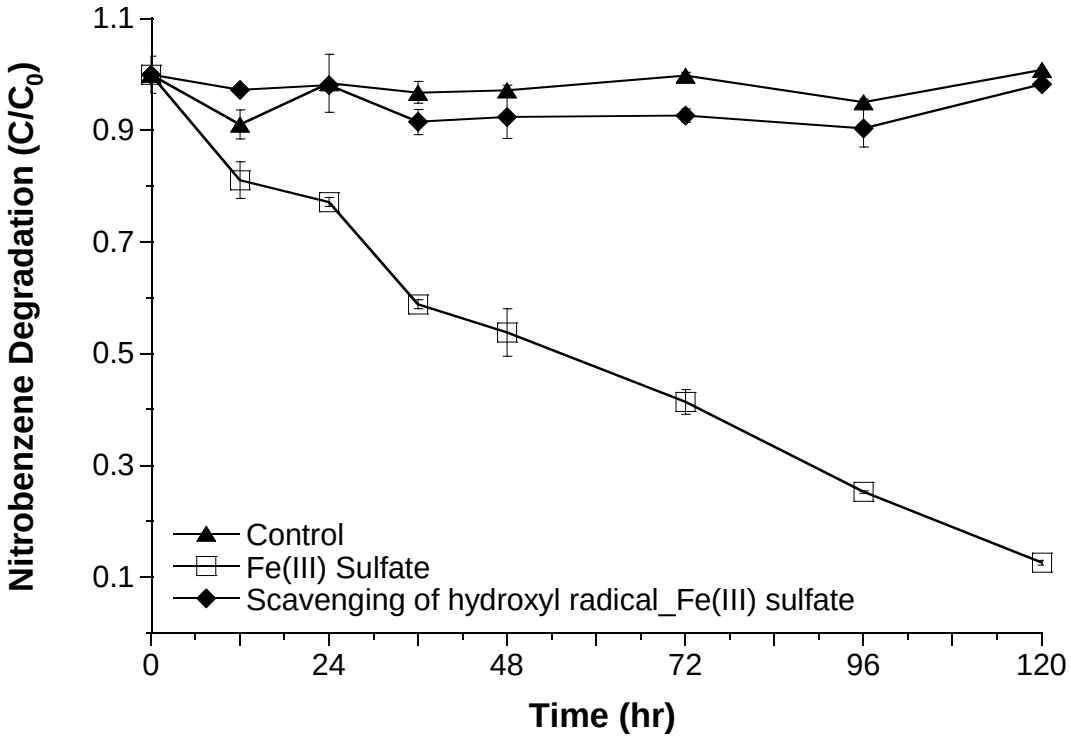
Nitrobenzene Degradation (C/C0)
1.1
0.9
0.7
0.5
0.3
0.1
0
24
48
72
96
120
Time (hr)
Control
Fe(III) Sulfate
Scavenging of hydroxyl radical_Fe(III) sulfate

(c)

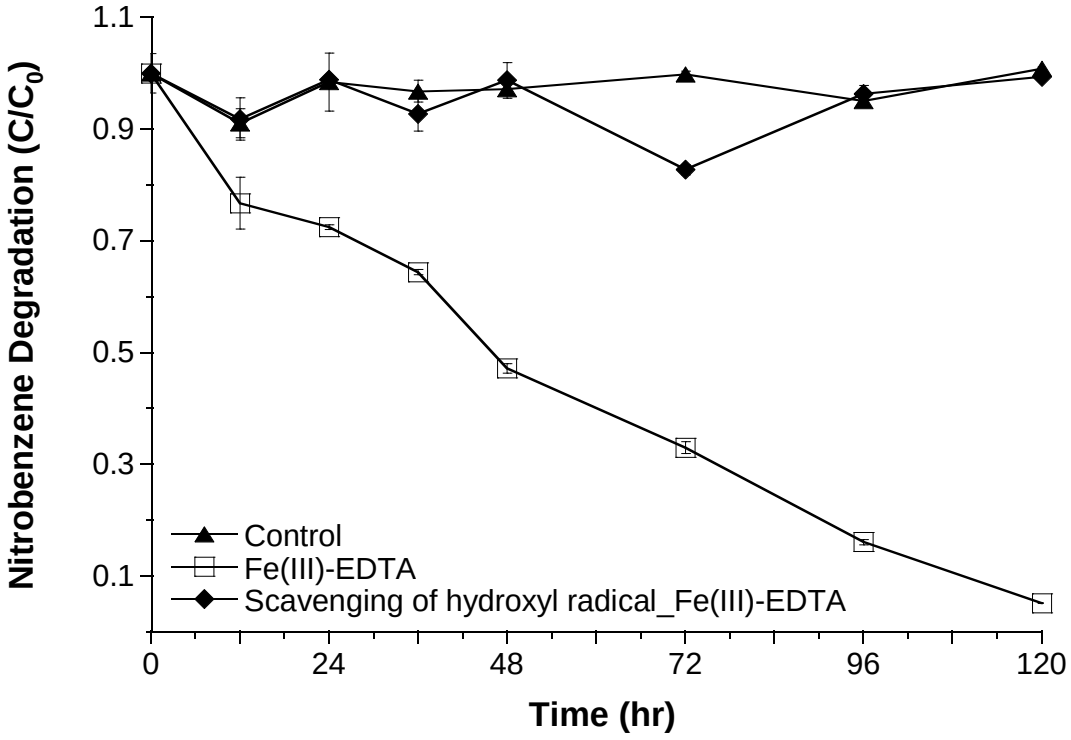
Nitrobenzene Degradation (C/C0)
1.1
0.9
0.7
0.5
0.3
0.1
0
24
48
72
96
120
Time (hr)
Control
Fe(III)-EDTA
Scavenging of hydroxyl radical_Fe(III)-EDTA

(d)

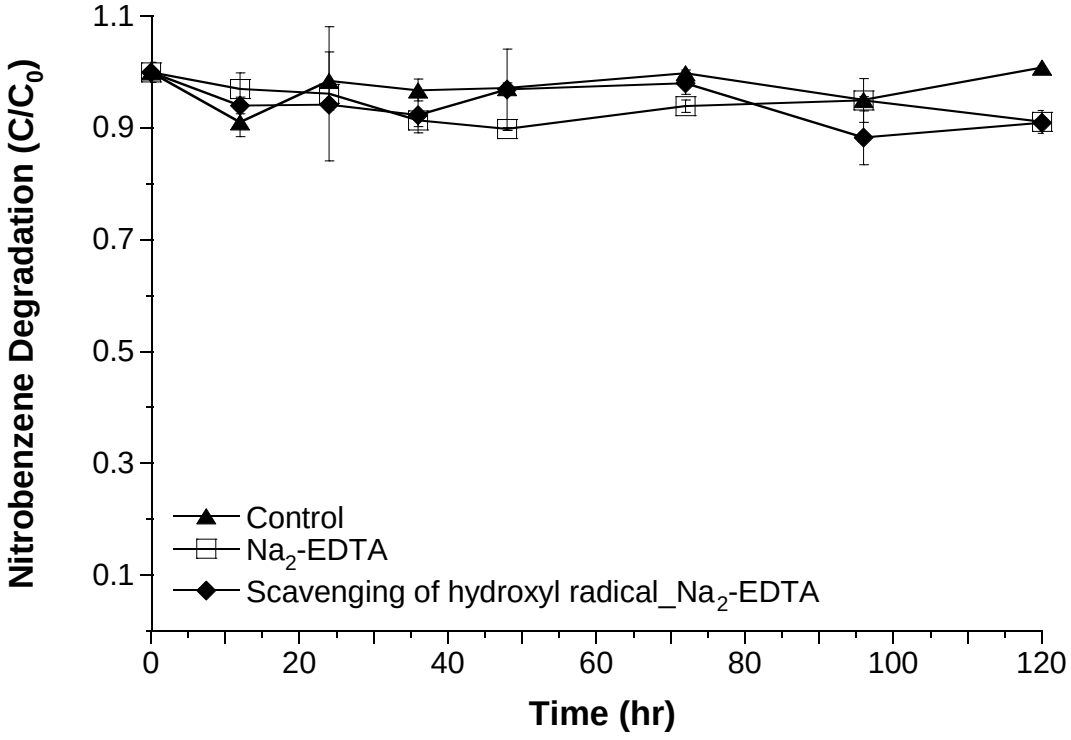
Nitrobenzene Degradation (C/C0)
1.1
0.9
0.7
0.5
0.3
0.1
0
20
40
60
80
100
120
Time (hr)
Control
Na2-EDTA
Scavenging of hydroxyl radical_Na2-EDTA

Figure 3

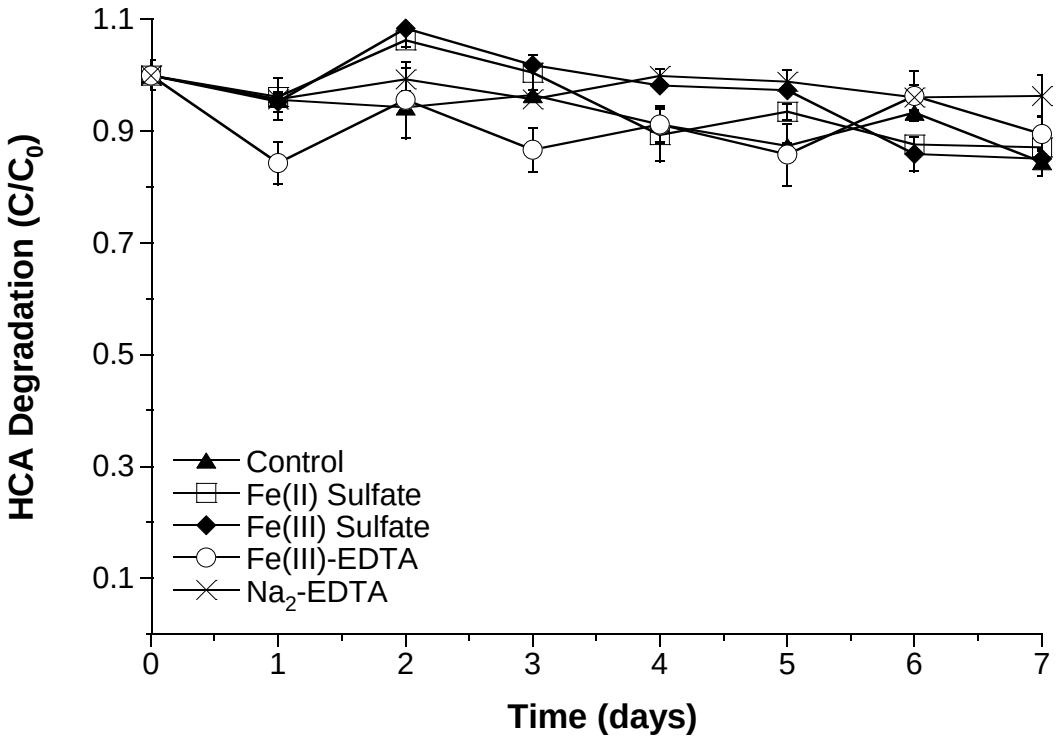
1.1
0.9
0.7
0.5
0.3
0.1
HCA Degradation (C/C0)
Control
Fe(II) Sulfate
Fe(III) Sulfate
Fe(III)-EDTA
Na2-EDTA
0
1
2
3
4
5
6
7
Time (days)

Figure 4 (a)

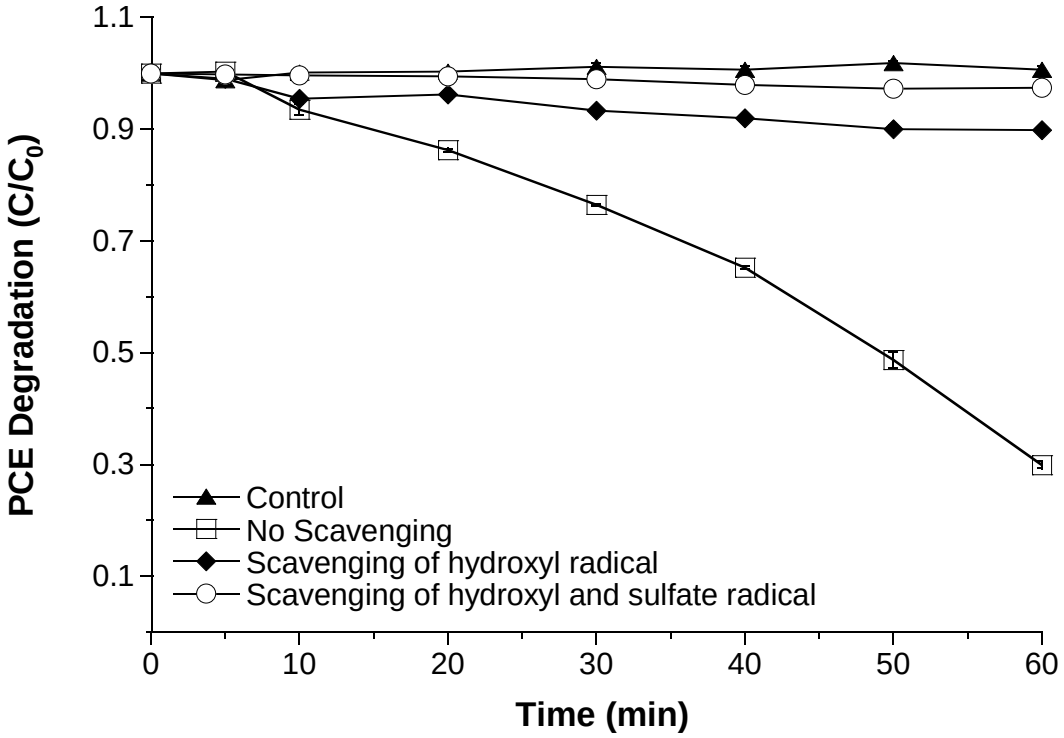
PCE Degradation (C/C0)
Time (min)
Control
No Scavenging
Scavenging of hydroxyl radical
Scavenging of hydroxyl and sulfate radical

(b)

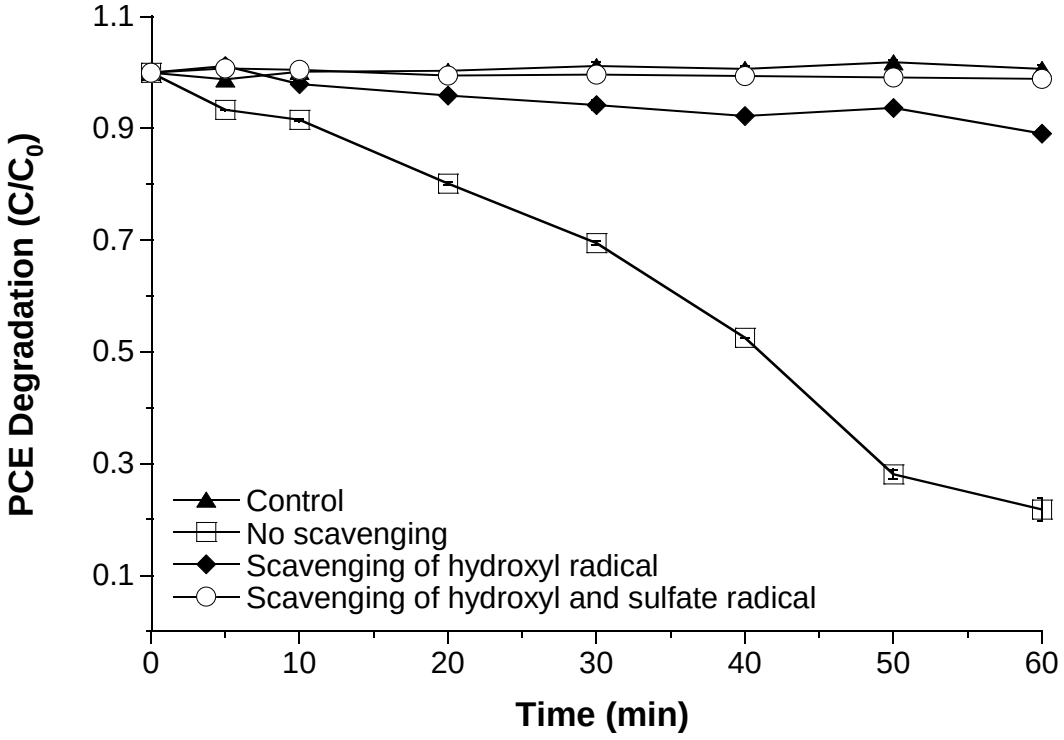
PCE Degradation (C/C0)
Time (min)
Control
No scavenging
Scavenging of hydroxyl radical
Scavenging of hydroxyl and sulfate radical

(c)

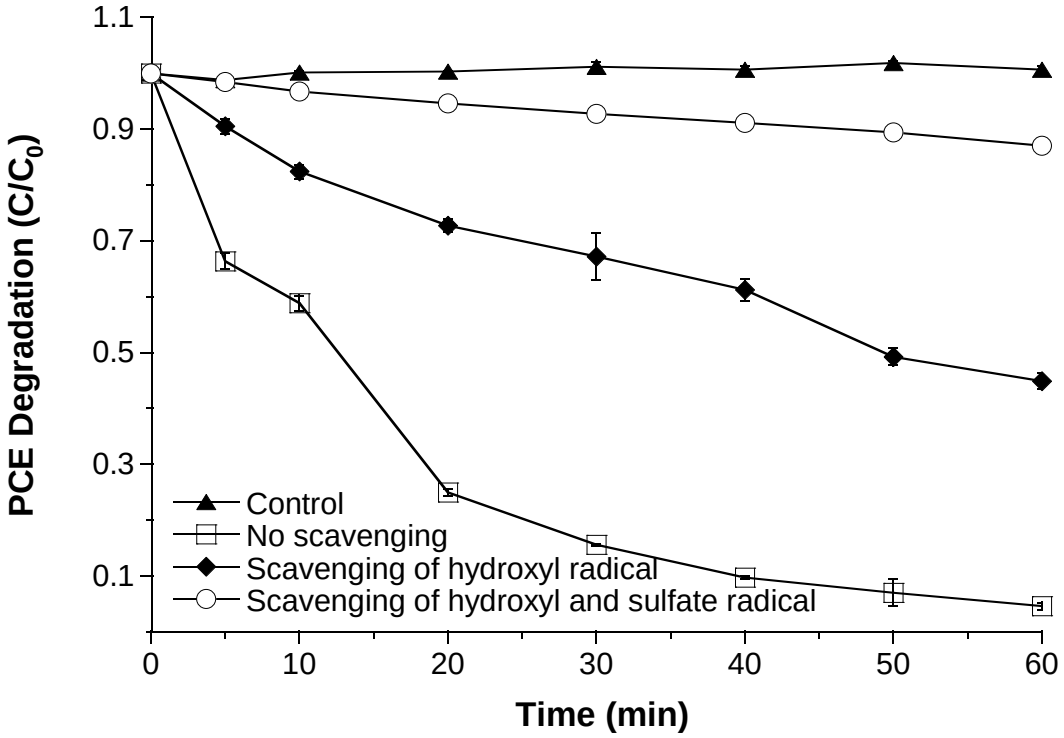
PCE Degradation (C/C0)
Time (min)
Control
No scavenging
Scavenging of hydroxyl radical
Scavenging of hydroxyl and sulfate radical

Figure 5 (a)

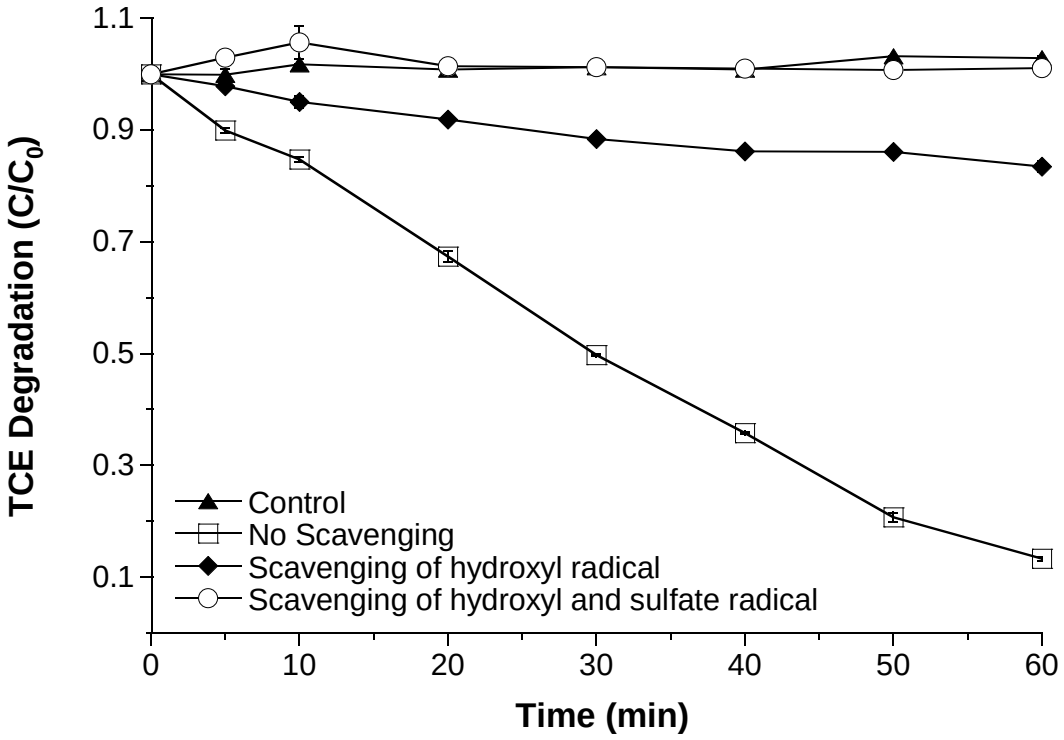
TCE Degradation (C/C0)
Time (min)
Control
No Scavenging
Scavenging of hydroxyl radical
Scavenging of hydroxyl and sulfate radical

(b)

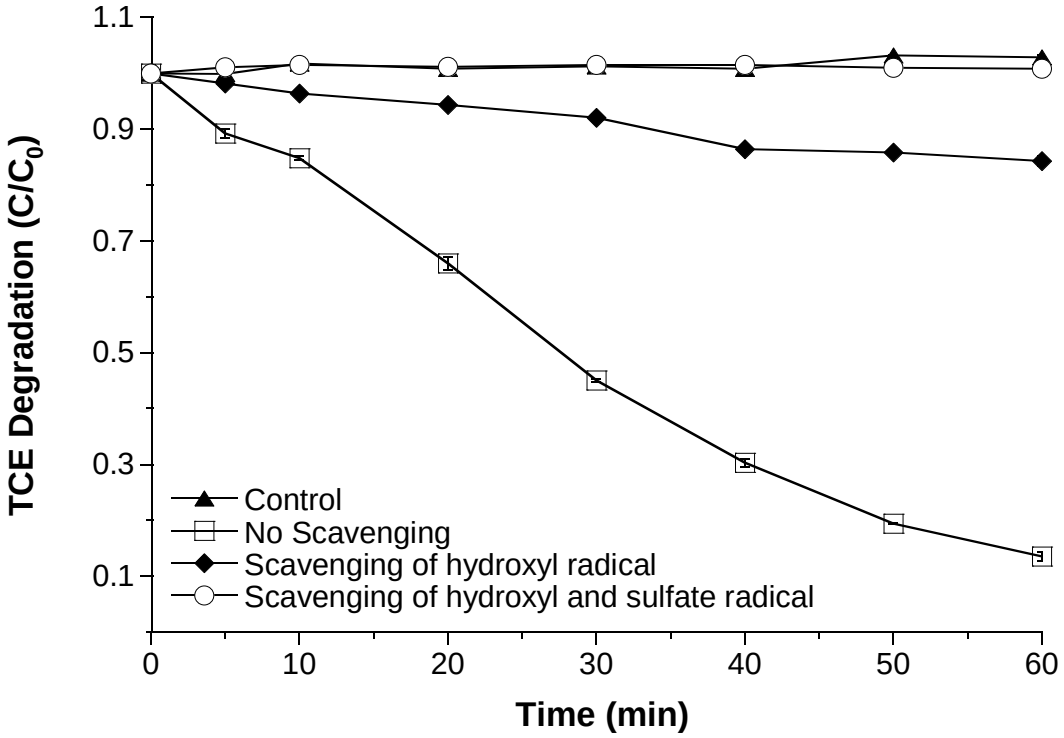
TCE Degradation (C/C0)
Time (min)
Control
No Scavenging
Scavenging of hydroxyl radical
Scavenging of hydroxyl and sulfate radical

(c)

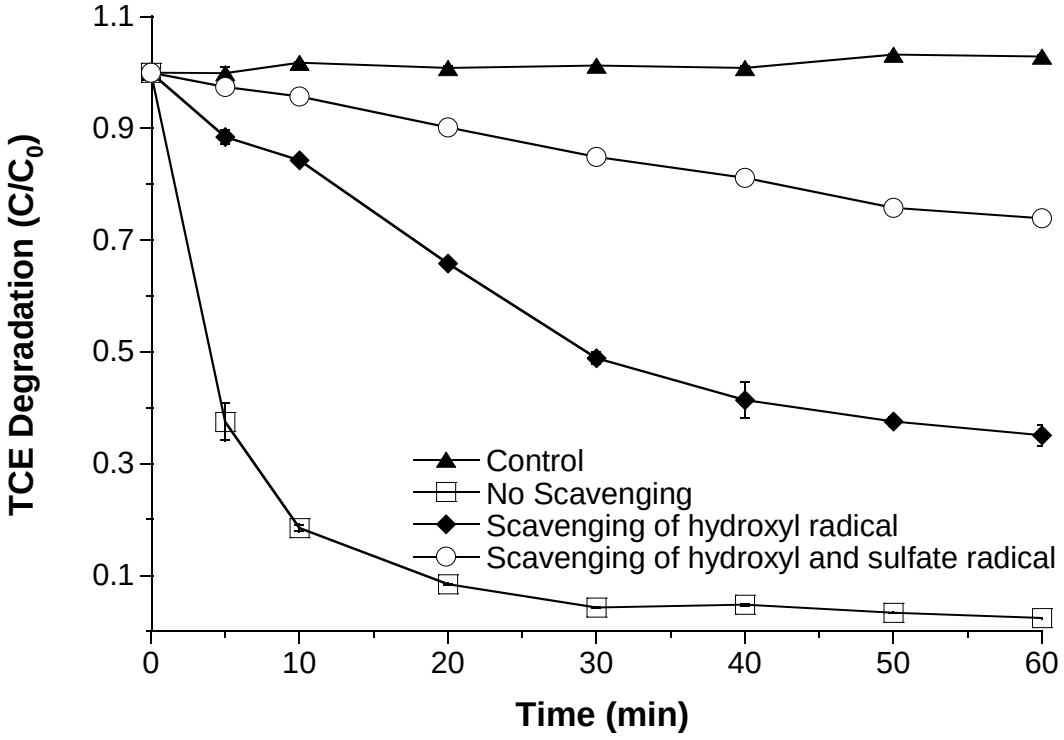
TCE Degradation (C/C0)
Time (min)
Control
No Scavenging
Scavenging of hydroxyl radical
Scavenging of hydroxyl and sulfate radical

CHAPTER 4

Reactive Species Generation in Modified Fenton's Systems with Different Concentrations of Hydrogen Peroxide

Introduction

Improper disposal of biorefractory and toxic organic pollutants has caused soil and groundwater contamination around the world, which has led to in situ chemical oxidation (ISCO) becoming a popular technology over the past twenty years for treating such contamination. Modified Fenton's reagent, also known as catalyzed hydrogen peroxide propagation (CHP), is one of the most important ISCO technologies that have widespread application for soil and groundwater remediation. CHP reactions are based on soluble iron, iron chelates, or minerals catalyzing the decomposition of hydrogen peroxide to generate reactive species such as hydroxyl radical. This is a modification of the standard Fenton's reaction in which dilute hydrogen peroxide is applied in excess with an aqueous iron (II) solution to generate hydroxyl radical (Walling 1975):

$$Fe^{2+} + H_2O_2 \rightarrow Fe^{3+} + OH^{\bullet} + OH^{-} \quad (1)$$

Hydroxyl radical is a strong and relatively nonselective oxidant that has high reaction rates ($k > 10^8\ M^{-1}s^{-1}$) with alkenes, aromatics or heterocyclic ring compounds. Due to its widespread reactivity, hydroxyl radical is considered the most important reactive species for contaminant degradation in ISCO. However, it is unreactive with highly oxidized compounds or halogenated alkanes (Dorfman et al., 1973; Buxton et al., 1988; Haag et al., 1992).

When higher concentrations of hydrogen peroxide (0.6–3.6 M) are used in CHP reactions, hydroxyl radical is not the only reactive species generated. The hydroxyl radical produced through the initial Fenton's reaction promotes the following propagation reactions to generate superoxide radical anion ($O_2^{\bullet-}$), perhydroxyl radical ($HO_2^{\bullet}$), and hydroperoxide anion (HO_2^-) (Watts and Teel, 2006):

$$OH^{\bullet} + H_2O_2 \rightarrow HO_2^{\bullet} + H_2O \quad (2)$$

$$HO_2^{\bullet} \leftrightarrow O_2^{\bullet-} + H^+ \ (pKa = 4.8) \quad (3)$$

$$HO_2^{\bullet} + Fe^{2+} \rightarrow Fe^{3+} + HO_2^- \quad (4)$$

Perhydroxyl radical is a relatively weak oxidant, and hydroperoxide anion is a strong nucleophile (David et al., 1999). Superoxide radical anion is a weak reductant and nucleophile in aqueous medium (Frimer et al., 1988). Superoxide can also be generated from hydrogen peroxide decomposition by iron (III) (Gutteridge, 1985), which is the superoxide-driven Fenton initiation reaction:

$$Fe^{3+} + H_2O_2 \rightarrow Fe^{2+} + O_2^{\bullet-} + 2\,H^+ \quad (5)$$

The widespread reactivity of reactive species generated through CHP reactions has been demonstrated in previous studies that elucidated the degradation mechanism of highly oxidized chlorinated compounds, such as chloroform, carbon tetrachloride, trichloroethylene (TCE) or perchloroethylene (PCE). Smith et al. (2006) found that for CHP systems with 2 M hydrogen peroxide catalyzed by a 5 mM iron (III)-chelate, carbon tetrachloride dense non-aqueous phase

liquid (DNAPL) was destroyed by the reactive species superoxide; however, both hydroxyl radical and superoxide were responsible for chloroform DNAPL degradation. As the chemical structures of PCE and TCE both exhibit the characteristics of degradation by oxidants and reductants, the mechanism of their degradation is more complex. Smith et al. (2009) showed that both hydroxyl radical and superoxide were involved in TCE and PCE DNAPL degradation, and the degradation may be due primarily to the activity of superoxide in CHP system. Since hydroxyl radical is short-lived and its reactivity is limited by diffusion-controlled rates in aqueous solutions, it may not be reactive with sorbed contaminants (Sedlak and Andren, 1994). However, the PCE and TCE degradation mechanism may be different when dissolved in water rather than in DNAPLs. Moreover, as the results from Smith et al. (2009) were based on a CHP system only with 2 M hydrogen peroxide, the PCE and TCE degradation under varying hydrogen peroxide concentrations in CHP requires elucidation. The purpose of this study was to investigate which reactive species were responsible for PCE and TCE degradation in aqueous phase and the reactive species generation in CHP systems with different concentrations of hydrogen peroxide.

Methodology

Chemicals

Hydrogen peroxide (50%, technical grade), iron (III)–perchlorate, perchloroethylene (PCE), trichloroethylene (TCE), and tetranitromethane were provided by Sigma Aldrich (St. Louis, MO). Nitrobenzene was purchased from J.T. Baker (Phillipsburg, NJ). N-hexane (95%) was obtained from Fisher Scientific (Fair Lawn, NJ). ORBO 32 gas adsorbent tubes were purchased

from Supelco (St. Louis). Double-deionized water (>18 MΩ·cm) was produced and purified using Barnstead NANOpure II Ultrapure water purification system.

Organic compounds and radical scavenger

PCE and TCE were used to study the degradation mechanism as a function of hydrogen peroxide concentrations in CHP systems. The initial concentrations of PCE and TCE were 100 μM. Nitrobenzene and tetranitromethane were used as reaction-specific probe compounds to identify the generation of reactive species in CHP systems. The initial concentration of nitrobenzene and tetranitromethane were 1 mM and 300 μM, respectively. Nitrobenzene was used as oxidant probe to detect hydroxyl radical because it has high reactivity with hydroxyl radical ($k_{OH\cdot} = 3.9 \times 10^9\ M^{-1}s^{-1}$) but not with reductants or nucleophiles. Because tetranitromethane has high reactivity with superoxide ($k_{O_2\cdot^-} = 1.9 \times 10^9\ M^{-1}s^{-1}$) and not with perhydroxyl radical ($k_{HO_2\cdot} < 10^4\ M^{-1}s^{-1}$) (Afanas'ev, 1989) or with hydroxyl radical, tetranitromethane was used as the superoxide probe. Isopropanol was used to scavenge the hydroxyl radical ($k_{OH\cdot} = 1.9 \times 10^9\ M^{-1}s^{-1}$) (Buxton et al., 1988). The molar ratio between scavenger and probe compounds was 1000:1.

Reaction procedures

CHP systems contained varying concentrations of hydrogen peroxide and 1 mM iron (III)–perchlorate. The concentrations of hydrogen peroxide varied at designated increments between 0.01M and 1M. The reaction system consisted of hydrogen peroxide, iron (III) and organic compounds. Reactions with organic compounds PCE, TCE, nitrobenzene or tetranitromethane were conducted in bench-scale 20 ml borosilicate vials, and an ORBO-32 gas absorbent tube was secured into the Teflon cap to capture volatilized PCE and TCE (Smith et al., 2006). The total

aqueous solution was 10 ml. Reaction vials and ORBO tubes were extracted using hexane (5 ml) at selected time points. All the organic compounds concentrations were quantified by gas chromatography (GC). In addition, control experiments were conducted using deionized water in place of CHP reagents. All reactions were conducted in triplicate at 20 ± 2 ℃.

Analysis

PCE, TCE or tetranitromethane extracts were analyzed by gas chromatograph equipped with a 30 m × 0.53 mm Equity-5 capillary column and electron capture detector. The injector and detector temperatures were 220 ℃ and 270 ℃, the initial and final oven temperatures were 100 ℃ and 160 ℃, respectively, with a program rate of 30 ℃ /min for PCE or TCE. The program for tetranitromethane was 50 ℃ and 160 ℃ at a rate of 50 ℃ /min. Nitrobenzene extracts were analyzed by gas chromatography (Hewlett-Packard 5890) with a flame ionization detector fitted with a 15 m × 0.53 mm SPB-5 capillary column. The injector temperature was 200 ℃, and the detector temperature was 250 ℃. The initial and final oven temperatures were 60 ℃ and 180 ℃, respectively, and the program rate was 30 ℃ /min.

Results and discussion

PCE and TCE degradation by CHP

The degradation of PCE and TCE by CHP is shown in Figure 1 and Figure 2, and the first order rate constants are listed in Table 1. PCE was destroyed by 87.3% in CHP with 0.01 M H_2O_2 over 30 minutes with a rate constant of 0.025 min^{-1}. Greater than 99% of PCE was degraded within 20 minutes at a rate constant of 0.152 min^{-1} in the presence of 0.025 M H_2O_2. When H_2O_2 concentrations increased to 0.05 M and 0.1 M in CHP, > 99% of PCE destruction was achieved

within 15 minutes ($k = 0.173\ min^{-1}$) and 10 minutes ($k = 0.191\ min^{-1}$), respectively. These results indicated that PCE degradation rate increased with respect to rising hydrogen peroxide concentrations from 0.01 M to 0.1 M, confirming that higher hydrogen peroxide concentration provides high stoichiometric ratios for reactive species generation (Watts et al., 2005). However, when hydrogen peroxide concentration was increased to 0.5 M, 99% of PCE degradation was achieved within 20 minutes at a rate constant of $0.135\ min^{-1}$, which was lower than that in CHP with 0.1 M H_2O_2. Moreover, with 1 M H_2O_2 in CHP, 87.2% of PCE was degraded within 30 minutes at a rate constant of $0.059\ min^{-1}$, which was 1.4 and 2.3 times smaller than that with 0.5 M and 0.1 M H_2O_2. These results suggest that when hydrogen peroxide concentration increased from 0.1 M to 1 M, the PCE degradation rate decreased, which did not correspond to the results from increasing hydrogen peroxide concentration from 0.01 M to 0.1 M.

Similar results were obtained with TCE in CHP systems. When hydrogen peroxide concentrations were 0.01 M, 0.025 M, 0.05 M and 0.1 M in CHP, the rate constants of TCE degradations were 0.06, 0.078, 0.246 and $0.297\ min^{-1}$, respectively. TCE degradation increased with rising hydrogen peroxide concentrations between 0.01 M and 0.1 M. However, at 0.5 M and 1 M hydrogen peroxide, TCE degradation rate constants were 0.270 and $0.164\ min^{-1}$, which were 1.64 and 1.8 times lower than the rate found at 0.1 M hydrogen peroxide. Volatilization in both PCE and TCE were negligible. Smith et al. (2009) demonstrated CHP degraded PCE and TCE DNAPLs, which is a similar result to those found by our team, in that PCE and TCE in aqueous phases were rapidly destroyed by CHP at degradation rates greater than volatilization. Since hydroxyl radical reacts with both PCE ($k_{OH\cdot} = 2.8 \times 10^9\ M^{-1}s^{-1}$) and TCE ($k_{OH\cdot} = 4.0 \times 10^9\ M^{-1}s^{-1}$) (Buxton et al., 1988), the aqueous-phase PCE and TCE degradation may be due to hydroxyl

radical generated in CHP. However, CHP system generates not only hydroxyl radical, but also a series of reactive species such as superoxide radical anion, hydroperoxide anion, etc (equations 3-5). Smith et al. (2009) concluded that the destruction of PCE and TCE DNAPLs occurred mainly because of the superoxide activity rather than due to hydroxyl radical. Further investigation of the degradation mechanism of aqueous-phase PCE and TCE in CHP is necessary.

PCE and TCE degradation in CHP with scavenger addition

To examine the reactive species responsible for PCE and TCE degradation in the aqueous phase, we conducted CHP treatments with the hydroxyl radical scavenger isopropanol. PCE degradation in CHP at determined hydrogen peroxide concentrations between 0.01 M and 1 M with or without isopropanol is shown in Figure 3(a-f). When hydrogen peroxide concentrations were 0.01, 0.025, 0.05 and 0.1 M, < 5% PCE degradation was achieved in CHP with isopropanol within 30 minutes. However, 87.3 % of PCE was degraded with 0.01 M H_2O_2 and > 97% degradation was achieved with 0.025, 0.05 and 0.1 M H_2O_2 without radical scavenger. When hydrogen peroxide concentrations increased to 0.5 M and 1 M, 97.1% and 87.2% of PCE were removed without isopropanol, and ~ 7% of PCE was removed in CHP with isopropanol, which was a slight increase compared with lower hydrogen peroxide concentrations. At each concentration level of hydrogen peroxide in CHP, the PCE degradation rates with isopropanol were not significantly different from the deionized water control system ($\alpha = 0.05$). The above results indicated that the PCE destruction was due mainly to hydroxyl radical in CHP; the superoxide activity is minimal for PCE degradation compared with hydroxyl radical activity.

The degradation of TCE in the presence of hydroxyl radical scavenger isopropanol in CHP is shown in Figures 4(a-f). At the hydrogen peroxide concentrations of 0.01 M and 0.025 M, the TCE degradation with isopropanol was 5.1% and 6.2% respectively within 20 minutes while the degradation of TCE were 83.0% and 97.6% without scavenger. At hydrogen peroxide concentrations of 0.05 M and 0.1 M in CHP, the TCE degradation was 9.1% and 9.5 % with isopropanol, and 97.2% and 98.4% without scavenger, respectively. When hydrogen peroxide increased to 0.5 M and 1 M, with isopropanol present, the TCE degradations levels increased to 13.0% and 19.8%; when scavenger was absent, the degradations of TCE were 98.9% and 95.1%, respectively. These results demonstrated that, although hydroxyl radical was the major reactive species for TCE loss, higher superoxide activity was observed and contributed to more TCE destruction as hydrogen peroxide concentrations were increased from 0.01 M to 1 M. Smith et al. (2004) reported that the presence of hydrogen peroxide acts as a cosolvent to increase the superoxide radical anion activity in CHP. This may be the reason why the superoxide activity contributes more to the contaminant destruction when there are higher concentrations of hydrogen peroxide in the system. As we found that both hydroxyl radical and superoxide activities are tied to hydrogen peroxide concentration, we conducted a further study to investigate the generation of hydroxyl radical and superoxide at different hydrogen peroxide concentration levels.

Generation of hydroxyl radical in CHP systems

Nitrobenzene was used as a probe compound to investigate hydroxyl radical generation in CHP with specific hydrogen peroxide concentrations between 0.05 M and 1 M. The degradation of

nitrobenzene in CHP over 15 minutes is presented in Figure 5, and the first order rate constants are listed in Table 2. With 0.05 M and 0.1 M hydrogen peroxide, over 99% of nitrobenzene destruction was achieved within 10 minutes at first order rate constants of 0.316 and 0.397 min^{-1}, respectively. However, in the presence of 0.5 M hydrogen peroxide in CHP, the nitrobenzene degradation only reached 93.1% within 15 minutes ($k = 0.182\ min^{-1}$). Moreover, when the hydrogen peroxide concentration was increased to 1 M, destruction of nitrobenzene was 66.9% within 15 minutes ($k = 0.077\ min^{-1}$). The maximum nitrobenzene destruction rate was achieved with 0.1 M hydrogen peroxide. The degradation rate of nitrobenzene in the presence of 0.1 M hydrogen peroxide was 1.26 times higher than that found with 0.05 M hydrogen peroxide. However, the degradation rate in the presence of 0.5 M and 1 M hydrogen peroxide were 2.18 and 5.16 times lower than that found with 0.1 M hydrogen peroxide. These results correlate with the PCE and TCE degradation trends, indicating that more hydroxyl radical was generated as hydrogen peroxide concentration increased incrementally between 0.01 M to 0.1 M. However, less hydroxyl radical existed in CHP systems as hydrogen peroxide concentration levels continued rising from 0.1 M to 1 M. This may be because a series of propagation reactions occurred in higher hydrogen peroxide concentrations (0.6-3.6 M) in CHP. The hydroxyl radical generated through initial Fenton's reaction promotes the generation of other reactive species such as superoxide radical anion (Watts and Teel, 2006). In this case, higher concentration of hydrogen peroxide may result in a lower amount of hydroxyl radical, which was consumed by additional hydrogen peroxide to promote the propagation reactions.

Generation of superoxide radical anion in CHP systems

Modified Fenton's reagent not only oxidizes contaminants in soil and groundwater, but also reduces oxidized compounds (such as carbon tetrachloride and tetranitromethane) as well (Teel and Watts, 2002). To investigate the generation of superoxide radical anion in CHP systems with different hydrogen peroxide concentrations, tetranitromethane was used as probe compound for the study. The degradation of tetranitromethane in CHP over a 5 minute-period is shown in Figure 6, and the first order rate constants are listed in Table 2. With 0.05 M and 0.1 M H_2O_2 in CHP, 70.7% and 78.4% of tetranitromethane was degraded within 5 minutes with rate constants of 0.106 min^{-1} and 0.386 min^{-1}, respectively. When H_2O_2 concentration increased to 0.5 M and 1 M, the degradation percentage went up to 80.6% and 83.4% with rate constants of 0.503 min^{-1} and 0.521 min^{-1}, respectively. Unlike the nitrobenzene degradation findings, tetranitromethane degradation increased with greater concentrations of H_2O_2. Similar results were found by Smith et al. (2004); as hydrogen peroxide concentrations increased from 0.1 M to 1 M in CHP systems with 0.5 mM iron (III), greater carbon tetrachloride transformation was observed, due to increased superoxide generation. The results indicated that higher generation of superoxide was achieved with greater concentrations of H_2O_2 because the high hydrogen peroxide concentrations (> 0.3 M) promote propagation reactions that form transient reactive oxygen species other than hydroxyl radicals (such as superoxide radical anions) (Watts et al, 2005). Additionally, the presence of hydrogen peroxide enhances the reactivity of superoxide in modified Fenton's reagent (Smith et al., 2004).

Conclusion

The destruction of PCE and TCE by modified Fenton's reagent was investigated, and the addition of radical scavenger isopropanol was used to evaluate the reactive species responsible

for their degradation. Greater PCE and TCE degradation was achieved in CHP systems with higher hydrogen peroxide concentrations from 0.01 M to 0.1 M. However, less PCE and TCE degradation was achieved when hydrogen peroxide concentrations continued to increase to 0.5 M and 1 M. The addition of a hydroxyl radical scavenger suggested that hydroxyl radical was responsible for the degradation of PCE and TCE. However, higher TCE degradation was obtained in the presence of scavenger when hydrogen peroxide concentration increased from 0.01 M to 1 M, indicating that higher H_2O_2 concentrations may result in more superoxide generation. Next, nitrobenzene and tetranitromethane were used as probe compounds to investigate the activities of hydroxyl radical and superoxide with different hydrogen peroxide concentrations. Lower nitrobenzene degradation was achieved with 0.5 M and 1 M hydrogen peroxide, compared with higher hydrogen peroxide concentrations that resulted in greater tetranitromethane destruction. Our findings indicated that, in CHP systems with hydrogen peroxide concentrations from 0.1 M to 1 M, superoxide displayed greater activity. The results of this study demonstrate that modified Fenton's reagent with high concentrations of hydrogen peroxide may provide an effective process to destroy oxidized organic compounds in in situ chemical oxidation.

References

Afanas' ev, I.B. 1989. Superoxide ion: chemistry and biological implications. Volume I.

Buxton, G. E. P., V., Greenstock, C. L., Helman, W. P., Ross, A. B., 1988. Critical review of rate constants for reactions of hydrated electrons, hydrogen atoms and hydroxyl radicals in aqueous solution. J. Phys. Chem. Ref. Data; 17(2):513–886.

David, M. D., Seiber, J. N., 1999. Accelerated hydrolysis of industrial organophosphates in water and soil using sodium perborate. Environ. Pollut.; 105:121.

Dorfman, L. M., Adams, G. E., 1973. Reactivity of the Hydroxyl Radical in Aqueous Solutions; U.S. Department of Commerce, National Bureau of Standards NSRDS-NBS 46.

Frimer, A. A. In Oxygen Radicals in Biology and Medicine. Eds. Simic, M. G., Taylor, K. A., Ward, J. F., von Sonntag, C. Plenum Press: New York, 1988.

Gutteridge, J.M.C., 1985. Superoxide dismutase inhibits the superoxide-driven Fenton reaction at two different levels. FEBS Letters; 185(1,3):19–23.

Haag, W. R., Yao, C. D. D., 1992. Rate constants for reaction of hydroxyl radicals with several drinking water contaminants. Environ. Sci. Technol.; 26:1005.

Sedlak, D. L. and Andren, A. W., 1994. The effect of sorption on the oxidation of polychlorinated biphenyls _PCBs_ by hydroxyl radical. Water Res.; 28(5):1207–1215.

Smith, B.A., Teel, A.L., Watts, R.J., 2004. Identification of the reactive oxygen species responsible for carbon tetrachloride degradation in modified Fenton's systems. Environ. Sci. Technol.; 38:5465–5469.

Smith, B.A., Teel, A.L., Watts, R.J., 2006. Mechanism for the destruction of carbon tetrachloride and chloroform DNAPLs by modified Fenton's reagent. J. Contam. Hydrol.; 85(3-4)z;229–246.

Smith, B.A., Teel, A.L., Watts, R.J., 2009. Destruction of trichloroethylene and perchloroethylene DNAPLs by catalyzed H_2O_2 propagations. J. Environ. Eng.; 135(7):536–543.

Teel, A.L., Watts, R.J., 2002. Degradation of carbon tetrachloride by modified Fenton's reagent. J. Haz. Mater.; B94zz;179–189.

Walling, C., 1975. Fenton's reagent revisited. Acc. Chem. Res.; 8(1):125–131.

Watts, R.J., ASCE, Teel, A.L, 2005. Chemistry of Modified Fenton's Reagent (Catalyzed H_2O_2 Propagations–CHP) for In Situ Soil and Groundwater Remediation. J. Environ. Eng.; 131:612–622.

Watts, R.J., Teel, A.L., 2006. Treatment of contaminated soils and groundwater using ISCO. Pract. Period. Hazard. Tox. Radio. Waste Manag.; 10(1):2–9.

Table 1 First Order Rate Constants for Degradation of PCE and TCE.

	PCE		TCE	
H_2O_2 concentration	k_{obs} (min^{-1})	R^2	k_{obs} (min^{-1})	R^2
0 M (Control)	n.d.	n.d.	n.d.	n.d.
0.01 M	0.025	0.94	0.060	0.81
0.025 M	0.152	0.92	0.078	0.64
0.05 M	0.173	0.93	0.246	0.93
0.1 M	0.191	0.93	0.297	0.91
0.5 M	0.135	0.97	0.270	0.99
1 M	0.059	0.87	0.164	0.99

n.d.: not determined.

Table 2 First Order Rate Constants for Degradation of Hydroxyl Radical Probe Nitrobenzene and Superoxide Probe Tetranitromethane.

	Nitrobenzene		Tetranitromethane	
H_2O_2 concentration	k_{obs} (min^{-1})	R^2	k_{obs} (min^{-1})	R^2
0 M (Control)	n.d.	n.d.	n.d.	n.d.
0.05 M	0.316	0.88	0.106	0.76
0.1 M	0.397	0.77	0.386	0.88
0.5 M	0.182	0.99	0.503	0.97

1 M	0.077	0.98	0.521	0.96

List of Figures

Figure 1

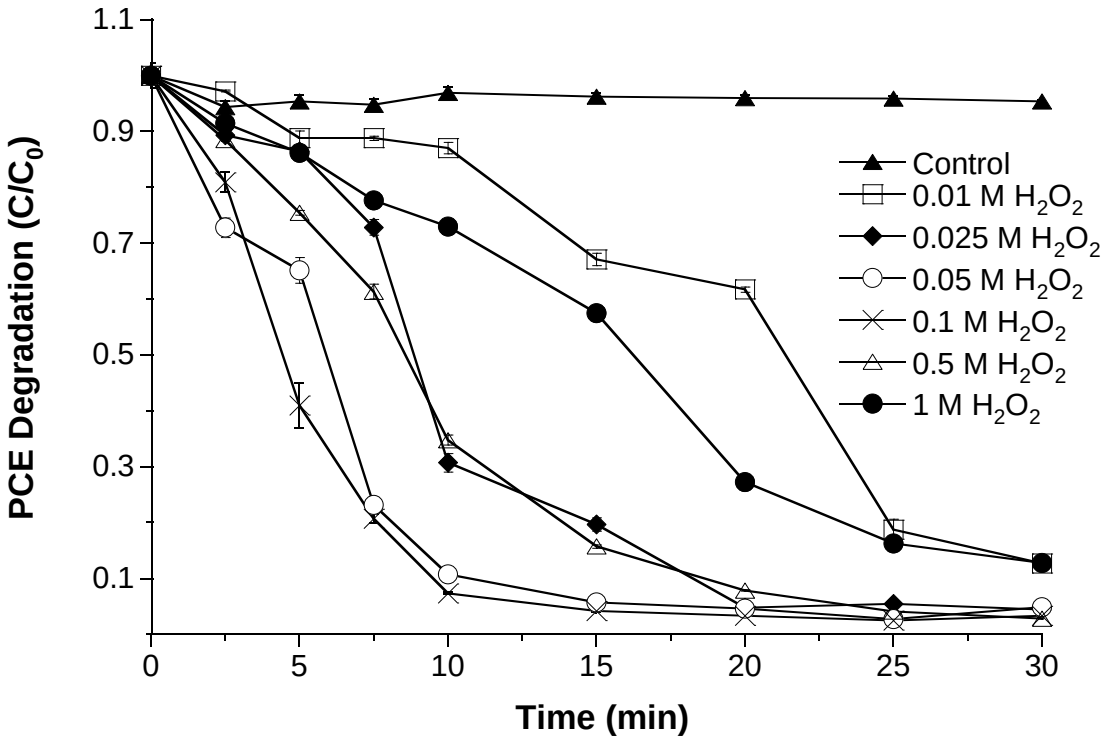
PCE Degradation (C/C0)
Time (min)
1.1
0.9
0.7
0.5
0.3
0.1
0
5
10
15
20
25
30
Control
0.01 M H2O2
0.025 M H2O2
0.05 M H2O2
0.1 M H2O2
0.5 M H2O2
1 M H2O2

Figure 2

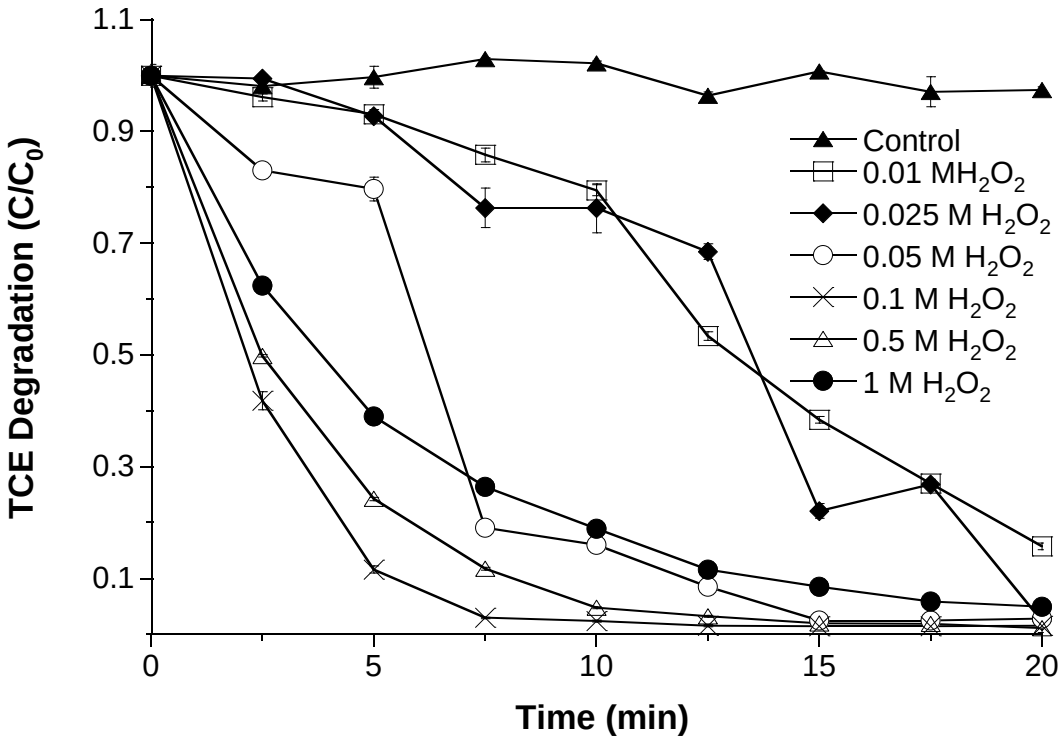
TCE Degradation (C/C0)
Time (min)
Control
0.01 MH2O2
0.025 M H2O2
0.05 M H2O2
0.1 M H2O2
0.5 M H2O2
1 M H2O2
1.1
0.9
0.7
0.5
0.3
0.1
0
5
10
15
20

Figure 3 (a)

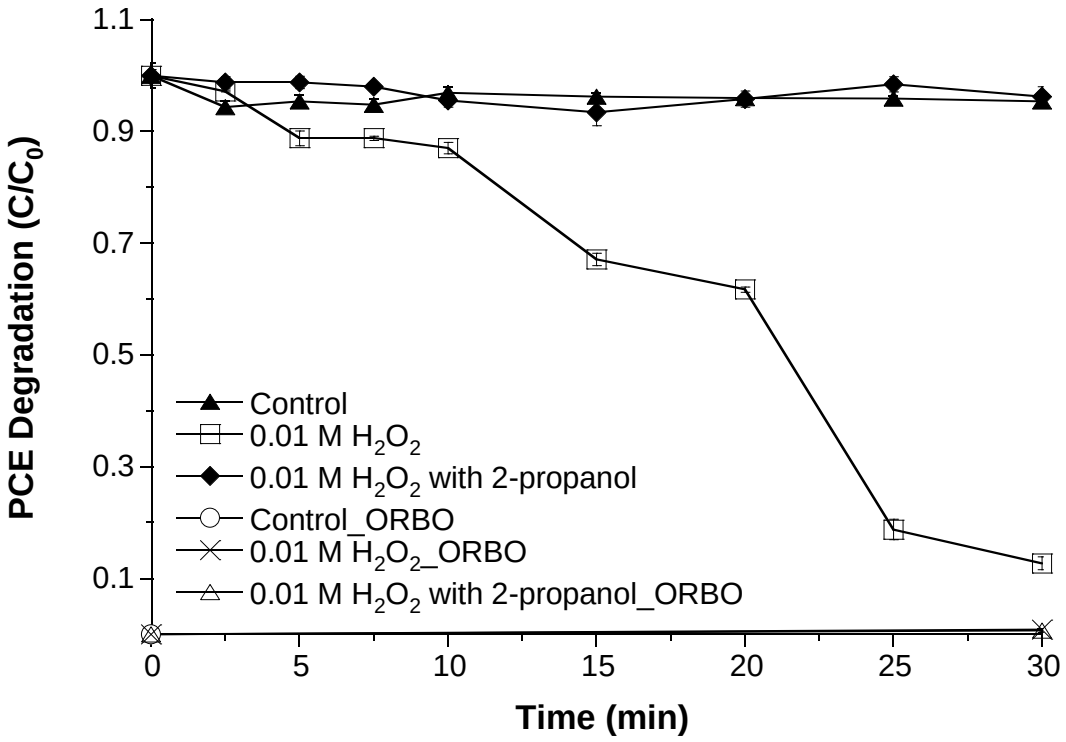
PCE Degradation (C/C0)
Time (min)
1.1
0.9
0.7
0.5
0.3
0.1
0
5
10
15
20
25
30
Control
0.01 M H2O2
0.01 M H2O2 with 2-propanol
Control_ORBO
0.01 M H2O2_ORBO
0.01 M H2O2 with 2-propanol_ORBO

(b)

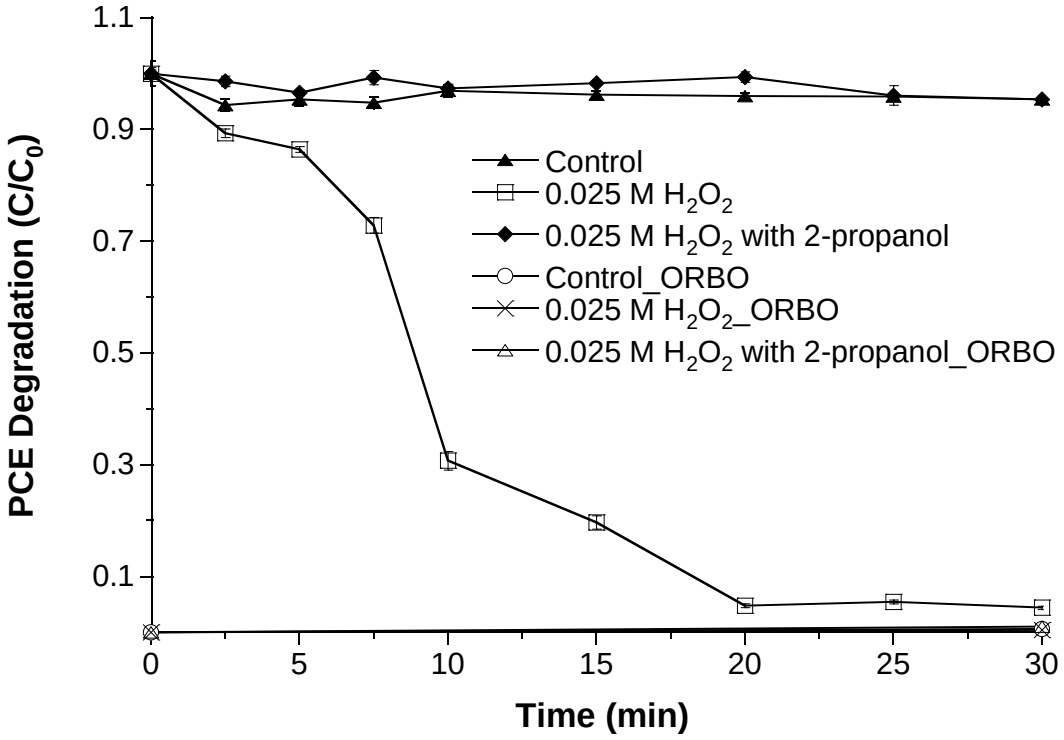
PCE Degradation (C/C0)
Time (min)
1.1
0.9
0.7
0.5
0.3
0.1
0
5
10
15
20
25
30
Control
0.025 M H2O2
0.025 M H2O2 with 2-propanol
Control_ORBO
0.025 M H2O2_ORBO
0.025 M H2O2 with 2-propanol_ORBO

(c)

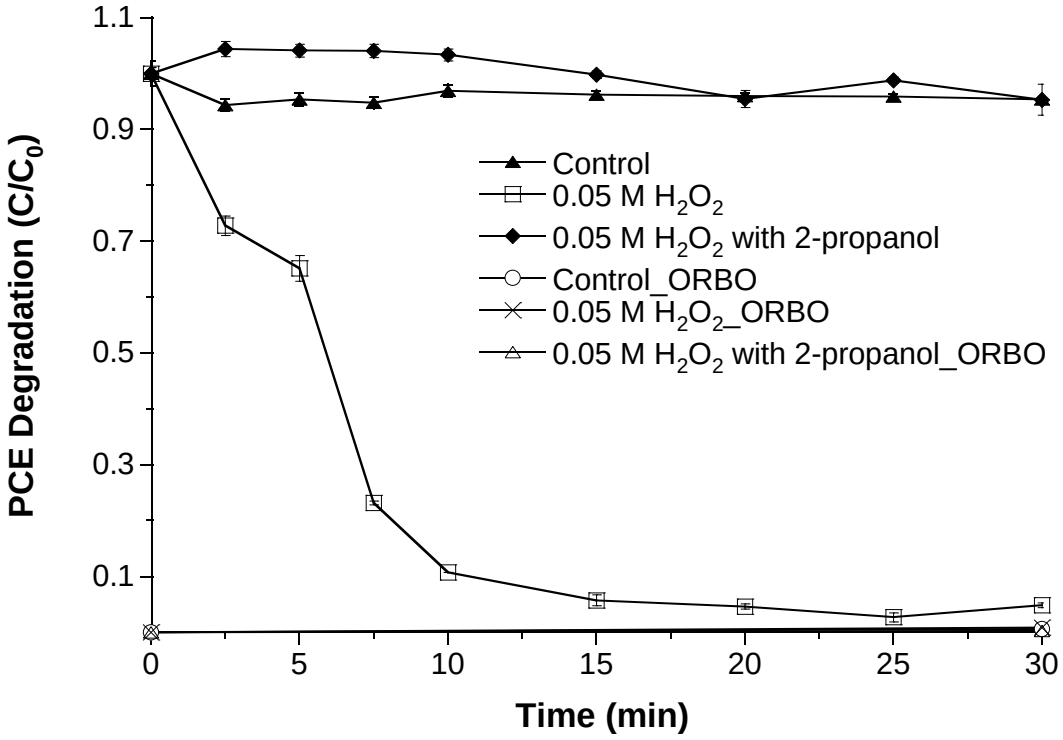
PCE Degradation (C/C0)
Time (min)
1.1
0.9
0.7
0.5
0.3
0.1
0
5
10
15
20
25
30
Control
0.05 M H2O2
0.05 M H2O2 with 2-propanol
Control_ORBO
0.05 M H2O2_ORBO
0.05 M H2O2 with 2-propanol_ORBO

(d)

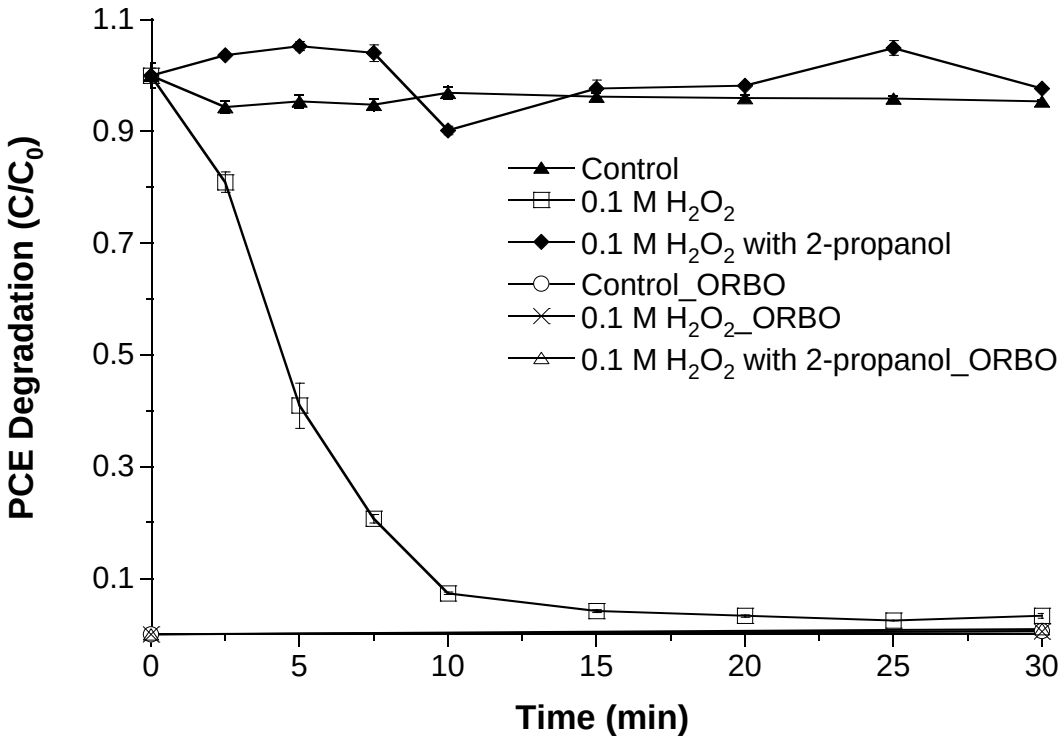
PCE Degradation (C/C0)
Time (min)
1.1
0.9
0.7
0.5
0.3
0.1
0
5
10
15
20
25
30
Control
0.1 M H2O2
0.1 M H2O2 with 2-propanol
Control_ORBO
0.1 M H2O2_ORBO
0.1 M H2O2 with 2-propanol_ORBO

(e)

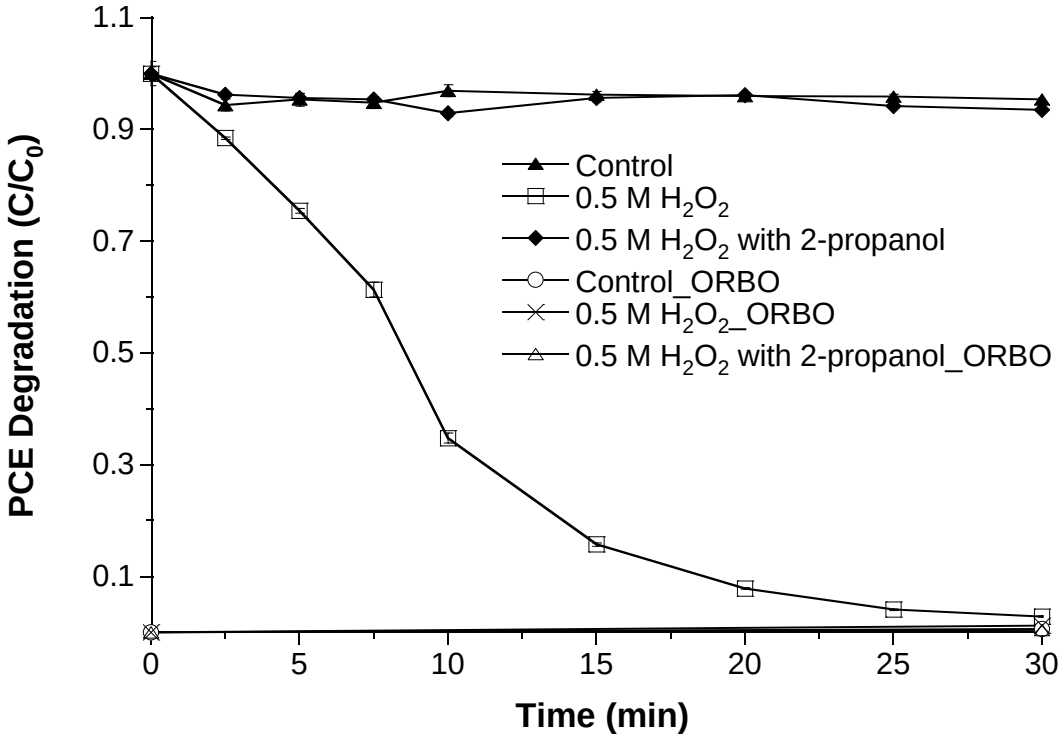
PCE Degradation (C/C0)
Time (min)
1.1
0.9
0.7
0.5
0.3
0.1
0
5
10
15
20
25
30
Control
0.5 M H2O2
0.5 M H2O2 with 2-propanol
Control_ORBO
0.5 M H2O2_ORBO
0.5 M H2O2 with 2-propanol_ORBO

(f)

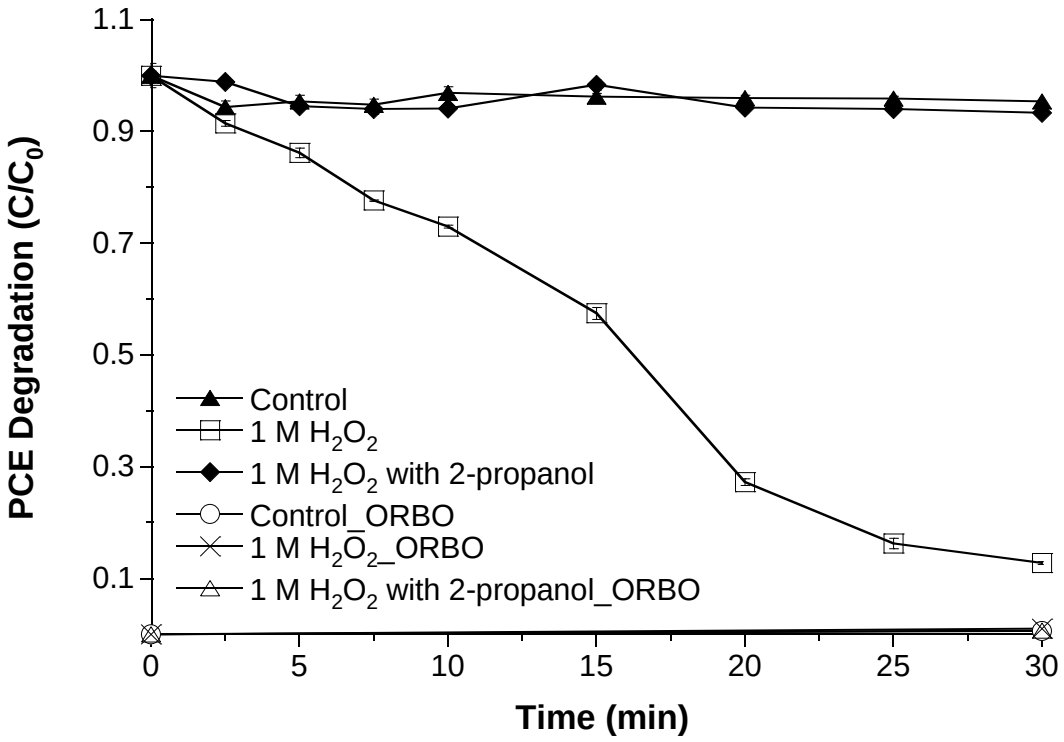
PCE Degradation (C/C0)
Time (min)
1.1
0.9
0.7
0.5
0.3
0.1
0
5
10
15
20
25
30
Control
1 M H2O2
1 M H2O2 with 2-propanol
Control_ORBO
1 M H2O2_ORBO
1 M H2O2 with 2-propanol_ORBO

Figure 4 (a)

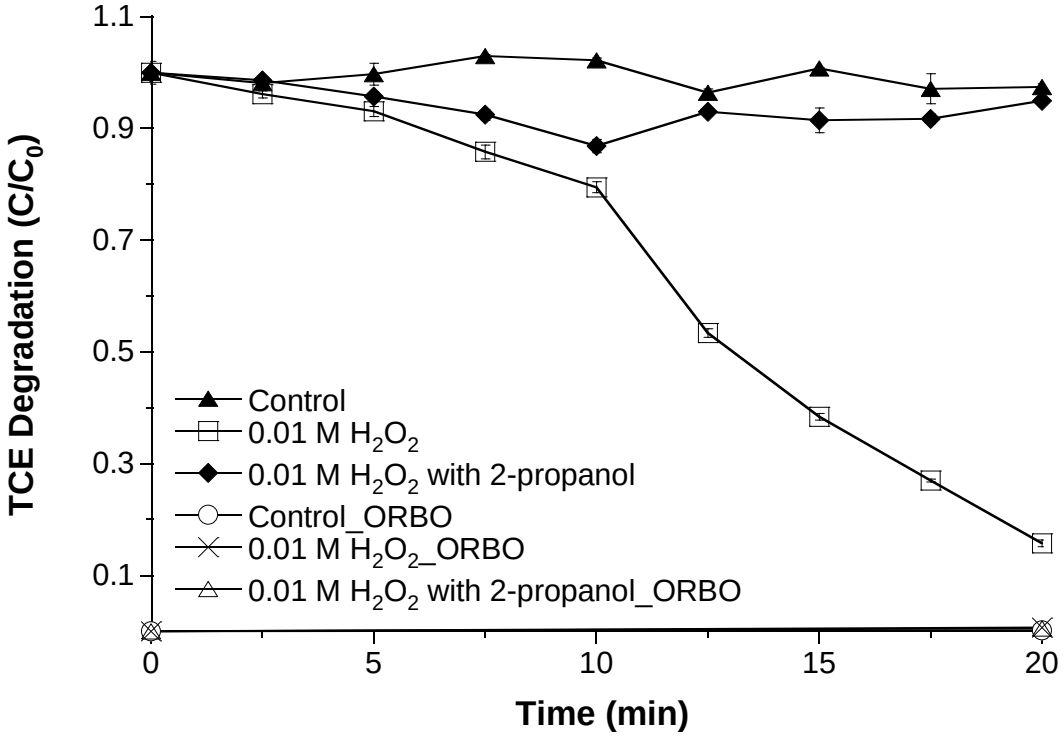
TCE Degradation (C/C0)
Time (min)
1.1
0.9
0.7
0.5
0.3
0.1
0
5
10
15
20
Control
0.01 M H2O2
0.01 M H2O2 with 2-propanol
Control_ORBO
0.01 M H2O2_ORBO
0.01 M H2O2 with 2-propanol_ORBO

(b)

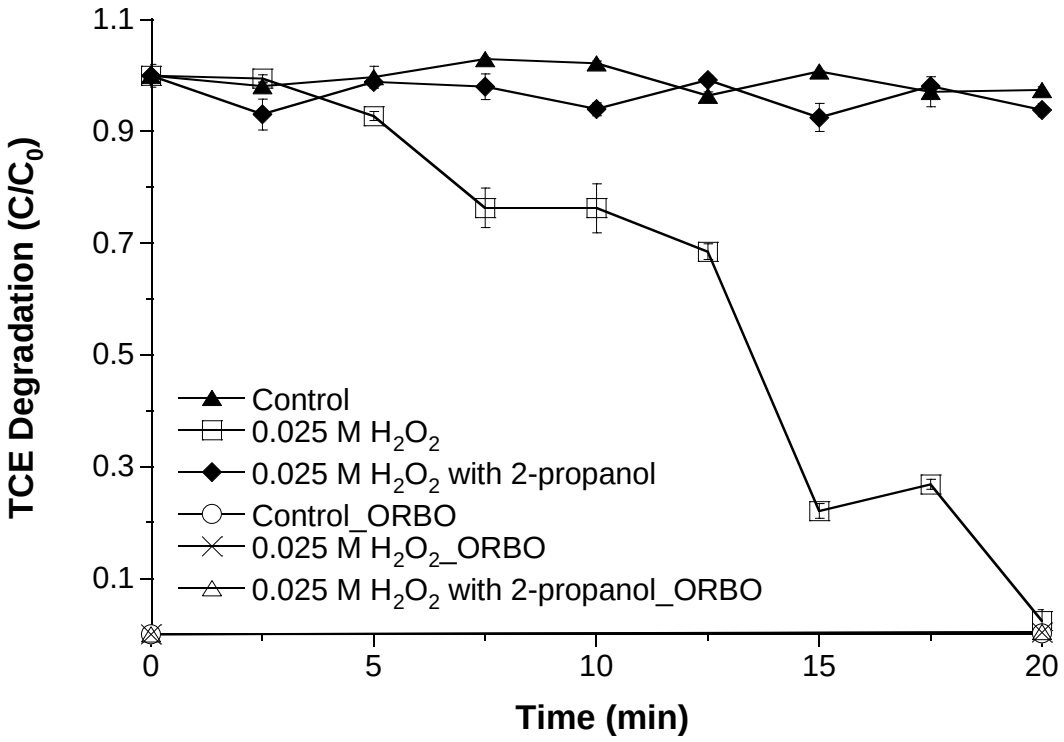
TCE Degradation (C/C0)
1.1
0.9
0.7
0.5
0.3
0.1
0
5
10
15
20
Time (min)
Control
0.025 M H2O2
0.025 M H2O2 with 2-propanol
Control_ORBO
0.025 M H2O2_ORBO
0.025 M H2O2 with 2-propanol_ORBO

(c)

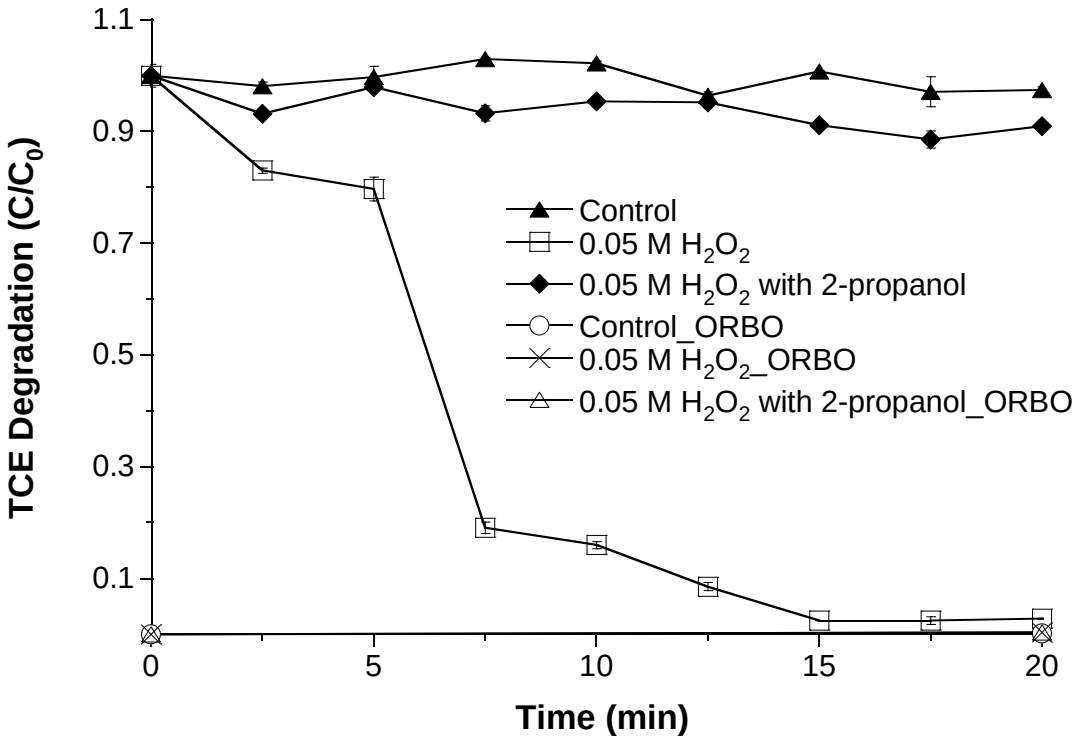
TCE Degradation (C/C0)
Time (min)
1.1
0.9
0.7
0.5
0.3
0.1
0
5
10
15
20
Control
0.05 M H2O2
0.05 M H2O2 with 2-propanol
Control_ORBO
0.05 M H2O2_ORBO
0.05 M H2O2 with 2-propanol_ORBO

(d)

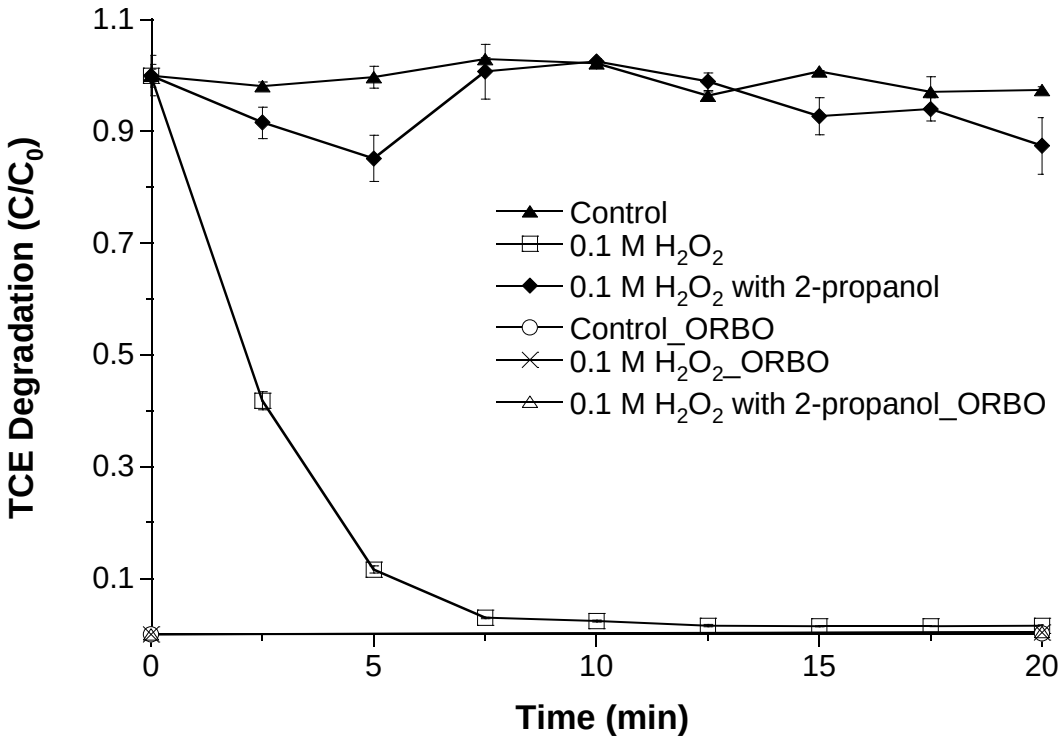
TCE Degradation (C/C0)
Time (min)
1.1
0.9
0.7
0.5
0.3
0.1
0
5
10
15
20
Control
0.1 M H2O2
0.1 M H2O2 with 2-propanol
Control_ORBO
0.1 M H2O2_ORBO
0.1 M H2O2 with 2-propanol_ORBO

(e)

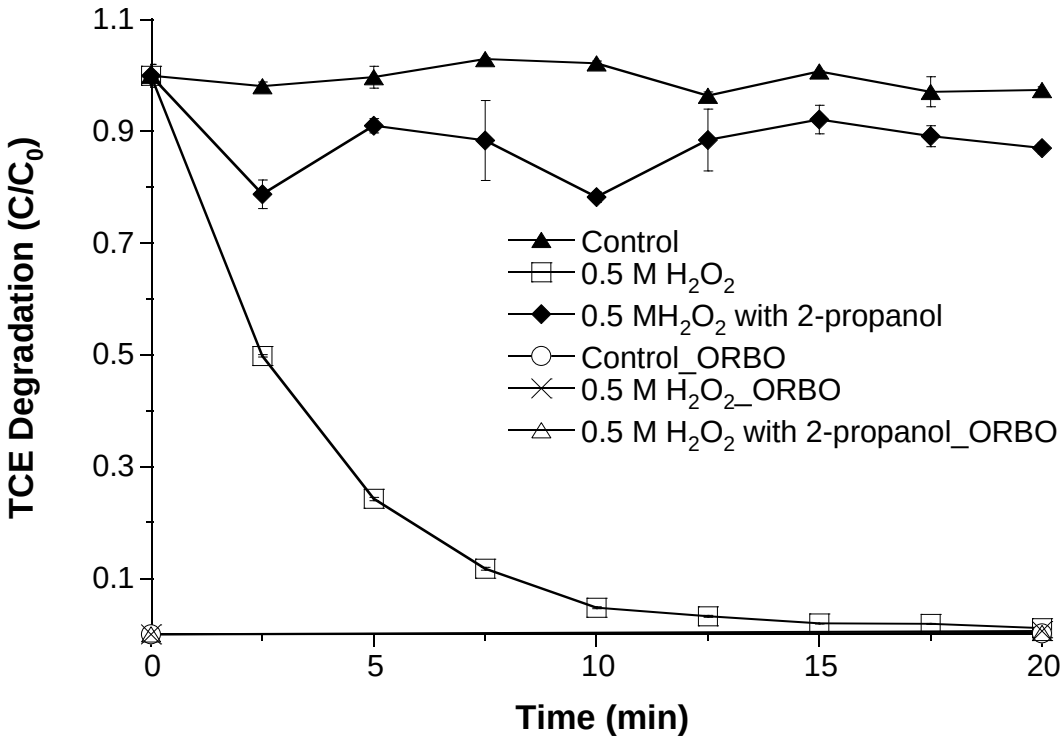
1.1
0.9
0.7
0.5
0.3
0.1
TCE Degradation (C/C0)
0
5
10
15
20
Time (min)
Control
0.5 M H2O2
0.5 MH2O2 with 2-propanol
Control_ORBO
0.5 M H2O2_ORBO
0.5 M H2O2 with 2-propanol_ORBO

(f)

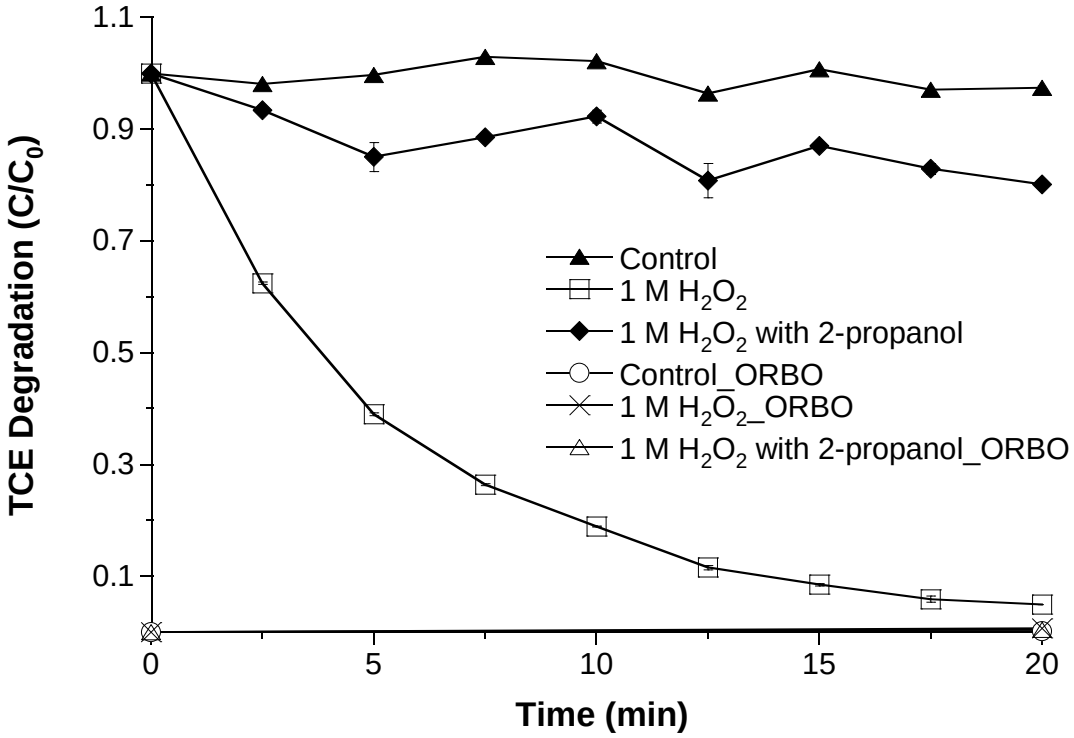
TCE Degradation (C/C0)
Time (min)
1.1
0.9
0.7
0.5
0.3
0.1
0
5
10
15
20
Control
1 M H2O2
1 M H2O2 with 2-propanol
Control_ORBO
1 M H2O2_ORBO
1 M H2O2 with 2-propanol_ORBO

Figure 5

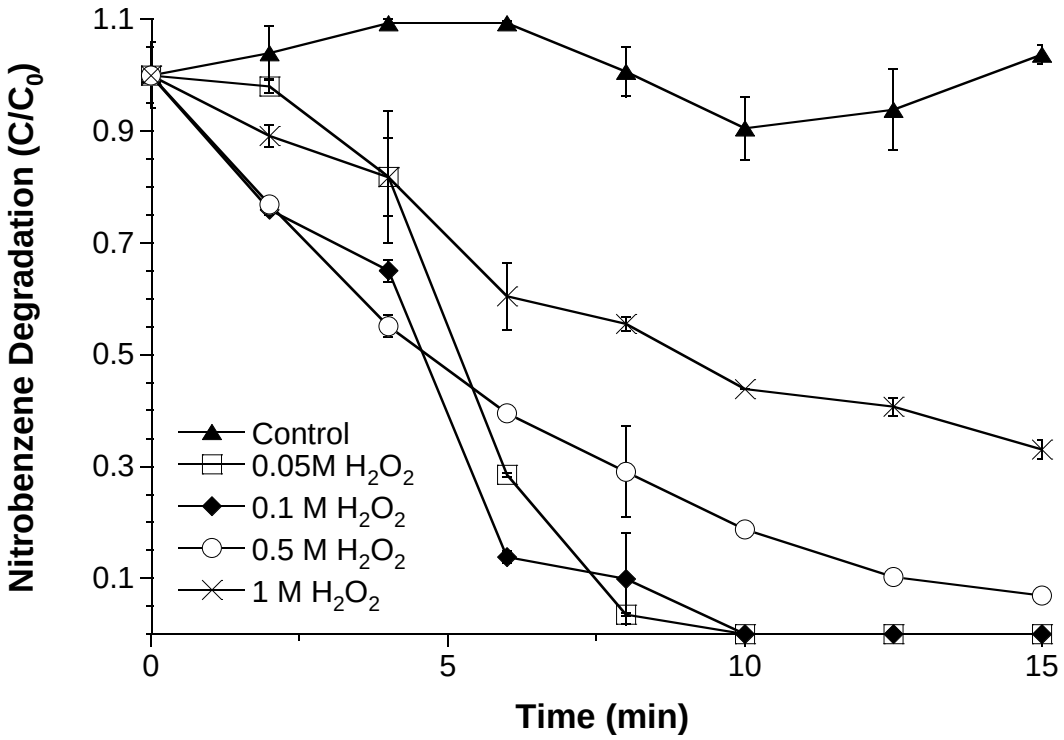
Nitrobenzene Degradation (C/C0)
Time (min)
1.1
0.9
0.7
0.5
0.3
0.1
0
5
10
15
Control
0.05M H2O2
0.1 M H2O2
0.5 M H2O2
1 M H2O2

Figure 6

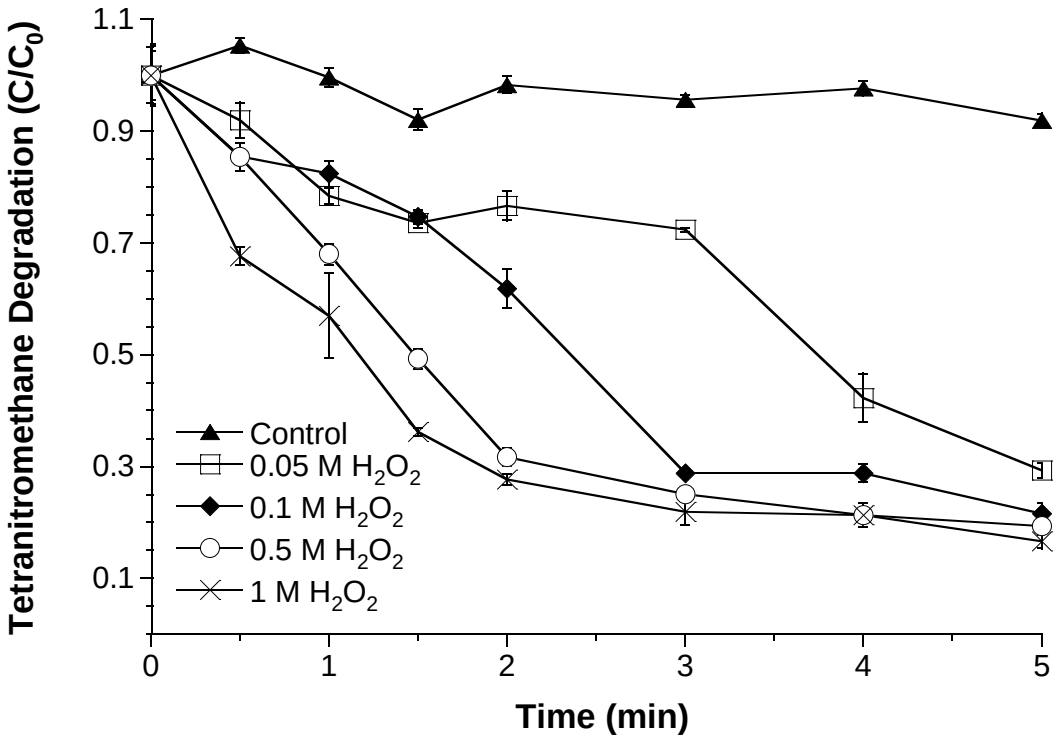
Tetranitromethane Degradation (C/C0)
Time (min)
Control
0.05 M H2O2
0.1 M H2O2
0.5 M H2O2
1 M H2O2
1.1
0.9
0.7
0.5
0.3
0.1
0
1
2
3
4
5